The Northern European Enclosure Dam

A study on the technical feasibility of the enclosure dam

Master Thesis

Pim Koch

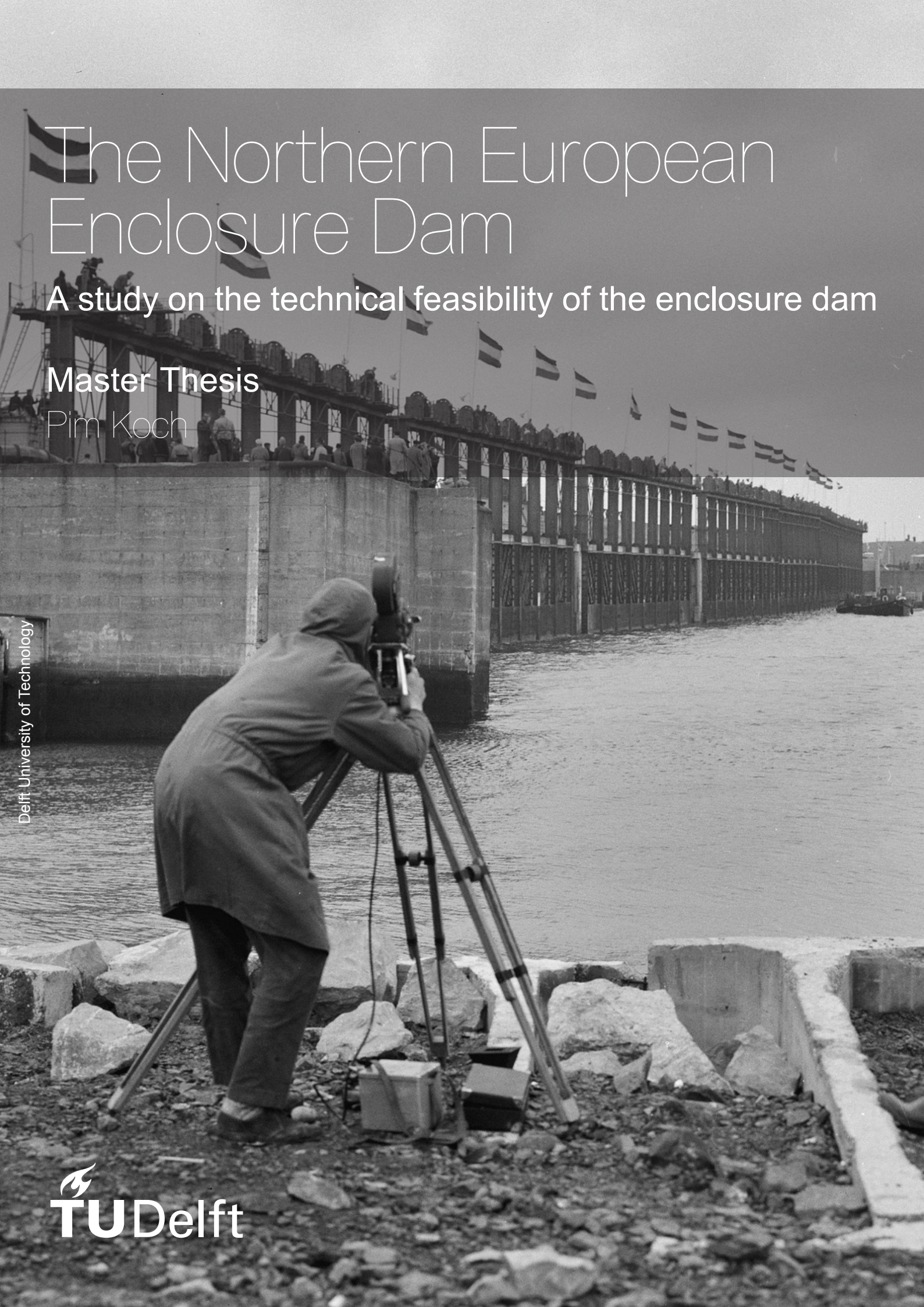

Delft University of Technology

TU Delft

The Northern European Enclosure Dam

A study on the technical feasibility of the enclosure dam

Master Thesis

To obtain the degree of Master of Science in Hydraulic Engineering at Delft University of Technology

Pim Koch

Student Number:
4350421

April 1, 2022

Graduation Committee

Prof. dr. ir. S.N. Jonkman	TU Delft (Chair thesis committee)
Ing. C. Kuiper	TU Delft, Witteveen+Bos (Daily supervisor)
Dr. S. Groeskamp	NIOZ

Cover Image: Permanent closure of the Veerse Gat (Nationaal Archief)

TU Delft

Preface

This thesis is written to obtain the master's degree in Hydraulic Engineering at the TU Delft. Although most of this thesis was written during the covid pandemic, spending a lot of time working in my room, I enjoyed his project. During the project, I gained a lot of knowledge about building huge dams. This master thesis allowed me to apply the knowledge gained during my study in Delft.

I would like to thank my daily supervisor Coen Kuipers for his feedback, time, and guidance throughout the duration of this thesis. I would like to thank Bas Jonkman for his input and shared knowledge during the committee meetings. And I would like to thank Sjoerd Groeskamp for his suggestions and thoughts.

Lastly, I would like to thank my fellow students, in particular Menno, Sven, and Zhi Yang, friends, and housemates for their help and support during this thesis.

Enjoy reading!

Pim Koch
Nieuwkoop, April 2022

Summary

Sea level rise caused by climate change directly affects and threatens low-lying countries. In August of 2021, the report of the IPCC was published, and the findings were disturbing. The sea could rise by a few meters in the coming centuries, causing floods in large parts of West-Europe. Groeskamp and Kjellson proposed a solution to adapt to the effect of extreme sea-level rise, a Northern European Enclosure Dam (NEED). The dam stretched from Bergen in Norway to the north of Scotland and from Ploudalmézeau France to the Lizard Heritage Coast England. Figure 1 illustrates the location of the NEED proposed by Groeskamp.
main objective of this thesis is to investigate the technical feasibility of the NEED. To fulfill this objective, the following aspect were studied in more detail: the location and layout of this dam, the favorable cross-section of the dam, and the most likely closure scenarios.

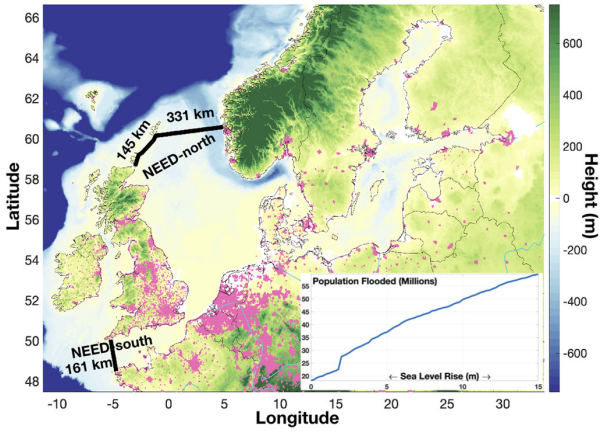

Figure 1: The proposed location for the Northern European Enclosure Dam by Groeskamp. [22]

The first step was to find out what the optimized location was. The proposed location from Groeskamp was compared to an optimized location based on the boundary conditions. The two alignments are distinguished by their length, depth, and location. These were compared by using multicriteria analysis, with the four criteria being:

1. The total length and maximum depth of the alignment.
2. The difference in the number of people that the dam will protect by the dam.
3. The constructability of the damper alignment, based on the loads (tide and wave).
4. The geotechnical stability based on the requirements by Huis in 't Veld

An engineering perspective was used to evaluate the alignments. The outcome of the multicriteria analysis (MCA) was that the initial alignment by Groeskamp was most favorable. However, a different perspective can result in a different conclusion, and it is therefore advised to look in further detail to come up with a well-founded decision.

For the favorable cross-section, two types of closure dams were investigated to determine the best dam design, the caisson dam, and the earthen dam. Both designs were dimensioned based on safety criteria. These safety criteria were derived from the Dutch guidelines for primary flood defenses, with the top event, inundation of west Europe, given a probability of failure of 1:10 000 per year. A Monte Carlo analysis was constructed to determine the dimensions of both dams. Two failure mechanisms are assessed fully probabilistically as these are considered to be the most relevant. The ULS (ultimate limit state) and SLS (serviceability limit state) conditions are considered per failure mechanisms. The main difference between the resulting designs is the sizes; the earthen dam needs a mild slope to be

stable (1:5), requiring a tremendous amount of material. The earthen dam requires seven times more material than the caisson dam. This results in the caisson dam being a more technically feasible design for the NEED than the earthen dam. Figure 10.1 shows the most feasible design of the NEED. The caisson is made of concrete filled with sand. Rock protection and concrete foot protection blocks to protect the sill from erosion.

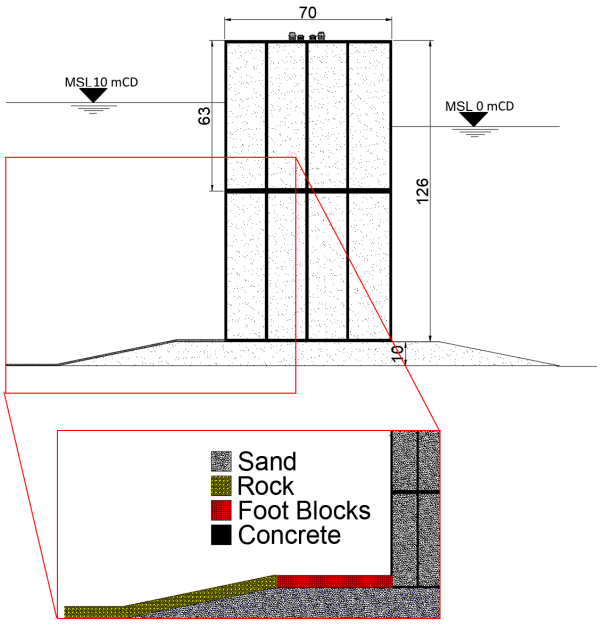

Figure 2: The caisson dam, units in meters.

The closure procedure depends on the flow velocities inside the closure gap. The occurring flow velocities during the closure determine the feasibility. These velocities were calculated using the shallow water equation. A critical boundary condition for the caissons closure is that the maximum flow velocity in the gap is less than 2.5 m/s. For higher flow velocities, placement of the caissons is impossible. Based on the model, a closure procedure was proposed in which this essential condition is met. The most likely closure scenario is that first, the Southern dam is closed to ensure that the flow velocities do not exceed the critical value. The next step is to fulfill the Northern dam closure. The gap is closed until the maximum velocity is approximately 2m/s. The last part is then closed using sluice caissons. These caissons are placed openly in the gap and closed between 1 tidal cycle, completing the dam. The location of the final gap is at the Norwegian trench.

The results from this research are that the NEED is expected to be technically feasible. However, the enormous size of the NEED poses new challenges and effects. Further research is required to comprehensively analyze all impacts of the NEED in order to make it feasible.

Contents

Nomenclature

Abbreviations

Abbreviation	Definition
AIC	Akaike Information Criteria
DWL	Design Water Level
GEBCO	General Bathymetric Chart of the Oceans
IPCC	Intergovernmental Panel on Climate Change
KNMI	Koninklijk Nederlands Meteorologisch Instituut
MC	Monte Carlo
MCA	Multicriteria Analysis
MDP	Multidisciplinair Project
MHWS	Mean High Water Springs
MLWN	Mean High Water Neaps
MLWN	Mean Low Water Neaps
MSc	Master of Science
MSL	Mean Sea Level
NOAA	National Oceanic and Atmospheric Administration
NEED	Northern European Enclosure Dam
NIOZ	Koninklijk Nederlands Instituut voor Onderzoek der Zee
QGIS	Quantum Geographic Information System
SLR	Sea Level Rise
SLS	Serviceability Limit State
SSP	Shared Socioeconomic Pathways
SWL	Still Water Level
TU	Technical University
ULS	Ultimate Limit State

Symbols

Symbol	Definition	Unit
Acc	Accretion area	[m^2]
B	Width berm	[m]
c	Wave velocity	[m/s]
cf	Friction coefficient	[-]
d	Still water depth	[m]
d_h	Distance berm and still water level	[m]
Fr	Froude number	[-]
g	Gravity of Earth	[m/s^2]
D_{n50}	Nominal median rock diameter	[m]
D_{15}	15 percent value grainsize distriburion	[m]
D_{70}	70 percent value grainsize distriburion	[m]
H_{m0}	Significant wave height	[m]
H_1	Upsteam energy level	[m]
h_2	Energy level on top of the sill	[m]
h_3	Downstream energy level	[m]
ΔH	head difference	[m]
ΔH_c	critical head difference	[m]

Symbol	Definition	Unit
i	critical gradient	[-]
k	Wave number	[rad/m]
L	Deep water wave length	[m]
M	Mass upright section (Goda)	[kg/m]
N	Number of waves during storm	[-]
n_f	Porosity of filter layer	[-]
q	Discharge per unit width	[m^3/s/m]
Q	Discharge	[m^3/s]
R	Hydraulic radius	[m]
R_c	Freeboard	[m]
R_u	Run up	[m]
S	Damage level	[-]
Δs	Space step	[m]
t	Horizontal distance centre of gravity	[m]
Δt	Time step	[m]
$T_{m-1,0}$	mean spectral wave period	[sec]
u	flow velocity	[m/s]
U	Uplift force caisson	[kN/m]
Z_{acc}	Accretion height	[m]
α	Slope	[$\circ$]
β	Angle of attack wave	[$\circ$]
γ_b	Influence factor berm	[-]
γ_β	Influence factor angle of attack	[-]
γ_f	Influence factor slope	[-]
γ_p	Volumetric weight of sand	[kN/m^3]
γ_w	Volumetric weight of water	[kN/m^3]
Δ	Relative density	[-]
ε	Breaking parameter	[-]
η	Drag coefficient	[-]
θ	Rolling resistance	[$\circ$]
κ	Intrinsic permeability	[m^2]
μ	Friction Coefficient Goda	[-]
ψ	Shields parameter	[-]
ρ_s	Density of sediment	[kg/m^3]
ρ_w	Density of water	[kg/m^3]
ϕ	Angle of internal friction	[$\circ$]
ν_w	Kinematic viscocity water	[m^2/s]
χ	Bed resistance coefficient	[-]

List of Figures

List of Tables

1 Introduction

1.1. Background

Climate change is perhaps the greatest threat humanity faces today. Sea level rise is a direct effect of the increasing temperature and threatens low lying countries. Due to the increase of CO2 emissions since the industrial revolution, the global average temperature has increased by about 1 degree[31]. This increase in temperature is still continuing with a rate of +0.29 degrees Celsius per decade [18]. When greenhouse gasses emissions are not reduced, the earth's average temperature will continue to rise. This causes the polar ice caps to melt and the sea level to rise. Sea level rise is detrimental for low-lying countries, especially the Netherlands.

Although the Paris Agreement has been signed in 2012, the global temperature will continue to rise by 2.6 to 3.1 degrees over the next 100 years [41]. The causes of sea level rise due to the rise in temperature are, water expands the earth's gravitational field changes by the redistribution of water, land underneath the melted polar ice rises, and the previous ice-free land sinks. Combining all these effects results in a relative mean sea-level rise in the Netherlands of 50 cm in 2100 [31]. A recent paper argues that the sea level will rise by 2 meters in case of a strong global temperature increase [23]. A higher sea level will result in a higher water level in rivers because of sedimentation. This increases the likelihood that areas close to rivers will flood. The rise in sea level is a threat to west Europe and the Netherlands, but also due to global warming, storms will intensify. Resulting in higher waves and a more extensive wind setup. Recently a new research by the IPCC [3] was published about climate change and the effects, this report share the same conclusion. The results of that study is analysed in more detail in chapter 2.

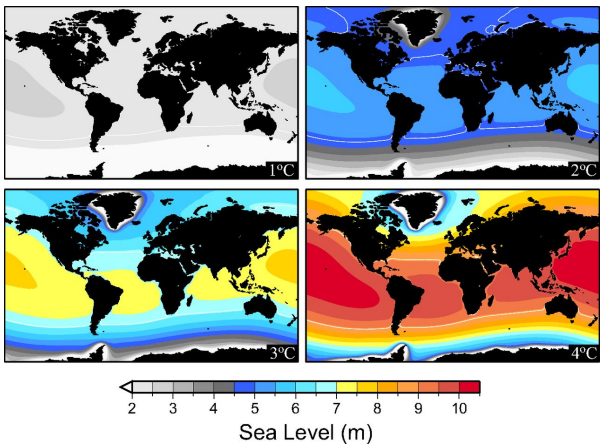

Figure 1.1: Regional patterns of sea-level change for scenarios of 1, 2, 3, and 4 °C of warming for the next 2,000 Years [35]

By raising and strengthening the dikes, these effects can be mitigated. However, if the temperature continues to rise, the sea level rise in the far future can reach a value between 5 -11 meters [35]. This enormous rise is threatening for the Dutch coast and the entire coastline of the North sea. Therefore, ensuring that the coastal areas remain safe and habitable will be a massive economic and technical challenge.

1.2. Northern European Enclosure Dam

Groeskamp and Kjellson proposed a solution to mitigate the effect of extreme sea level rise, a Northern European Enclosure Dam (NEED). The dam stretched from Bergen in Norway to northern Scotland and from Ploudalmézeau France to the Lizard Heritage Coast England [22]. The NEED turns a large part of the North sea into a closed basin. The NEED reduces the coastline under immediate wave attack from the ocean and thereby defends the coastal region of the low-lying areas bordering the North and Baltic sea. In addition, the NEED protects 25 million people living below 2-meter sea-level rise against flooding resulting from climate change [22].
By jointly tackling the effects of climate change, the countries of western Europe can be better protected.

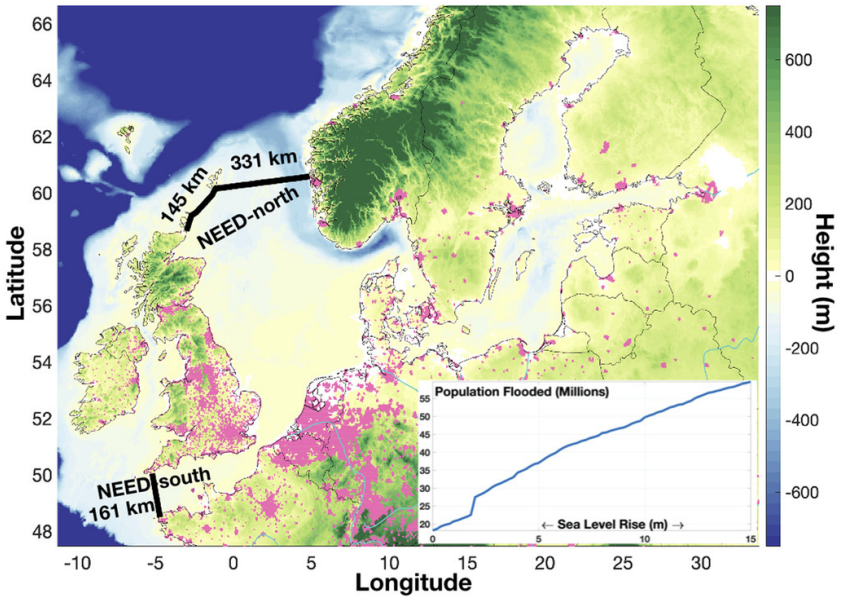

Figure 1.2: The proposed location for the Northern European Enclosure Dam by Groeskamp. [22]

The Northern part of the enclosure dam's existing layout is projected to be 476 km long, consisting of 2 separate parts. The first part with a length of 145 km from Scotland to the Isle of Noss, with an average depth of 49 meters. The second part from the Isle of Noss to Norway (distance 331 km) with an average depth of 127 meters. The depth varies considerably over the dam's length. Just off the coast of Norway, a deep trench is located; this trench has a depth of 321 meters as described. The southern enclosure dam, see figure 1.2, is projected to be 161 km long with an average depth of 85 meters; the maximum depth is significantly less than the northern dam, 102 meters. The combined length of the dam is equal to 637 km. A critical aspect resulting from the southern enclosure dam's construction is the blockage of the entire shipping route through the canal.
The canal's passage is one of the busiest trade routes globally and of vital importance for northern European ports like Rotterdam, Antwerp, and Hamburg. To make these ports accessible, locks must be built to accommodate the sea traffic. This dam's construction also significantly impacts nature like, aquatic life, fishing industry and sediment transport. The dam is also financially very costly and politically sensitive. According to Groeskamp and Kjellson, this project should be seen as a last resort if we have failed to decrease greenhouse gasses emissions drastically. Groeskamp stated, 'if we have to build this, we have basically failed.'
Before this project can be carried out, many hurdles still have to be overcome, but in the paper published by Groeskamp and Kjellson, they have shown that it could be realized. However, more research

needs to be done to detail the implications and the construction of the enclosure dam.

1.3. Problem description and Relevance

New IPCC data [3] showed that the sea level rise is accelerating. When drastic measures are not taken to damp the accelerated sea level rise, large parts of western Europe could become flooded. Groeskamp and Kjellson have proposed a dam to protect west European countries against sea-level rise, the Northern European Enclosure Dam. The NEED is a massive project, and when built, the dam will become the largest civil engineering structure globally. The effect of the construction and use impacts a vast area. The location of the NEED described in the paper was a first estimate. The dam is long and some optimisations may be considered. Also the material volumes are enormous. The current estimates are based on rough estimates of the cross-section. However, in-depth research on the technical feasibility has not been investigated yet. This thesis will elaborate on the dam layout, and consider different dam cross-section to determine the material volumes. Finally this thesis also touches major construction aspects as the closure of the gaps and the location of the dam.
The technical feasibility is by determining the optimum layout from technical point of view. This is the basis to create typical cross-sections for the different sections which will be evaluated using a MCA. The selected cross-section will be used to provide a realistic estimate of the material volumes for these dams

To summarize the problem and relevance of the research:

- Ongoing sea-level rise threatens West Europe.
- Groeskamp proposed to completely block the North Sea by creating a dam, the NEED.
- Detailed calculations to demonstrate the technical feasibility of the dam is lacking.

1.4. Objective

Based on the problem description, the research question can be formulated as:

What is the technical feasibility of building the NEED based on the location, cross-sectional designs, material use, construction duration, and the closure of the final gap?

Three subquestions have been formulated to provide a correct answer to the main question. The subquestions are structured based on the design process, starting with location investigation and narrowed down to the investigation of the resource use and total duration. The subquestions are:

1. **What is the most optimal location of the closure dam, according to a multi criteria analysis?**
2. **What is the optimal cross-section that fulfills the required safety criteria?**
3. **What is a feasible closure strategy?**

1.5. Research approach

The thesis gives a answer to three sub questions based on, the location of the dam, the cross-section and evaluation, and the design of the final closure. First a review of the existing literature, background of the NEED and the environmental description is conducted, chapter 2. Three studies already made some predictions of the consequence of the dam. These predictions are shortly summarized in this section. The current flood protection systems, safety norms, and types of structures are briefly assessed. More insight into the recent measures to mitigate the effects of sea-level rise is explored. The IPCC [3] report published in August 2021 forms the foundation of this thesis. The sea-level rise predictions are used as the primary input for determining the design of the NEED. Two reference projects are analyzed for practical information, the Afsluitdijk and the Saemangeum Seawall.
The link between the location, design and final closure depends on the environmental data. Data about the area will form a separate chapter, 3, because it is crucial for the technical design. Data that need to be collected are bathymetry, bed material, waves, river discharge, analysis of the area that needs to

be protected, and the tide. Some data are sparsely available; assumptions and expert knowledge will replace the missing data to develop a good dam design.

For the first sub-question, the optimal location is being determined in chapter 4. For both the northern and southern dam, one alternative design is proposed. First, the different alignments are shortly discussed. In the following sections, the alignments are tested against the evaluation criteria. Eventually, the concepts are evaluated using a multi-criteria analysis. These criteria also form the requirements of the dam, as will be explained in this chapter. The criteria are:

- The total length and maximum depth of the Alignment.
- The difference in the number of people that the dam will protect by the dam.
- The constructability of the dam, based on the loads.
- The geotechnical constructability based on the requirements by Huis in 't Veld [25].

The last section of this chapter contains the final decision. The decision is fully based on the results from the multi-criteria study. For the second research question, the probabilistic design conditions, and the cross-section design are described in chapter 5 and 6.
Multiple design steps are made to assess the safety of the designed cross-section; these design steps are based on the Hydraulic Engineering Method explained in Appendix B. Two types of dam solutions are proposed the earthen dam and the caisson dam. First, an overview is made of the failure mechanisms that can occur. The ultimate limit state (loss of function) per failure mode is determined for each failure mechanism. A fault tree is constructed to get insight into the correlation between the different failure modes. The serviceability limit state (hindrance) is depicted in the next section. The most stringent of the two determines the design conditions of the dam. Next, a probabilistic method is described that will help to assess the dam, and the minimum amount of runs based on the coefficient of variation is determined.

The next chapter, 6, consists of the design of the cross-section. Multiple failure mechanisms are fully probabilistically assessed. This means that for each input parameter, distribution should be fitted. For the most critical parameters, wave height period and direction, a multivariate distribution is used. This type of distribution is used to take the correlation between the wave properties (direction, height, and period) into account. For each location of interest, two designs are made and probabilistically assessed. Based on the designs, a conclusion is made on which type of dam is most feasible. From the most feasible concept the needed building material are discussed. The main production stages are explained and an estimation is made based on the total duration, chapter 7.

The last research question consists of the final gap closure, chapter 8. Generally, four methods can be distinguished: horizontal, vertical, combined, and sudden closure. The closure is verified using the Navier-stokes equation that calculates the flow velocities through the gap. The maximum occurring flow velocities determine the feasibility of closure. A numerical model is made using several simplifications, these simplification are described in detail.

With this information an answer to the main research question can be provided.

1.6. Readers Guide

An overview of the different chapters is shown below using a flowchart.

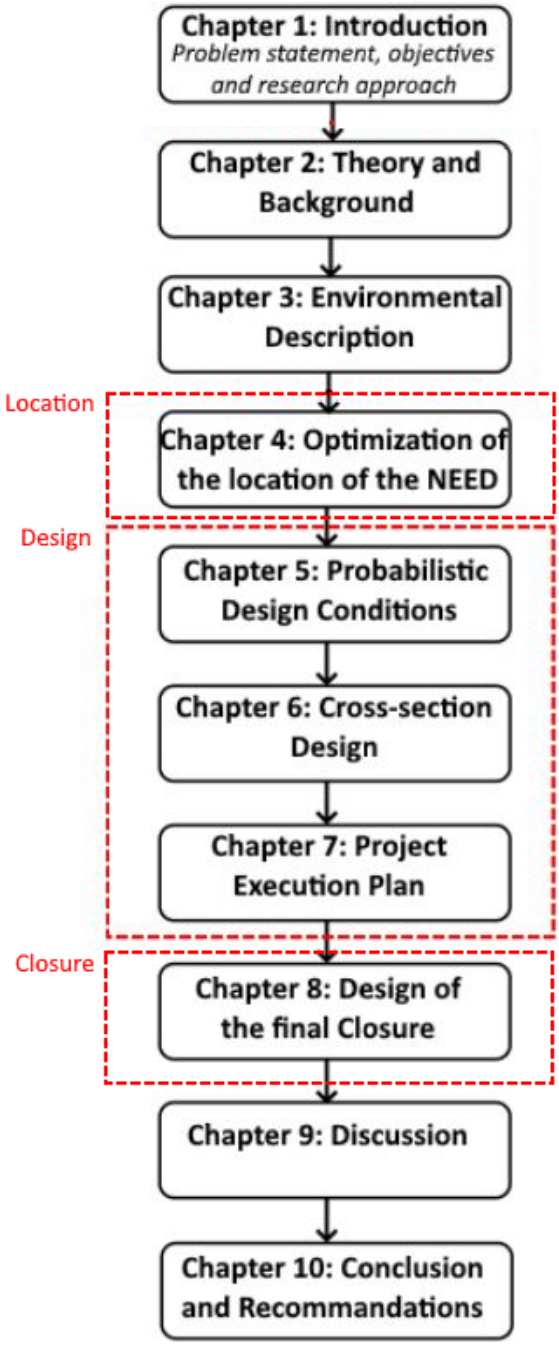

Figure 1.3: Readers Guide

2

Theory and Background

2.1. Flood Protection West Europe and safety in the Netherlands

This section explained the different flood defenses applied to protect west-European coasts. The safety norms discussed in this section are applied in the Netherlands to give insight into the allowable probabilities for flood defenses. Low-lying parts of western Europe are protected by a series of flood gates, dikes, dunes, and barriers. Examples of West-European flood defense structures are the Thames barrier, the sigma plan to protect the harbor of Antwerp against flooding, and the Delta works in the Netherlands. Most of these structures can be found in the Netherlands because 59% of the Netherlands is prone to frequent flooding if not protected. Flood defenses are essential to protect the low-lying area. In Figure 2.1, the areas vulnerable to a 1:100 year storm are indicated with a red dot if there was no flood defence system.

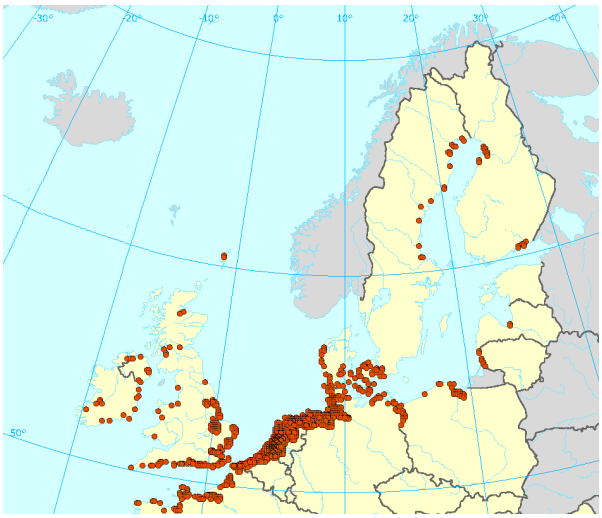

Figure 2.1: Coastal flood damage potential West-Europe 1:100 year storm.[2]

Most of these areas are protected by a flood defense to minimize the risk of a flood. There are different types of flood defenses that protect west Europe such as a dike, dam, storm surge barrier, dunes and a flood wall. These are further explained below.

- A dike is a water-retaining structure that can retain the water under extreme conditions. A dike lies between water and land and is mostly made from soil.
- A dam separates two bodies of water and is not always constructed from sand/stone. In mostly deep water conditions, a caisson (a watertight retaining structure made of concrete and steel) is used. An example of a dam is the Afsluitdijk and the Delta Works.

- A storm surge barrier prevents high water levels from moving upstream rivers or estuaries. A moveable barrier temporarily closes the waterway if the water level exceeds a certain threshold. During normal conditions, the barrier is open. The Thames barrier and Maeslantkering are well-known examples of storm surge barriers.
- Dunes are natural protection that are formed along the coasts. Dunes protect due to their enormous volume preventing water from eroding through. Dunes can be found along the entire Dutch and Danish coasts and some parts of the UK, France, and Belgium. And are therefore the most important protection against floods.
- A flood wall is a concrete wall that retains the water. Flood walls are mostly concrete or steel and need a solid foundation. These are mostly built near cities where space is limited.

2.2. Safety Standards

In the past, the height of the flood defenses were based on the highest recorded water level. This method was applied to every flood protection system. But after the flood in Zeeland in 1953, a new approach was developed. The delta committee proposed different safety levels depending importance of an area inside a dike ring—the flood defense was designed to withstand a hydraulic load with a probability of exceedance. For the primary flood defenses, this value was 1:10,000 per year.
In 2017 new safety standard program was introduced, which focuses more on the consequences of a failure. This approach is more risk based approach. Risk is defined as the probability of a failure times the consequences resulting from that failure. Flood defenses were designed for a given allowable probability of failure. Also, not the entire dike ring has the same acceptable probability of failure. Dike systems were subdivided into smaller sections of 10-15 km 'trajectories'.
The consequences of a flood and thereby the safety standard of the dike sections and other flood protection structures is determined based on the most stringent of the three criteria: Individual risk, societal risk, economic risk. The individual risk is the probability of an individual being killed by a flood. The risk is based on the location, whether it is near the risk source, and the effects of being evacuated [28]. The societal risk is the probability of an accident with multiple fatalities. An FN curve is often used to visualize the likelihood of a fatality compared to the number of deaths. The economic risk is based on the monetary value of a specific area; it balances the cost of investment of risk reducing measure and the cost of the risk itself (probability X consequence). The design conditions of flood protection are based on these safety standards; the safety standards can differ significantly between different dike sections, as shown in Figure 2.2.The design calculations performed in later chapters are based on the lasted knowledge in flood protection in the Netherlands, therefore this risk based approach is used. As a side note, the flood protection standards are much lower for the other countries bordering the North Sea. The value is approximately around 1:1000 per year [47].

Figure 2.2: Maximum allowable failure probability for a flood defence according to the new safety standards [55].

2.3. Sea level rise predictions

In August of 2021, the report of the IPCC [3], the international panel on the climate of the United Nations, was published. More than a hundred scientists contributed to this report from 66 different countries. The main conclusion of this report was that climate change is a real threat to existing life and that the rate of change of the climate has never been observed for the past thousands of years. The report concluded that the leading cause of climate change is the emissions of greenhouse gases in the atmosphere by human activity. The effects of climate change are already noticeable everywhere, extreme droughts, increased storm intensity, sea level rise, etc. When the carbon dioxide emissions continue in the coming decades, extreme weather events will become increasingly frequent.
The first part of the report indicates that each of the last four decades has been successively warmer than any decade previously (measurements from 1850). The average surface temperature between 2011-2020 was 1.09 degrees warmer compared to 1850-1900. This temperature increase leads to a rise in the global mean sea level by 0.2 m between 1901 and 2018. The rate at which the sea level rises increases from 1.3 mm per year between 1901 and 1971 to 1.9 mm per year in 1971 and 2006 and 3.7 mm per year from 2006 to 2018 [3]. The IPCC stated that human influence was very likely the primary driver of these increases, 'Humans influence has warmed the climate at an unprecedented rate in at least the last 2000 years'.
In the next part the IPCC considered six possible emission scenarios; for all the scenarios, the temperature keeps rising until around 2050. The worst-case scenario estimates a temperature increase between 2081 and 2100 of 4.4 degrees. The increase in global temperature direct result in increases in hot weather and heat waves, heavy precipitation, droughts, more intense tropical storm, and a reduction of the arctic sea ice, snow cover, and permafrost [3]. These effects increase with an additional increment of global warming. Many direct impacts of global warming have been irreversible for centuries, especially global sea level. The IPCC rapport simulated the global sea-level rise for the different scenarios. In 2100, the sea level rise for all six scenarios lay between 0.5 and 1-meter increases relative to 1900. In 2300, the sea level rise increases by a few meters. Even the 15-meter sea level rise is within the uncertainty range for one scenario. This scenario is very unlikely and makes some assumptions about the ice sheet instability. The report concluded that it is virtually certain that the regional mean sea level rise continues through the 21st century; this contributes to an increase in severity and frequency of coastal flooding and erosions amplifying the flood events.

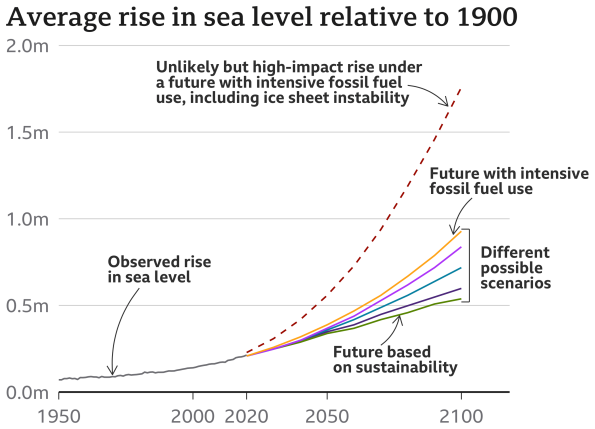

Figure 2.3: Global average sea level rise prediction to 1900 [3].

The KNMI report, 'Klimaatsignaal'21: hoe staat het ervoor met het klimaat in Nederland?', examines the consequences of climate change for the Netherlands. The KNMI report is based on the IPCC report. The KNMI concluded that the sea-level rise resulting from climate change would continue for the coming centuries. The KNMI conducted extra research because, the sea level – and therefore the increase in sea level – can differ in different regions. For example, the sea-level rise along the Dutch coast depends on various factors such as the expending of the water, change of salinity, reduction of mass on the poles, and local change of gravity. The KNMI expects that these effects will result in less sea level rise in the Netherlands than global values. An important aspect for sea level rise effects in

the Netherlands is subsidence; in the scenarios from the KNMI, subsidence level of 0.5 mm per year is used.
Since 1901, the total sea-level rise for the Dutch coast is approximately equal to global sea-level rise, namely about 22 cm. This includes the effect of subsidence.
The six scenario's as discussed before are all adapted to simulate the sea level rise of the Dutch coast. Between the current period and 2150, the KNMI does not distinguish between global sea-level rise and sea-level rise off the Dutch coast. This is partly due to the uncertainty of the mass loss of the Antarctic Ice Sheet. Figure 2.3 shows that the sea level rise continues to rise for all scenarios, even if the Paris agreements is fulfilled. The reasons for this are the slow response of the (deep) oceans to the warming and the loss of the ice caps. These processes have a long response time; a deployed change cannot simply be stopped.
If all processes are taken into account, including processes that we are not yet able to properly quantify (uncertain ice sheet processes), the sea level rise can hit a value up to 16 meters in 2300. It is expected that in 10,000 years, the sea level is in balance with the climate, and 6-7 meters will have risen as global warming peaks at 2°C; 10-24 meters at the peak of 3°C; and 28-37 meters at the peak of 5°C.

Long-term predictions are very uncertain; the measurements governments take to combat climate change will result in lower sea levels. To achieve this, far-reaching efforts are needed worldwide to reduce greenhouse gas emissions rapidly. Due to the uncertainty, the average of the three scenarios as shown in Figure 2.4 is chosen. This corresponds to a sea-level rise of 10 meters.

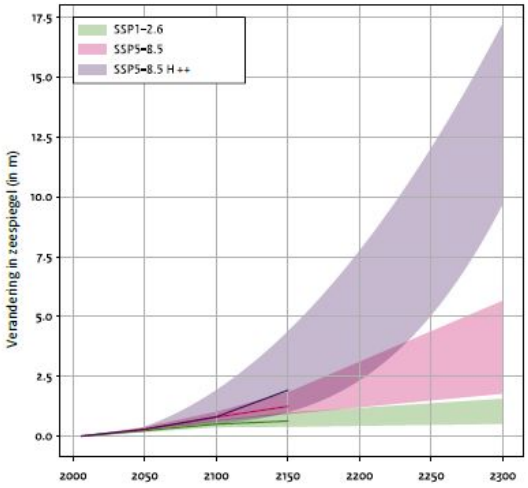

Figure 2.4: Sea level rise prediction off the dutch coast for three scenarios [16]. The SSP5-8.5 H++ considers the extreme ice loss of the Antarctic Ice Sheet; this scenario is extremely unlikely.

2.4. Conducted research into the NEED

Several studies on the effects and impact of the NEED have been conducted. The data obtained from these studies are used in this thesis. In this section, the initial paper of Groeskamp and Kjellson, the MDP, BSc thesis from Buder and the thesis from Nota are discussed, and the results of the three studies are summarized.

2.4.1. Initial idea by Groeskamp and Kjelsson

The Northern European enclosure dam is an idea of Groeskamp and Kjelsson [22] to protect the low-lying countries in west Europe against extreme sea-level rise. The proposed dam stretches from Bergen in Norway to northern Scotland and from Ploudalmézeau France to the Lizard Heritage Coast England. They globally assessed the effect on the maritime industry, the pumping capacity needed to pump out all the river discharge, and the financial feasibility.
The dam would impact the maritime industry; Groeskamp [22] proposed two solutions for this problem, to relocate major ports outside the basin at the ocean side. Or incorporate sluices to allow for ongoing ship traffic. Both solutions will affect the maritime industry. But without measures, the sea level rise will also impact ports to upgrade or relocate continuously.
The discharge of the rivers would lead to a sea-level rise of 0.9 m per year if not pumped out. Massive pumps must be installed to keep the water level equal to the initial state. To put the pumps needed for the NEED in perspective; when the same pumps would be used for the Afsluitdijk, less than 100 pumps are needed. The river discharge into the basin also leads to a drop in salinity in the basin. It is expected that the saltiness will be reduced by a factor of ten in about 100 years, impacting marine life, the ecosystem, and the fishing industry.
Groeskamp expects the NEED to cost 250-550 billion [22] euros spread over twenty years. He concluded that the costs are achievable and pose almost no financial limitation. Compared to dike reinforcement, the dam can become the cheaper solution.
More in-depth research was done on the impact on ocean dynamics and the environment. The ocean model NEMO was used to quantify the ocean circulations. Three simulations were performed using 15 tidal components. The models show the effect on the tide with and without the NEED. The tidal Kelvin wave propagates under current circumstances anticlockwise around the North Sea. After construction, the tidal wave is completely blocked, leading to very small tidal amplitudes inside the basin. The motion inside the basin is set up that is wind-driven, baroclinic circulation from water discharge and small tidal fluctuations. The new alignments create a slight increase in water level of 0.7 meters along the south-west coast and 0.4 for the northwest England coast. The NEED will also significantly impact outside the basin; changes in atmospheric circulation and rain patterns could occur.

2.4.2. Multidisciplinary Project

The report made by a group of students from the TU Delft (MDP) contains a research on the water levels, salinity temperature, and sediment transports changes in space and time within the North Sea basin [33]. The aspects concerning the technical feasibility of the NEED are discussed in more detail in this section. The water balance in the North Sea basin considers five fluxes: river inflow, precipitation, Baltic sea, evaporation, and pumps. These fluxes describe the water balance and are used to calculate the required monthly pumping rate. In the report, they took into account the effects of climate change. Due to climate change, the precipitation rate, evaporation, and river discharge will rise. These fluxes also have a seasonality; for example, the evaporation rate in the summer is higher due to the higher temperatures. Based on these two scenarios, the pumps have to pump 29200 m^3/s, based on a 5-11 meter sea-level rise, which uses 1.4 GW. The report chooses a constant pumping rate; therefore, the pumps are not over-dimensioned. The average water variability stays within the 16.2 cm range. To put the needed pumping capacity for the NEED in perspective, two pumping stations with six pumps each are used to keep the water level in a certain range. The total pump capacity is therefore 235 m^3/s. The NEED needs 125 times the total pumping of the Afsluitdijk [39].

The following research topic of the MDP was hydrodynamics. Because of the reduced fetch, the NEED could reduce the wave height in the North Sea basin. Even in fully developed wave conditions, the wave height can be limited due to the influence of the bottom. The MDP compared the wave heights

in the NEED to those in a fully developed sea state. It concluded that, on average, the wave climate would not significantly change.

The moon and sun will generate a small tide in the North Sea basin. Due to the limited water mass, the tide will be much smaller than in the original situation. By comparing the tide of comparable (semi)-closed basins Caspian, Black, and Baltic Seas, the tide in the North Sea basin are expected to be in the order of 20 cm. The northward Barotropic, eastward wind-driven, and tidal flow will dominate the circulation in the basin. The discharge-driven currents are an order smaller and can therefore be neglected. The average circulation is in the anti-clockwise direction of 0.035 m/s the velocity can fluctuate due to the variety in atmospheric forcing. The reduced current velocities result in more settlement of finer particles in the seabed and more transparent water.
The next topic was salinity. The saltwater influx is blocked by the dam, reducing the saltiness of the basin over time. Calculating the salinity is very complex, making the first-order approximation impossible. The report looked at the Baltic Sea as a reference case to overcome this. The resulting reduction in salinity over 50 years is from 35 PSU (particle salinity unit) to 3.5.
At last, the temperature change was analyzed, the redistribution of temperature will lead to an average reduction of 0.3 degrees centigrade. The seasonal change will increase compared to the initial state. The surface temperature will increase during the summers and decrease during winter.
The main conclusion of the MDP report was that the NEED has substantial consequences within the basin. If the NEED outbalances the negative impacts of climate change are still open for debate.

2.4.3. Bachelor Thesis Buder

The report made by Buder investigates the effect of the NEED on the North and Baltic sea. Unlike the MDP, Buder uses a model to predict the changes in salinity and temperature [6]. Buder's model is based on the Flexible Ocean and Climate Infrastructure developed by GEOMAR. The model simulated 60 years change in hydrodynamics inside and outside the basin. It predicts a decline in salinity in the North Sea from 34 PSU to 20 after 60 years. Using a formula fit on the generated data, Bruder expects the salinity to drop to 13.6 PSU in the coming 100 years. On average, the temperature will decrease by 1 degree compared to the initial situation. Both results strongly deviate from the results obtained by the MDP group. Further analysis is required to determine the accuracy of the predictions. Due to an error in the model, the data obtained at the Baltic Sea and the Atlantic ocean are unreliable.

2.4.4. Master Thesis Nota

Nota investigated the applicability and economic benefit of the NEED compared to raising the current flood protection systems. Based on the current flood protection systems, an inundation map is developed that combines information on several projections of the tidal change, land elevation, and sea-level rise. Nota concluded that for the most extreme projection (SSP5 with RCP8.5 2080 see report Nota), a total of 15 000 km^2 would be inundated. This affects 9.5 million people that fall in the protection range of the NEED—the total economic damage amount to 1 trillion euros. It is evident that adapting the current flood defenses or building the NEED is crucial to protect west-Europe from the rising sea. Nota compared the two adaptation strategies: Regional flood protection systems and the NEED to conclude the financially favorable strategy.
Based on the inundation maps, roughly 6 000 km of coast needs to be protected by 2080 if the NEED is not constructed. The total costs range between 245 and 335 billion euros for a 1-meter sea-level rise and increase by 170 to 235 billion euros for every extra meter.
Nota designed an earth-fill (the NEED) dam with a slope of 1:6 in detail. And also made some prediction with smaller slopes. The most critical components of the dam consist of a sand core, revetment, geotextile, pumps, and sluices. It is projected that the dam will cost 1.1 trillion euros for the scenarios SSP5 and RPC8.5. Adapting the regional flood protection system for SLR between 1 to 5 m is financially favorable. The two strategies intersect, ranging between 5.1 and 7.85 meters with an estimated cost of 1.12 and 1.17 trillion euros.

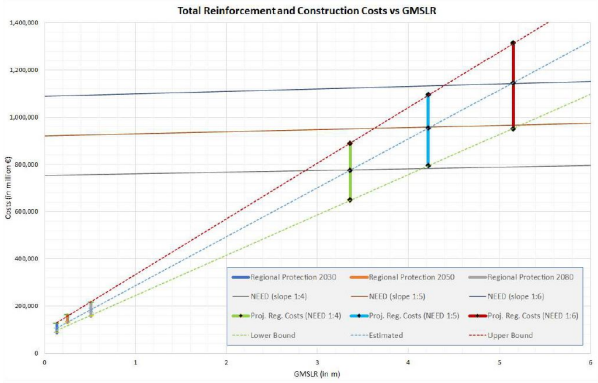

Figure 2.5: Comparison between regional reinforcement of flood protection and building the NEED (earthen dam) construction costs as a function of GMSLR. For three different slopes [37].

2.5. Closure Dams around the world

Several closure dams have been built all over the world. Land reclamation and flood protections are the main incentives for construction. In this section, the two largest dams, the Afsluitdijk and the Saemangeum Seawall are shortly discussed to gain insight into current dams' construction phases and dimensions. In Appendix C more information about the construction and background of the Afsluitdijk is provided.

2.5.1. Afsluitdijk

The plan of a large-scale dam (the NEED) is not new to the Netherlands. With its 32.5 kilometers, it is the longest dam in Europe. In late 1800, plans were already made for the dam's construction by ir. Lely, but the devastating flood of 1916 accelerated the process. The construction started in 1927, and the final gap was closed in 1932. A year later, it was finally opened for road traffic. Similar to the NEED, the main reason for the dam was that strengthening the existing dikes was too complicated and expensive. The development of the Afsluitdijk resulted in a great deal of knowledge in the field of hydraulic engineering, the knowledge that is still crucial to the fight against water. Several physical tests were performed in the waterloopkundig laboratory to investigate the strength and performance of the closure and the sluices. Lorenz developed new numerical models to determine the effects of the dam in the surrounding [48].
The Afsluitdijk separates the Waddenzee from the IJsselmeer through a dam creating a non-tidal lake not influenced by storm surges. The dike crest was originally designed based on the highest storm surges level determined by the Lorenz committee combined with the maximum wave run-up. The crest height differs slightly along the length of the dam near the coast of North Holland is the highest point. The cross-section material consists primarily of sand; only at the exterior boulder clay was used to protect the dam from erosion. A road connection ensures that Friesland was accessible via North-Holland.

Currently the Afsluitdijk is being renovated to withstand extreme weather conditions and sea-level rise again until at least 2050. Higher waves and water levels results in larger crest levels and heavier protection. Nature plays an essential role in the renovation plans of the Afsluitdijk. An example of this is the fish migration river. The fish migration river creates a connection between the Afsluitdijk and the Wadden Sea. It is expected that millions of fish will use this passage in the future.
New types of protection have been designed to give it an authentic appearance, the so-called Xblocplus and Quatroblocks. The renovation will be completed in 2025.

2.5.2. Saemangeum Seawall

Another similar project is the Saemangeum Seawall, which is 33 km long and thereby the longest dam in the world. The dam enclosed the entire estuary of the Mangyeong and Dongjin rivers and is located on the coast of the Yellow sea in South Korea. The reason for building the dam is to create new land and a freshwater lake. The dam was constructed in two parts, the northern and southern parts, and in between a small island is located. The average height of the dam is 36 meters due to the significant tidal differences [32].

There was a lot of controversy around the construction of the dam. A conservation organization said the government failed to see the project's impact on local wildlife transparently and conducted an observation-only program in 2006. Seabird fish depend on the tidal mudflat that surrounds the Saemangeum bay. Wildlife organizations estimated that the dam's construction would result in the decline of the species. After a long struggle between the government and environmental activists and several court decisions, the dam was closed in April 2006. It was decided that the newly reclaimed land should be managed sustainably and contribute to the prosperity of the local residents [32].

3

Environmental Description

This chapter presents an overview of the project area. It offers input to develop different variants of the dam that will be assessed using a multicriteria anlysis in Chapter 4. The data is also used for the closure procedure, and the cross-section development. Aspects discussed are: location bathymetry, river discharge, impact sea level rise, wave climate, and the astronomical tide.

3.1. Project Area

The North Sea is a shelf sea located in western Europe. It is connected to the Atlantic ocean in the north and to the Baltic sea in the east. In the south, it is connected by the English Channel and the Strait of Dover to the Atlantic ocean. The North sea is bordered by seven countries, namely, the United Kingdom, France, Belgium, the Netherlands, Denmark, and Norway. The total surface area is 575 300 km^2 making it one of the largest shelf seas in the world. The maximum length of the North Sea is 660 km and the width is 580 km.

3.2. Bathymetry North Sea

Information about the bathymetry is retrieved from GEBCO general bathymetry chart. GEBCO provided elevation data on a 15 arc seconds interval grid, which is approximately 500 meters and the depth is measured from the chart datum. The North Sea sits on a broad continental shelf, a feature of a trailing edge coast, and has a sudden drop indepth, the continental break. The shallow sea has a significant effect on hydrodynamics. These water areas result in larger effect on storm surges. During a storm, the water level near the coast can rise to 8 meters [28] and is the leading cause of dike failure.
On the other hand, wind waves are generally lower, due to depth induced breaking.
The shallow North Sea can be split into two sections, depth ranging from 20 to 40 meters below sea level and between 50 to 100 meters. In the middle of the North Sea, a shallow area is present, the Dogger Bank. The Dogger Bank is the largest sandbank in the North Sea. It is on average just 13 meter deep. The deepest part of the North Sea is located just of the Norwegian coast, a trench with the deepest depth of 700 meters. Erosion caused by the glacial retreat formed the trench. The trench width and depth vary along its length; in the south of Norway, the trench is the deepest. Near the Norwegian city of Stavanger, the depth of the trench is considerably reduced to less than 200 meters. This part of the trench will be the best location for the dam to cross it.
In Figures 3.1a the bathymetry of the North Sea is plotted, the range is set from 0 to 400 meters; this makes the parts of the North Sea deeper than 400 meters green. The relatively shallow stretch of the trench can easily be distinguished in the figure. As is the different depth variation in the sea itself. In Figure 3.1b, the range is set from 100 meters and 500 meters, the white area is the continental shelf and the boundary between the green and white area is the continental break.

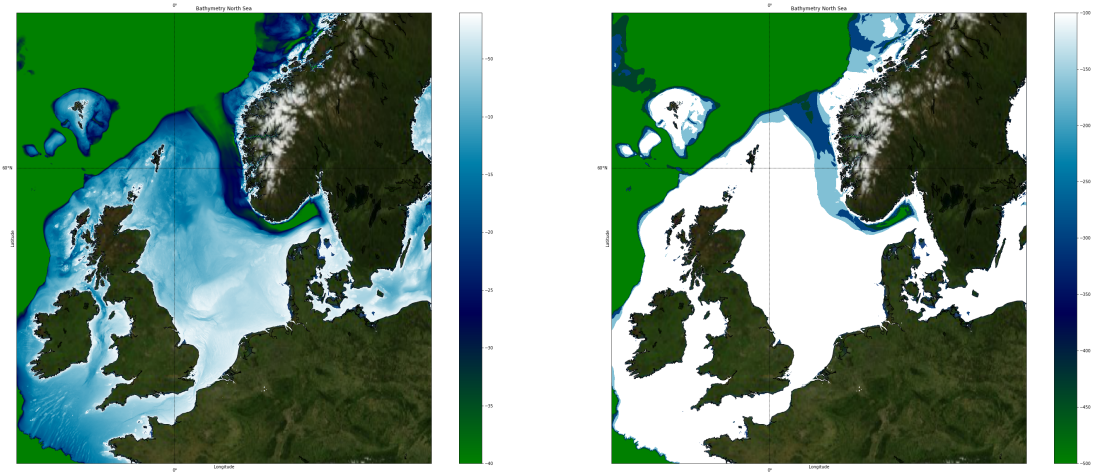

(a) Bathymetry North Sea color bar ranging from 0 to -400 m **(b)** Bathymetry North Sea color bar ranging from -100 to -500 m

Figure 3.1: The Bathymetry of the North Sea, data retrieved from GEBCO

3.3. Sea bed material North Sea

The North Sea bed consists primarily of fine sediment due to the particle abrasion and weathering during transport downstream by the river systems flowing into the North Sea. These sediments are also called continental sediments, as they come from Europe. The sediment has accumulated in the North Sea for the most significant part during the Holocene and Pleistocene era, creating a shallow basin in the North sea.

The relative frequency of different sediments is strongly correlated by climatic factors, i.e., latitudinal zonality. Hayes found a relation between the latitude and the sediment types for up to 60 meters depth as explained in the book by Bosboom [5]. Based on his analysis, a rough estimation of the sediment distribution can be determined. The future dam is located between 50 and 60 degrees latitude, resulting in the type and share of sediment: 50 % sand, 15 % mud, 35 % rock and gravel, and 5 % shell, based on the analysis of Hayes. A map of the seabed substrate in the North Sea from Marine regions, Figure 3.2, shows that the Hayes relationship is a little bit off for the North sea. The seabed of the North Sea consists mostly of sand, with a small parts consisting of mud. The data is collected and harmonized using different surveys within the EMODnet-Geology project (European Marine Observation and Data Network). The map is multiscale, meaning that some parts of the map have higher accuracy. The part of interest, the North Sea, has, for the biggest part, a scale of 1:250 000. Near the North Sea cost, the scale is 1:25 000 and a small section in the middle 1:1 000 000. The substrate is defined using the modified Folk triangle. The Folk triangle is a standard sediment classification and is widely used among geologists. The seven indicates the different seabed material distinguish.

Sand is the most abundant material the two other common bottom materials in the North sea are mud to muddy and coarse substrate. The substrate is distributed as follows: the northern part of the North Sea consists of mud the shallow area is more dominated by erosion, and in deep or sheltered water, fine particles can accumulate. Sand is evenly distributed, with large stretches just off the Dutch coast and the middle of the North Sea; the coarse substrate is mainly located along the British coast. The flow velocities near the British coast are relatively high; as a result, tiny particles cannot accumulate. In the English channel, the substrate consists mainly of the coarse substrate, with some small patches of boulders and rocks near the French coast.

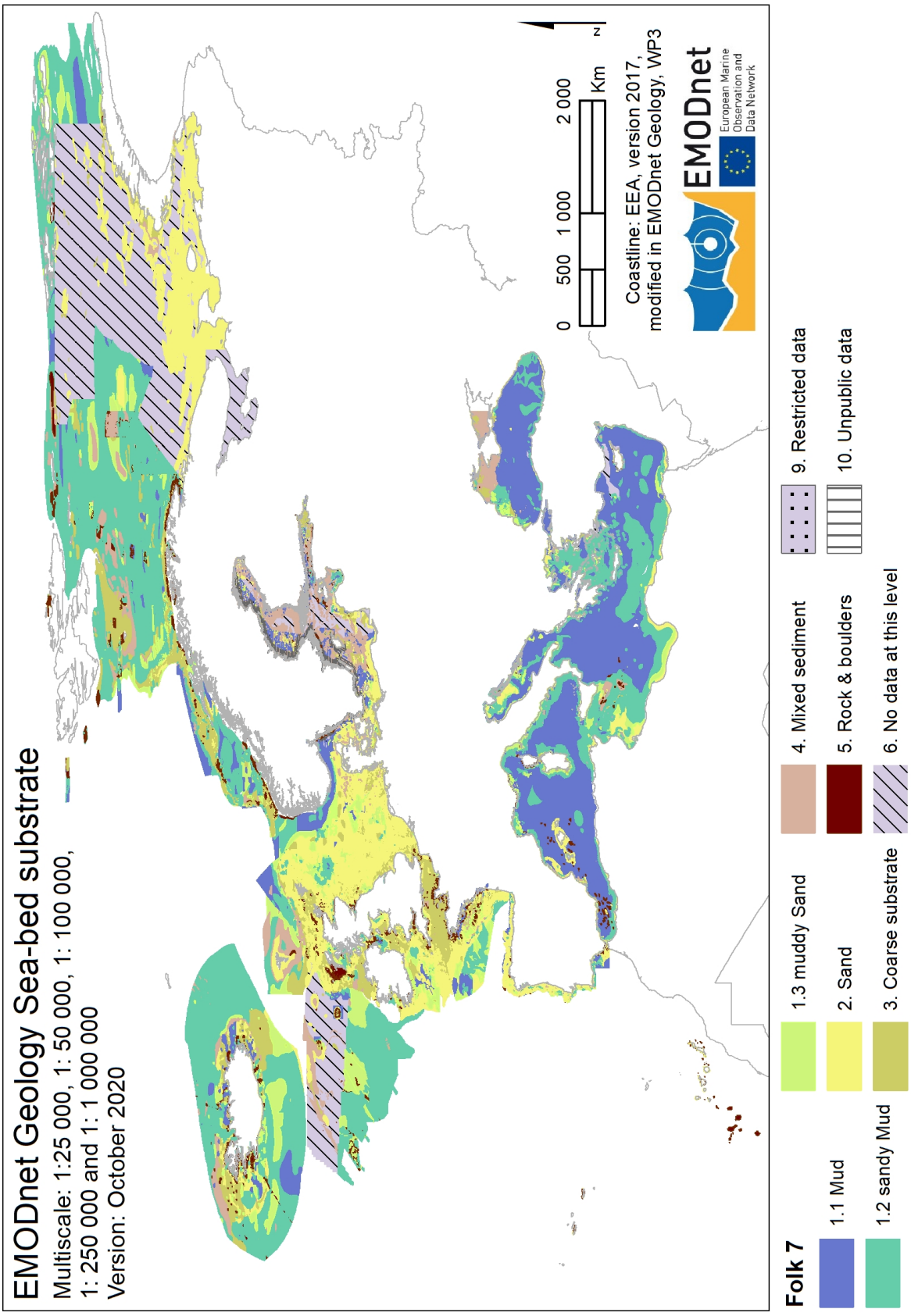

Figure 3.2: Multiscale seabed substrate in the North Sea [30].

3.4. Hydrodynamic parameters North Sea

The most critical hydrodynamic parameters are river discharge, the wave climate, the tide, and the wind setup. River discharge is taken into account when determining the final closure. The wave climate determines for a significant part the dimensions of the dam. The tide determines both the closure type and the size of the dam. Wind setup only occurs in the basin, where water can pile up. The water depth becomes too deep on the ocean side, minimizing the water built up. Wind setup is covered in more detail in chapter 6

3.4.1. Tide

The tide is characterized by two variables; its magnitude (the tidal range and vertical distance) and the tidal character. According to the report by Hutnance [26], the semi-diurnal lunar components (M2 Principal lunar semidiurnal and S2 the Principal solar semidiurnal) are the major contributor to the North Sea's tidal currents and water level. The tide is generated at the pacific ocean, and the wave travels to Europe. The difference between the celestial event and its appearance at the North Sea is about two days. For the English channel, it is just over one day.
The propagation of the tide is influenced by friction and the Coriolis force. Due to the Coriolis force and the landmass surrounding the ocean, the tide propagates in the counterclockwise direction in the North Sea. The point where the tidal amplitude is zero is called an amphidromic point. The further away from an amphidromic point, the higher the amplitude of the tide becomes. The tidal range lies between 2 and 4 meters in the North Sea.

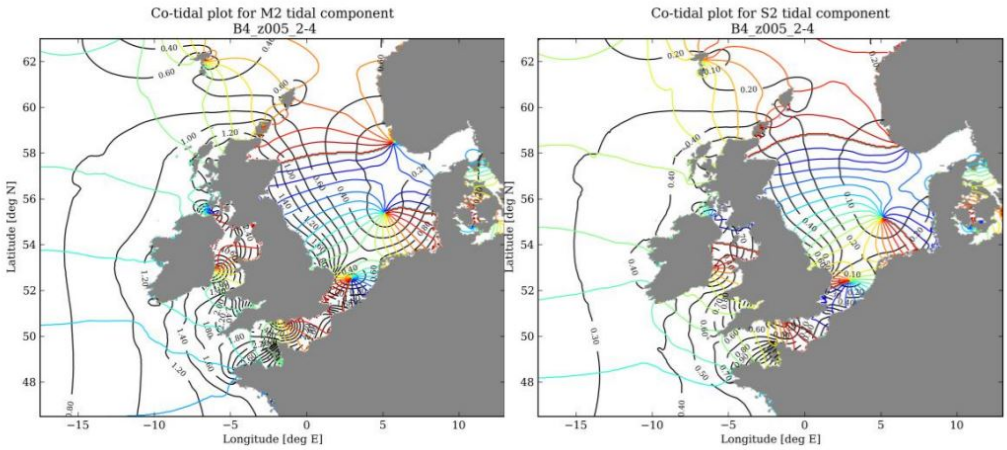

Figure 3.3: Co-tidal plots for the major harmonic constituents, M_2 (left) and S_2 (right). The labelled black lines give the tidal elevation and the coloured lines the phase.

In Figure 3.3, the propagation of the tide in the North Sea is presented [5]. The black lines are the co-tidal lines representing the simultaneous high water, and the coloured lines are the co-range lines representing the equal tidal range. There are three amphidromic points located in the North Sea: just off the Norwegian coast, the middle of the North Sea, and between the Netherlands and England. The largest tidal amplitudes occur along the English and French coast. In the English channel the maximum m2 tide is 5 meters. The most dominant tidal constituents in the North Sea are presented in Table 3.1. The tidal propagation through the English Channel and Skagerrak may slightly influence the tide in the North Sea, but this effect is minimal and is neglected.

Constituent	Period [sec]	Amplitude [m]
M2	44700	1.51
S2	43200	0.54
K1	86220	0.08
O1	92940	0.08

Table 3.1: Typical tidal constituents in the North Sea near the Edinburgh.

The principles lunar constituents are the most dominant tidal component and result in the highest amplitude. When the M2 and S2 components are in phase, it is spring tide. The character of the tide can describe by dividing the diurnal components (K1 O1, the Lunar diurnal consituents) by the semi-diurnal components, see Formula 3.1.

$$F = \frac{K1 + O1}{M2 + S2} \tag{3.1}$$

This results in a value of F of 0.0733, which corresponds to a semi-diurnal tidal character.
A harmonic formula is used to combine the different tidal constituents. The harmonic formula can reproduce the tidal wave elevation; the formula is presented in equation 3.2.

$$\eta(t) = a_0 + \sum_{n=1}^{N} a_n \cos\left(\omega_n t - \alpha_n\right) \tag{3.2}$$

Where,
η is the tidal elevation compared to the mean water level.
a_0 is the mean water level.
a_n is the amplitude of the tidal
ω_n is the angular velocity.
α_n is the phase angle.
t is the time.
N is the number of harmonic components.

In Figure 3.4, the tidal amplitude at the Scottish coast is calculated and compared to an observation from a nearby measuring station. It is compared to the calculated tidal water level elevation using Equation 3.2. The tide is the dominant effect of the water level elevation near Scotland; the small effect of wind setup is also visible. The graph shows that the maximum tidal range near Scotland is 2.5 meters. The North Sea is dominated by the semidiurnal components meaning that when adding up the two tidal constituents near Edinburgh, Figure 3.3 results in approximately the same value. The tidal elevation outside the dam will slightly change and completely be blocked inside the basin this change is analyzed in further detail in the next chapter.

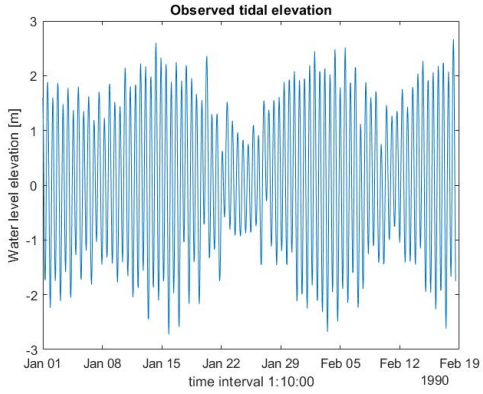

(a) Observed tidal elevation near the city of Edinburgh

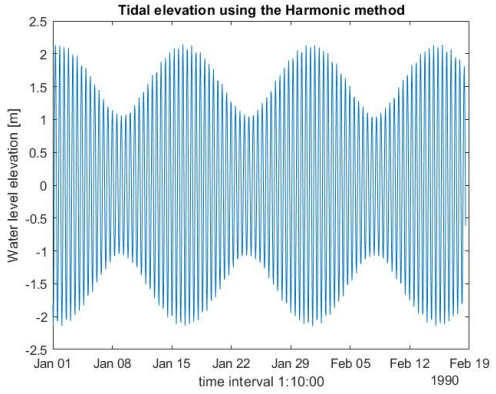

(b) Calculated tidal elevation near the city of Edinburgh

Figure 3.4: Compare the calculated tidal elevation to the observed.

3.4.2. River Discharge

Several large river systems drain into the North and Baltic sea, the future basin. Knowing these discharges is essential for further analysis of the dam concerning the final closure and dimensions of the dam. An overview of the largest rivers concerning discharge is presented in Table 3.2. The discharges are averaged; seasonal effects result in higher discharges in the winter months. The data is retrieved from the Natural Earth data collection supported by the NACIS (North American Cartographic Information Society). By summing all the discharges, including smaller rivers, the total yearly discharge flowing to the North and Baltic Sea equals 824 km^3/y.

River	Discharge [m^3/s]
Rhine	2900
Nova	2500
Vistula	1080
Elbe	870
Glomma	698
Daugava	678
Neman	678
Göta älv	575
Seine	560
Kemijoko	556
Oder	540
Lule älv	506

Table 3.2: River discharge into the North and Baltic Sea.

The water that needs to be pumped out of the future basin will not be equal to the total amount of water coming from the rivers. Aspects such as evaporation, precipitation, the ideal location of the dam, and other water uses will influence the amount of discharge that needs to be pumped out. The MDP report concluded that based on the design by Groeskamp [22] the monthly pumping rate is based on four fluxes, the rivers flux, precipitation flux, evaporation flux, and the monthly influx from the Baltic sea. They assumed a rise in yearly precipitation of 5 to 20 percent, a change in precipitation distribution over the year, and an increased evaporation rate. In the MDP report [33], they assumed a constant pumping rate of the pumps over the year. Combining all these aspects resulted in the pumps having to pump 29200 m3/s, with maximum water level variability in the North Sea of 37.2 cm. This variability should be taken into account for the design of the dam.

Figure 3.5: QGIS map of the largest rivers in Europe discharging in the North Sea.

3.4.3. Wind Waves

Understanding the wave climate is essential for the design of the dam. According to J.L. Davies and Clayton [12], the North Sea exhibits a storm wave climate based on their classification. Meaning that

the waves are highly variable in height, period, and direction. The variability is especially present during winters and summers. Winters storm create high waves and most summers are relatively mild with relative low waves. The shallow water depth inside the North Sea effect the amplitude, therefore limited the maximum height. The following characteristics belong to a storm wave climate:

- Westerlies are the dominated wind condition.
- The waves are a combination of wind waves and swells.
- The wave height in deep water is between 2 to 3 meters 90 % of the time and between 5 to 6 meters 10 %.
- During storms, the wave height is larger.

The height of wind waves strongly depends on the wind direction, speed, fetch, and duration. High waves in the North Sea occur when the wind is coming from the northwest direction, this is also the direction with the most significant wind set up. The result is that the northern part of the enclosure dam will be exposed to the strongest hydraulic forces. To better understand the long-term wave climate, information from wave buoys and poles is retrieved from the European CDI sea data net, and the British Cedas wave net is used. Due to the limited number of wave observation points in the North Sea, models can be used to hindcast the North Sea climate using wave buoys and weather stations as boundary conditions.
A hindcast model retrieved from the Copernicus program (the European Union's earth observation program) [43] will provide additional data and can be used to assess the variability. The hindcast model is generated using WAVEWATCH III with an aspheric cell of 3 by 1.5 km and has a resolution of 3 hours. The model describes gravity waves with a period between 3 and 30 seconds. The coverage is from 1980 to the present, and the temporal resolution is 3-hourly-instantaneous. In Figure 3.6, the 2020-02-12 15:00:00 is plotted. The arrows indicate the wave direction, often equal to the wind direction. The fetch is limited near the British coast; this shelter effect is clearly visible. The same phenomenon can be observed in the English channel

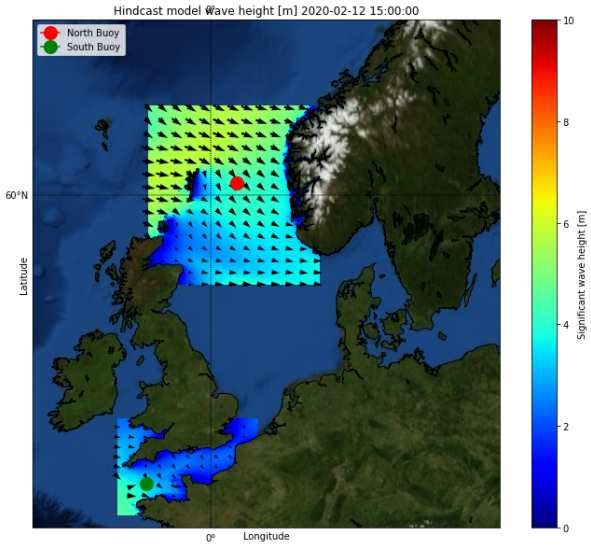

Figure 3.6: Significant wave height and direction 2020-02-12 15:00:00.

Figure 3.7 shows the distribution of the three-hourly significant wave heights over 40 years for both locations. The wave data is plotted using the scatter MATLAB tool. The maximum occurring wave height for the Northern dam is 10.2 m and the southern buoy 10.8 m. The scatter plot indicates the density of the measurements. The locations of the buoys are marked with a red and green dot in Figure 3.6. The red dot is the Northern Buoy, and the green dot is the Southern buoy. The more yellow area means that more points are in that spot. This concludes that the prevailing wave direction in the English channel is westerly and north in the North Sea from a northerly. In Chapter 6, a more detailed analysis is made of the wave data including an extreme value analysis.

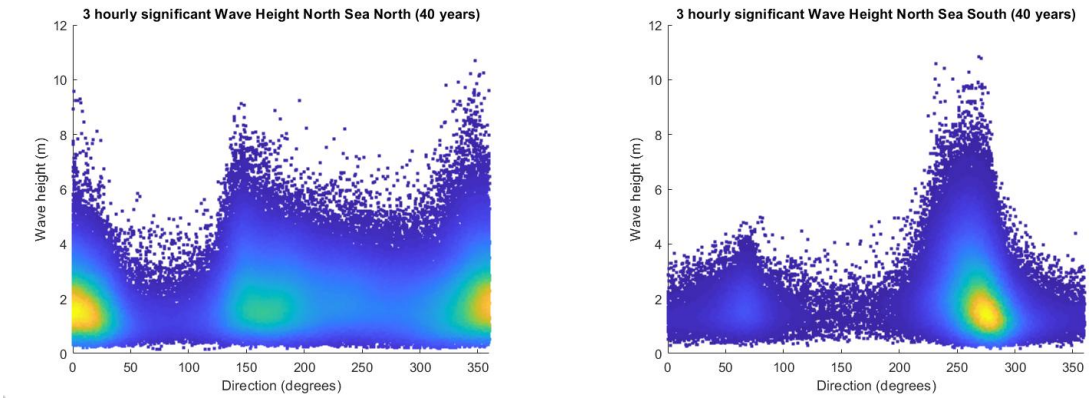

(a) Scatter plot North Sea North

(b) Scatter plot North Sea South

Figure 3.7: Histogram and fitted distribution wave height, based on data from Copernicus [11].

A wave rose provides a clear overview of the wave direction distribution combined with the wave height. The length of each spoke related to the percentage of waves deriving from a specific direction. The color represents the wave height classes, ranging from 0 to 12 meters. The wave rose is presented in Figure 3.8 for both the southern and northern parts of the North Sea. It shows that more than 80 % of the waves arrive from the south for the Southern part of the North Sea. This is due to the shape of the channel and the wind direction. The wave direction in the North of the North Sea arrives from the North and Southeast. Most of the waves are between 0 -4 meters. The wind rose follows the meteorological convention.

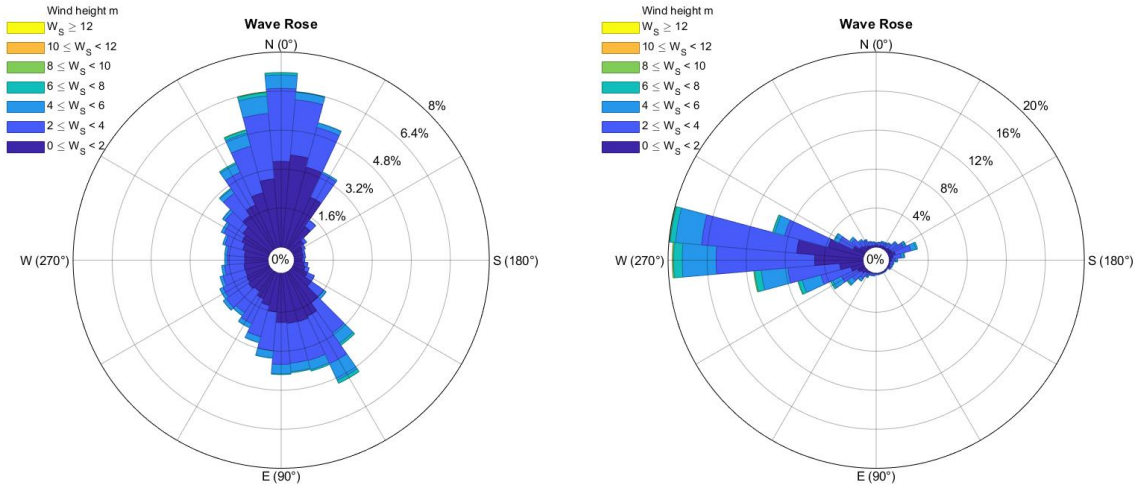

(a) Wave rose North Sea North

(b) Wave rose North Sea South

Figure 3.8: Wave rose of the North Sea and English Channel, location see Figure 3.6. The data used from Copernicus [11] .

3.5. Analysis of the area prone to flooding

The main goal for the NEED is to protect Europe against flooding. An analysis is made to understand better the area affected by sea-level rise. The data that is used is retrieved from the GEBCO Bathymetry Chart. Different water level rises are simulated to estimate the dam's area to protect. Figure 3.9 shows the area that becomes flooded for a water level rise of 10 meters. The 10 meter sea level rise is based on the high end prediction by Deconto [14] and the SSP5 scenario by the IPCC for the year 2300 [3]. The blue areas indicate the land that will be lost to the sea. West European countries will be hit hardest, with the Netherlands losing half its land size.

Other countries that experience server land loss by a sea-level rise of 10 meters are England, Belgium, Germany, and Denmark. Small coastal regions of Sweden and Poland will be hit but insignificant

compared to western Europe. Norway and Scotland will experience almost no loss of land for these sea-level rise predictions. Only a tiny strip of land near the coast will be lost. The total land loss in west/mid-Europe is expected to be 107980 km^2 for a sea-level rise of 10 meters. Using QGIS, the number of people impacted by sea-level rise is correlated to the area lost to the sea. The inhabitants of cities, towns, and villages in the blue area are summed and presented in the same table. Data on the amount of population is retrieved from Openstreetmap.

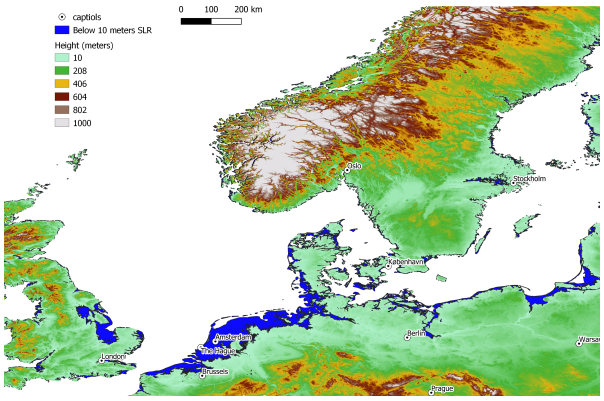

Figure 3.9: QGIS 10 meters Sea-level rise.

In Table 3.3, the area losses and population displacement for the countries that are hardest hit. From the figure, it follows that the most vulnerable areas are protected if the dam is built on the location proposed by Groeskamp and Kjellson. Even optimization is possible, and the southern and northern dam can be replaced to reduce the length of the dam. The protection of the vulnerable area will not be affected after replacement.

Table 3.3: QGIS flooded area and number of displaced people [10]

Country	Area of land loss [km^2]	Number of displaced people millions [-]
Netherlands	$2.4596 * 10^4$	10.9
Belgium	$3.6457 * 10^3$	1.57
United Kingdom	$1.4414 * 10^4$	1.75
Denmark	$9.5675 * 10^3$	1.05
Germany	$2.0429 * 10^4$	3.25

The modulations in Table 3.3 are made compared to NAP, meaning that wind setup and tidal variation are not yet considered. So two more modulations are carried out for 20 and 30 meters to check whether the conclusion is still valid, see Appendix D. Based on these two sea level increases, loss of land in the western part is increased; even parts of central Scandinavia, Poland, the Baltics, and Russia are affected. Nevertheless, Scotland and Norway are not impacted by the sea level rise.

3.6. Design water level

The Northern European Enclosure dam will be designed for a water level of 10 meters at the ocean side and the current water level at the lake side. The water levels are based on the high-end prediction by DeConto [14] and the SSP5 scenario by the IPCC [3] for the year 2300. Groeskamp concluded that the project could become financially viable for sea level rises above 10 meters. The water level inside the basin is kept to the current level disregarding the sea level rise during construction and planning. These numbers are used in further chapters of this thesis.

3.7. Conclusion

The bathymetry of the North Sea ranges between 30 meters near the coasts to more than 200 meters just off the Norwegian coast. The bed consists primarily of mud, sand, and coarse substrate, which can

be used as construction material for the dam. Three important hydrodynamic parameters essential for a good dam design are: the tide, the river discharge, and the wave climate. Several large rivers flow into the North Sea, providing it with fresh water. The amount of discharge is vital for modeling the final closure. The wave and the tide are essential for the height of the dam a hindcast model can be used to include the length effect. Last, the area that is prone to sea-level rise is analyzed.
The current location of the NEED is based on the report by Groeskamp and Kjellson, the main factor that determines that location is the amplification of the tide. An alternative configuration is proposed in the report; the southern part of the NEED is moved northwards and the northern part southwards. By replacing the dam its length is decreased significantly, but it also affects the amplification of the tide. The increase in water level due to the change of location would be within one order of magnitude. The depth of the trench that needs to be bridged is significantly shallower, and the wave climate is calmer compared to the first configuration. The new configuration makes almost no concessions regarding protecting the sea-level rise prone area. In the next chapter, the different locations are compared using a multi-criteria analysis.

4

Optimization of the Location of NEED

In this chapter, the most optimal dam location is determined. The first section describes the four alignments, and a calculation is made for the total amount of volume it takes to build the dams , the constructability is analysed and a difference in protection is investigated. In the next section, the evaluation criteria for the multi-criteria analysis are discussed. The last section contains the final decision, based on the results from the multi-criteria study.

For both the northern and southern dam, one alternative design is proposed, as shown in Figure 4.1. In the following sections, the alignments are tested against the evaluation criteria used in this study (no ecological and political criteria have been applied).. Eventually, the concepts are evaluated using a multi-criteria analysis. These criteria also form the requirements of the dam and are explained in the literature review. The criteria are:

- The total length and maximum depth of the Alignment.
- The difference in the number of people that the dam will protect by the dam.
- The constructability of the dam per alignment, based on the loads (tide and wave).
- The geotechnical stability based on the requirements by Huis in 't Veld [25].

A weight factor is given to each criterion to indicate the importance of the requirements.

4.1. Alignments NEED

For the design of complete closure, a sea-level rise of 10 meters is considered, as explained in the previous chapter. At first glance, the area flooded as result of a sea-level rise of 10 meters is mainly located south of Norway and Scotland. The location of the flood prone area allows an optimization to be possible to decrease the dam size and make the project more feasible.
Based on the bathymetry chart, two different alignments are proposed. The high-end projection of sea-level rise means that a partial closure can be ruled out. The partial closure dampens the tide and will slightly decrease the amount of wind set up, but this will not be enough to protect the flood-prone area. The first alignment is based on the report by Groeskamp and Kjellson. The second alignment is optimized by protecting an area as large as possible and at the same time minimizing the volume of soil used to create the dam. The two alignments are shortly described in section 4.1.1 and 4.1.2.

4.1.1. Alignment Groeskamp and Kjellson

The proposed alignment by Groeskamp and Kjellson is plotted on top of the bathymetry chart by GEBCO, Figure 4.1. The alignments consists of a northern part connecting the northern tip of Scotland to the Orkney Islands and the Orkney Islands to Norway (near Bergen), with a combined distance of 475 km. And a southern part connecting France (near Ploudalmezeau) to England (the Lizard Heritage Coast), stretching 161 km. The total length of the dam alignments by Groeskamp and Kjellson is equal to 636 kilometer. The proposed alignment protects the major West-European cities against sea-level rise and creates a large freshwater lake. The northern dam crosses the deep trench located just of the

coast of Norway. The deepest point reaches a depth of 400 meters below sea level. The first part of the dam, between Scotland and Orkney island, is shallow, where the deepest part is just 100 meters below sea level. In the second part between Orkney and Norway, the depth continues to be 100 meters. Moreover, the last section of approximately 100 km the trench is located. The depth of the southern dam is relatively uniform. The average depth is approximately 100 meters. The total cross-sectional area is calculated using the Riemann approximation.

This results in a total cross-sectional area for both alignments that can be found in Table 4.1.

Section	Length [m]	Area [km^2]	Volume [m^3]
North Optimized	452 000	58.57	35.55E9
North Groeskamp	475 000	62.70	47.51E9
South Optimized	40 000	0.96	0.23E9
South Groeskamp	161 000	13.17	5.23E9

Table 4.1: Dimensions Optimized and Groeskamps alignment.

The amount of volume is an essential aspect for determining the feasibility of the dam. In this section, a simple design is chosen to review the alignment. The volume is based on a design with a slope of 1:3 and 50 meters dam width on top; in a later stage, the design will be improved and adjusted. The areas and volumes are obtained using the Riemann approximation. The sea-level rise of 10 meters and the resulting dam height increase is also taken into account. The amount of volume is presented in Table 4.1.

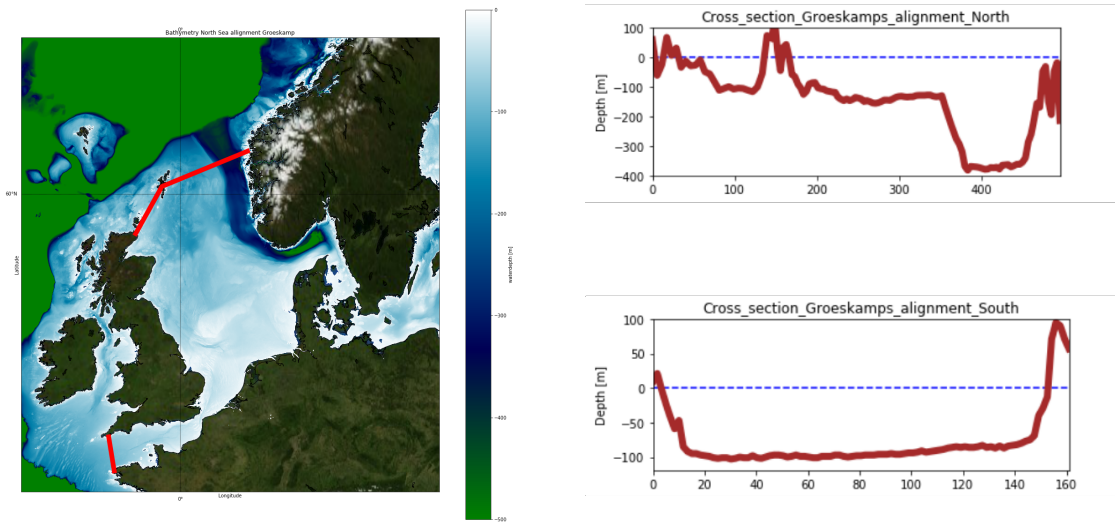

(a) Location Groeskamp's alignment

(b) Cross-section Groeskamp

Figure 4.1: Location Groeskamp's alignment with the cross-sections.

4.1.2. Optimized alignment

Based on the GEBCO bathymetry chart, an optimized design is created based on creating as large a basin as possible, thereby protecting as many cities and at the same time decreasing the amount of volume for building the dam. The northern dam of the optimized alignment is further south than the alignment made by Groeskamp; it connects Scotland (near Aberdeen) to Norway, near the city of Stavanger. The width of the trench it crosses is considerably smaller and less deep than Groeskamp's alignment. The maximum depth of the trench is reduced to 280 meters with a width of approximately 100 km. The southern alignment of the dam crosses the strait of Dover, the narrowest part of the English channel. The dam will be significantly shorter, spanning just 40 km with a maximum depth of 57 meters. It connects the two cities, Calais and Dover. The decrease in-depth results in a smaller

cross-section and less volume of soil to create the dam. In Table 4.1, the total volume of the future dam and cross-section is presented.

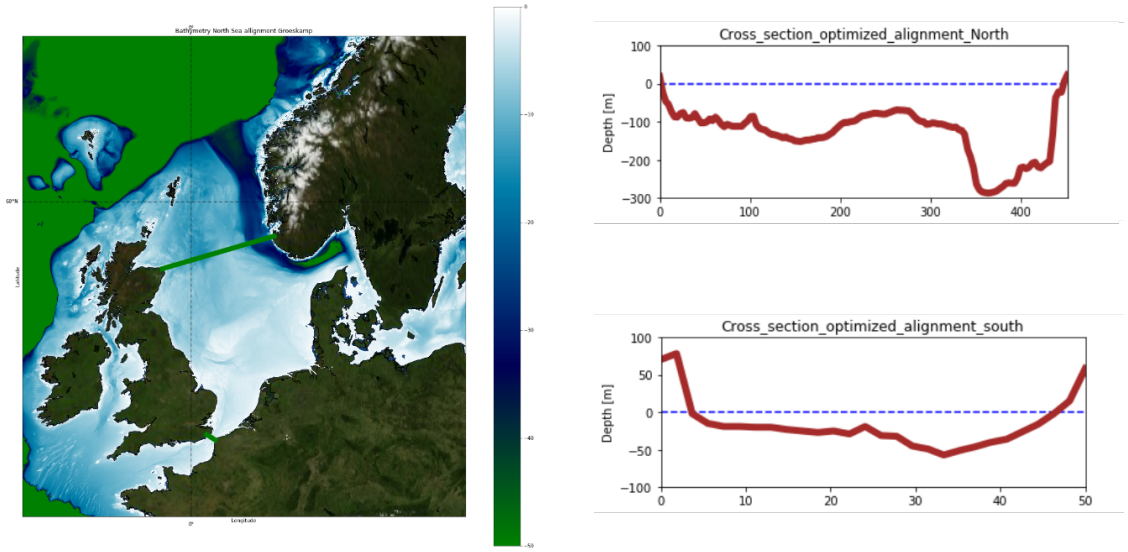

(a) Location Optimized alignment

(b) Cross-section optimized

Figure 4.2: Location Optimized alignment with the cross-sections.

4.2. Difference in protection of both alignments

The optimized alignment tries to minimize the total volume of the dam by relocating it to shallower waters. By migrating the dams, less area is protected against sea-level rise. This aspect is analyzed in further detail using Qgis. Qgis is an open-source geographical information program used for geographical calculations. All the cities, towns, and villages located below the 10-meter sea level rise (based on the prediction by DeConto) and between the two dam alignments are loaded in the program. The data on the location of the places and its inhabitant are retrieved from OpenStreetMap [10]. Figure 4.3 shows that a relatively small area is flooded. Although the flooded area is small many cities are affected, especially in France and Norway. The reason for this is that many places are all located close to the coast. Concluding that a relatively small loss of land surface has a significant effect on the number of relocated inhabitants. In Table 4.2, the number of inhabitants that will lose their homes is calculated.

Table 4.2: Number of unprotected people by 10 m slr per country between the 4 different alignments [10].

Part of Country	Number of relocated people
England	165 000
France	235 000
Norway	334 000
Scotland	31 000
Total	765 000

As a side note, the places in Qgis are represented as single dots (representing the center of the place). Therefore, the total number of inhabitants is slightly overestimated. However, the other way around is also present, when the center of the place is just above 10 m SLR.

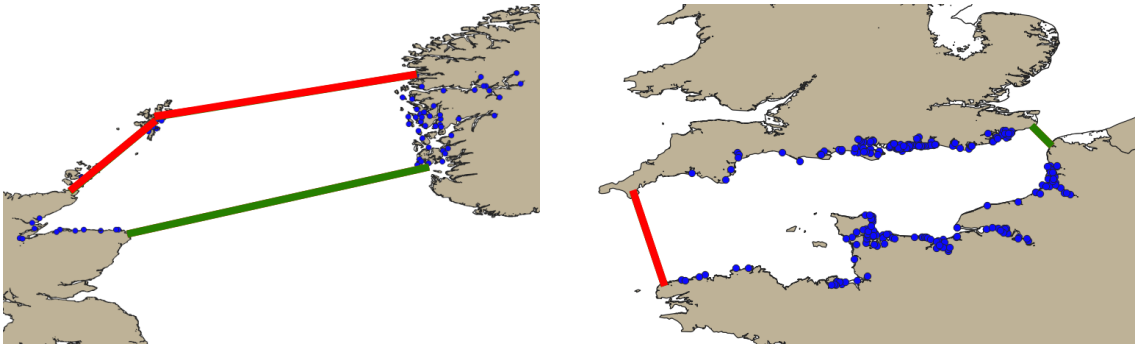

(a) Flooded place with a slr of 10 meters, northern alignments.

(b) Flooded place with a slr of 10 meters, southern alignments.

Figure 4.3: Qgis model of flooded places with a sea level rise of 10 meters.

4.3. Constructability based on the Tide and wave exposure

The dam will affect the tidal elevation outside of the basin. Groeskamp and Kjellson used the NEMO ocean model to simulate the effect on the tide. The model has a grid of 7 km and uses 15 tidal components [22]. The tidal elevations caused by the dam are compared to the tidal elevation without the barrier. The effect can be seen in Figure 4.4. The increase in amplitude at the dam is insignificant for the alignment made by Groeskamp. There is only a slight increase in elevation at the southern coast of England. A level of concern is the increase in tidal amplitude at the Bristol Channel. Just of the coast of Bristol, the amplitude will increase by 1 meter. This effect must be taken into account when choosing this alignment.

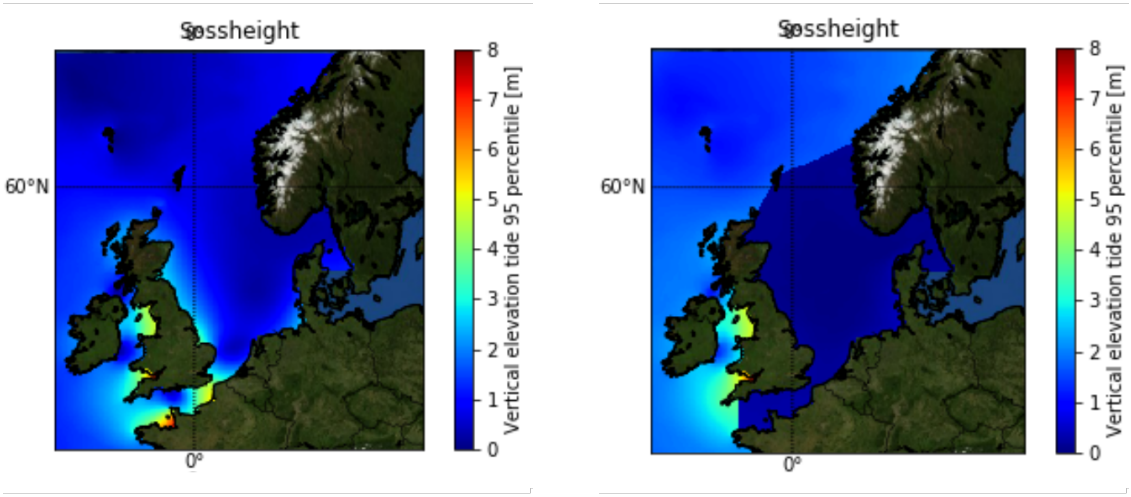

(a) Initial vertical tidal amplitude.

(b) Vertical tidal amplitude after construction of the dam.

Figure 4.4: Initial and result vertical tidal elevation North Sea.

Groeskamp and Kjellson also simulated the optimized southern dam this can be found in their paper [22]. The change in alignment resulted in a drastic increase of the water level. The funnel shape blocks the tide from flowing through the English channel into the North Sea resulted in a standing wave.
Also, the wave data is compared between the two alignments. The wave data is retrieved from the Copernicus hindcast model, explained in more detail chapter 6. Three points are chosen for both northern alignments and 1 for both southern alignments. Figure 4.5 shows the locations of the observation point. The data is further analyzed on the 5, 50, and 95 percentile to compare it, displayed in Table 4.3. The wave height for the ‘optimized’ alignment is significantly lower than the ‘Groeskamps’ alignment.

The ‘optimized’ alignment is more sheltered, decreasing the fetch. Another aspect is the shallower sea, limiting the wave height.

Table 4.3: Percentiles with the corresponding significant wave height for different wave observation buoys [m]

Percentile	Alignment Groeskamp				’Optimized’ alignment			
	pink	yellow	green	orange	red	black	purple	brown
0.05	0.836	0.77	0.96	0.872	0.28	0.60	0.68	0.70
0.5	2.05	2.02	2.31	2.12	1.00	1.71	1.80	3.84
0.95	4.90	4.68	5.25	5.23	3.03	4.01	4.32	4.45

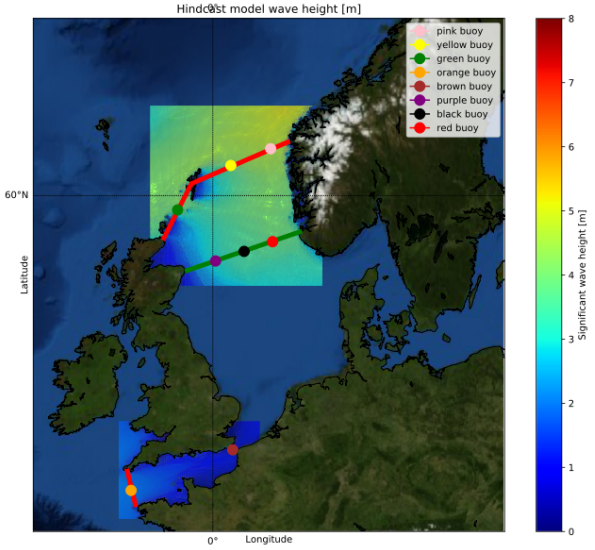

Figure 4.5: Location wave observation buoys both alignments.

4.4. Requirements Huis in ‘t Veld

The requirements from Huis in ‘t Veld are key bottom and shore characteristics that determine the feasibility of the dam alignment. The four requirements are; Configuration of the bed in situ, the composition of the bed, the connection to the shore, and the closure method. The requirements are elaborated in Appendix E. In this section, the four alignments are judged on those criteria. The weighting factors are assessed from the perspective of an engineer in particular a flood risk engineer. The reason for choosing this perspective is that the primary goal of this thesis is evaluating the technical feasibility.

4.4.1. Bed configuration

The bed configuration is requirement one and consists of three sub-requirements. The first sub-requirement is that the **deep parts need to be avoided**. The southern alignments satisfy these conditions; the optimized alignment has only a maximum depth of 60 meters. For the northern alignments, it is impossible to avoid the deep channel without compromising size of the protected area. However, the optimized difference between the maximum depth between the two northern alignments differs by 100 meters.
The second sub-requirement is that **the deep channel should be crossed perpendicularly**. These requirements only apply to the two northern alignments. Both alignments meet this requirement, as the trench is located parallel to the Norwegian coast.
The third sub-requirement holds that the closing gap should be **far away from any confluences**. Although the closing procedure is treated in a later chapter, this requirement is always met. There are no confluences adjacent to any of the four alignments.

4.4.2. Bed composition
The dam alignment should avoid weak bottom composition such as mud and clay. Figure 3.2 clearly shows the different bottom compositions of the North sea. The two southern alignments cross mostly bottoms consisting of coarse substrate and sand. Both the northern alignments cross the deep trench consisting of mud. Additional measures should be implemented to make a stable foundation, for example, by using ground improvement methods. The shallower parts of Groeskamps alignments cross mostly coarse substrate and sand. The optimized northern alignment scores worse, the shallower part of alignment crosses mostly muddy soils.

4.4.3. Connection to the shore
Essential for this requirement is the proximity of consisting infrastructure, such as road and railway networks. Also, if major urban areas are located at both sides of the dam, it can serve as an essential link between the two regions. These requirements also include the connection to the land, coastal outer bends should be avoided, and liquefaction prawn areas. All the alignments meet the last criteria. The 'optimized' alignment will score better when compared to the two southern alignments on the first criteria. The dam creates a link from Calais to Dover and will make the Eurotunnel absolute. The new connection reduces the time it takes to cross the channel. Groeskamp's southern alignment connects two sparsely populated areas and scores therefore worse than on the connection function of the dam. For the northern alignments, the 'optimized' alignment score is a little better on this aspect because it is closer to the urban area in Scotland. On the Norway side, both alignments are relatively close to Bergen, the largest city in the area.

4.5. Weighting score evaluation criteria
In this section, more information is provided on the weighting score of the different evaluation criteria. The weighting factors are determined by comparing the requirements to each other [54]. If a criterion on the columns is more critical (from a flood risk engineer perspective) than the one on the row, a value of 1 is given. The weighting factor on the column criterion is then given a 0. The sum of the given points given is equal to the weighting factor for each criterion. The importance of criteria also considers the influence on the technical feasibility of the alignment; particular assumptions are made to distinguish the significance. The cross-section of section 4.1.1 is used for the evaluation. First, the evaluation criteria are elaborated on the importance.

4.5.1. Length NEED
The length has a direct connection to the volume of material needed to build the dam. The amount of raw materials largely determines the duration, costs, and feasibility of the project. When the number of required raw materials increases, it may result in scarcity of readily available material, or mining those materials requires enormous investments. Fortunately, the dam is located in the North Sea, which is relatively shallow, and the bottom consists of several suitable building materials for the dam. Considering that the building materials are widely available, the volume is not an essential criterion for the feasibility of the dam.
Another aspect is the construction time that will increase with increasing length. The construction time should be minimized to be an excellent solution to mitigate the effect of sea-level rise. The availability of dredging vessels also plays an important role. The number of deployable dredgers is limited, and when more dredging work is required, the duration will also increase. Therefore from a time perspective, less volume is preferable. The increase in length doesn't necessarily increase the technical difficulties; it mostly repeats the same design. Transporting the material over a larger distance will become more complicated. The total points is set to 0.

4.5.2. Maximum Depth NEED
The increase in depth will also increase the total amount of volume to construct the dam. The use of scarce resources such as concrete and sand is also increasing. The depth will have a far greater effect; an increase in depth causes the volume to increase squared. Deeper parts of the dam also require inventive solutions to achieve a good design. Few dams are made in deep waters. As a result, an increase in depth contributes to the technical challenge of the design. The total points is set to 2.

4.5.3. Difference in protection of the two alignments

The most important aspect is the number of people protected by the dam. The main reason for constructing the dam is to mitigate the climate change effect by protecting the people living in the low-lying areas in western Europe; as the dam's area increases, the more value the dam gains as it protects more people. As the dam protects more people, the risk increases (probability times consequences), this will increase the safety criteria. In this case, the north and south alignment devised by Groeskamp is compared to the 'optimized' north and south alignment. The difference is in the number of protected people. Although the degree of technical challenge is not directly related to the difference in protection, this criterion is considered the most important. This results in the highest weighting criteria. The total points are set to 4.

4.5.4. The constructability based on the tide and wave climate

The effect on the tide and wave climate partly determine the height of the dam. The dam will be designed based on the acceptable amount of overtopping plus overflow. An increase in wave height and tidal elevation will result in extra material, dredging vessels, and costs. Compared with the increase in dam size due to the depth, the additional height increase due to the tide and wave climate is limited. The sea conditions in the North Sea are relatively mild compared to other locations where dams are built; this results in the low importance of this criterion. The total points is set to 1.

4.5.5. The geotechnical stability based on Huis in 't Veld

The requirements by Huis in 't Veld determine the technical feasibility of the dam. The requirements form the boundary conditions that need to be fulfilled to determine the best alignment. When all the requirements are met, the probability of a failure mechanism decreases, just like the complexity of construction. Otherwise, the complexity and costs increase because measures have to be taken to minimize the probability of failure and to overcome the resulting problems. The degree of complexity results directly in an increase in the technical challenge, making the importance of this criteria high. The total points are set to 3.

4.5.6. Results Weighting Factors

From Table 4.4 and the explanation in this section, it can be concluded that the difference in protection is the most important criterion. The mitigation of sea-level rise is the primary purpose of this thesis; protecting as many inhabitants in Europe as possible is a critical boundary condition and must be complied with as much as possible. The second criterion with a weight of three is the Constructability requirements by Huis in 'Veld. The least important aspect is the length, as an increase in length does not directly make the dam more complicated from a technical point of view.

Table 4.4: Relative Weighting Factor for each evaluation criteria

		A	B	C	D	E	Resulting Weighting Factor	Adjusted factor
Length NEED	**A**	X	0	0	0	0	0	1
Maximum Depth NEED	**B**	1	X	0	1	0	2	4
Different in Protection two alignments	**C**	1	1	X	1	1	4	8
Constructability based on tide and wave load	**D**	1	0	0	X	0	1	2
Geotechbical stability Huis in 't Veld	**E**	1	1	0	1	X	3	6
							sum	21

From the relative weighting factor, the final weighting factors for each criterium can be determined. This is done by dividing the individual score by the sum of the scores. The score of zeros will imply that the length factor has no value in the multicriteria process. This is, of course, not true; therefore, a value of 1 is given to this criteria. To keep the approximately the ratio between all criteria, the values are multiplied by two (excluding the length factor) [54]. All the elements are multiplied by 100 to end up with round numbers.

Table 4.5: Weighting factor for each criterium.

		Score
Length NEED	**A**	100*(1/21) = 5
Maximum Depth NEED	**B**	100*(4/21) = 19
Difference in Protection two alignments	**C**	100*(8/21) = 38
Constructability based on Tide and Wave Load	**D**	100*(2/21) = 10
Geotechnical Stability Huis in 'Veld	**E**	100*(6/21) = 29

4.6. Conclusion

The total score can finally be calculated based on the analysis given above. The weighting score of the different criteria is multiplied by the score given to the item. This is done for each alignment and summed. The alignments (north and south) with the highest score are the most optimal alignment. In Table 4.6, an overview is given of the individual scores of each alignment. The result of the multi-criteria is that for both the northern and southern dam, the alignment of Groeskamp scores best.

Table 4.6: Multi-criteria analysis alignments.

Criteria	Weighting Factor	North		South	
		Groeskamp	**'Optimized'**	**Groeskamp**	**'Optimized'**
Length NEED	5	2	4	6	10
maximum Depth NEED	19	2	4	6	8
Difference in Protection two alignments	38	10	6	10	6
Constructability based on Tide & Wave	10	6	6	6	6
Geotechnical Stability Huis in 'Veld	29	6	8	6	8
Total		**662**	616	**758**	722

The values of the weighting factors are being determined from the perspective of an engineer (flood risk engineer). A closer investigation is needed to find the best location using different perspectives, for example, the ecologist, government, etc. Different perspectives result in other weighting criteria and diverse scores. The scores are all set to one to assess the impact of the weighting scores. The results in the same conclusion, Groeskamp's alignment scores best.

Table 4.7: Overview of the values of the most important aspects.

	North		South	
	Groeskamp	**'Optimized'**	**Groeskamp**	**'Optimized'**
Length NEED [km]	475	452	161	4010
Maximum Depth NEED [m]	-400	-300	-100	-50
Volume NEED slope (1:3) [m3]	47.51E9	35.55E9	5.23E9	0.23E9
Difference in Protection Groeskamp - Optimized	365 000		400 000	
Significant Wave Height 95 percentile [m]	4.68	4.01	5.23	4.32

5

Probabilistic Design Conditions

In this chapter, the design conditions for the NEED are analyzed. Multiple design steps are made to assess the safety conditions that needs be fulfilled for designing the cross-section. First, an overview is made of all the failure mechanisms that can occur. The fault tree is constructed to get insight into the correlation between the different failure modes. The ultimate limit state (loss of function) per failure mode is determined for the most important failure mechanism, using the dutch guidelines. Next, the serviceability limit state (hindrance) are depicted, based on literature. The most stringent of the two determines the design conditions of the dam. Last, the probabilistic method is described that determine the dimensions of the dam.

5.1. Design definition

5.1.1. Requirements NEED

The requirements can be subdivided into two sub-specifications, the functional requirement, and the aspects requirements. The functional requirements describe the system's different functions, and the aspects requirements consider safety and reliability. The functional requirement of the Northern European Enclosure Dam are:

- The dam protects West-Europe against the rising sea level. In this thesis, the water level rise is set to 10 meters NAP at the Ocean side. The water level in the basin is kept equal to the current water level.
- The dam also has a transport function, meaning that there must be room on top of the dam for road or railway connection to both ends of the dam. This is explained in further detail in Chapter 6.
- The dam may be closed for traffic at most once a year due to storm conditions.

The aspects requirements for the Northern European Enclosure Dam are:

- The dam will be designed for 100 years, a class 4 design work-life structure. This does not mean that the dam becomes obsolete after that period, but extensive maintenance or adaptive measurements should be performed.
- The consequence class that best fits this project according to EN 1990 is CC3, which means high consequence for loss of life, economic or environmental [50].
- The main event is inundation of west-Europe, this probability is set to 1/10 000 per year, which is typical for Dutch primary flood defenses. The probability of failure of the dam is set to a lower maximum allowable probability of 1/20 000 per year. This is explained in more detail in section 5.3.

5.1.2. Boundary Conditions

The boundary conditions restrict the possibilities of designs and must be included in the design of a dam. The boundary conditions consist of: natural boundary conditions, e.g., loads due to wind and

waves, soil properties, and artificial boundary conditions such as traffic. The most important boundary conditions are the hydraulic loads. Multivariate distributions are fitted to the wave height, direction, and period to account for the correlation between these individual elements. The wave height is set to be the dominant wave parameter as it most influences the design. Other boundary conditions are already explained in Chapter 3; this includes the bathymetry, sea bed material, river discharge, windset up, and the area to be protected. These parameters are taken deterministically.

5.1.3. Two Concepts of the closure dam

There are generally two types of dams: dams consisting of individual structures such as a caisson and an earthen dam made by sand dumping on the seafloor.
The latter is the most straightforward type of dam; it is constructed from several layers, which creates a barrier that blocks the waves and tide. This type of structure is very durable and maintainable. The energy from the incoming waves dissipates on the slopes minimizing the impact on the structure. The side back of an earthen dam is that it requires a tremendous amount of material when constructing in deep water. This is due to the mild slope is necessary the make the dam stable. Steeping the slope will on the one hand reduce volume of the dam but on the other hand reduce the stability. Berms can be used to optimize the volume of the dam. The berm breaks and slows down the wave, reducing the necessary height and width.
The other type of dam is a caisson dam. A caisson dam is a concrete vertical box structure. These boxes can be transported to the final location and sunk with ballast, to fix the caisson permanently, (e.g., dredges material). The caisson method is very efficient and quick in deep water [36]. There is no limit for the height of caissons; it is usually a more attractive solution for water depths from 15 meters or more. The type of concept depends, among other things, on the availability of material (rock, sand in the area. The height of the caisson is structurally proven for water depths up to 50-75 meters [36]; larger caisson sizes make the transportation very complicated. Stacking the caisson can overcome the large water depth, complicating the watertight connection. Divers will have to connect the caissons to each other. The connecting part is not further treated in this thesis.
This thesis elaborates on both concepts, and conceptional designs are made.

5.2. Failure Mechanisms

A dam section can fail due to different failure mechanisms. In Figure 5.1, a schematic overview of possible failure mechanisms of an earthen and caisson dam are shown. Most failure mechanisms are also applicable for both concepts, except for revetment failure, sliding slope, and failure due to overtopping. The failure mechanism overtopping is not much of a thread for a caisson, but it must still take into account for the SLS state. SLS conditions is the serviceability limit sate and is explained in section 5.4. A failure tree is used to get more insight into the dependency of the failure of a dam section. In section 5.2.1, the most common failure types (on which the dam is being designed) are explained, and the underlying processes are described.
For the caisson dam, some additional failure mechanisms should be considered. These failure mechanisms are retrieved from the research by Goda [21]. The failure mechanisms are shown in the figure below.

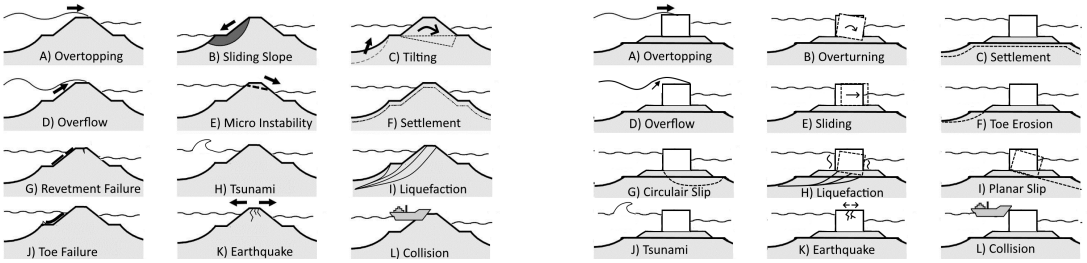

(a) Failure mechanisms of an earthen dam section, based on Flood Defence lecture note [28]

(b) Failure mechanisms of a caisson section.

Figure 5.1: Schemetic overview failure mechanisms for both earthen and caisson dam.

5.2.1. Fault trees

The top event of the failure tree is the inundation of West-Europe. There are three main causes for this event:

1. Failure of one or multiple sections of the dam during a storm. When a specific section of the dam fails, a flood wave is created that can cause the parts of West-Europe to inundate.
2. The NEED is damaged and is not repaired before the next storm/high water.
3. High waves and wind setup in the newly created basin that causes the current flood defenses of West-Europe to fail and inundate the land.

The connection between the main events is an OR-gate, meaning that the highest probability of failure is the probability of the top event. For this situation, the three events are correlated, as storm conditions increases the probability of inundation for all three events. The basin behind the dam is extensive, so when the dam fails, it does not immediately result in inundation of low lying parts of West-Europe. If immediate measures are taken, the risk of failure can be prevented. When a small breach is formed, the rapid measurements must be executed. After a particular time, the gap will become so large that closing it will be almost impossible. In this thesis it is assumed that a dam breach will result in inundation.
Conditions inside can also lead to inundation. Wind setup and high waves can still threaten the low-lying countries along the newly formed basin. Due to the enormous size of the basin, the wave setup due to the construction of the NEED hardly changes.
The last item is if the damages of the dam are repaired too late. Weak spots in the dam pose a thread if not repaired before the next storm. The SLS conditions given later in this chapter provide an indication of the probability of repairing the dam. A fault tree is constructed to show the events leading to the inundation of West-Europe. The fault tree can consist of two gates, an AND-OR gate. The And gate is true if both inputs are true, and the Or gate is true if any of the inputs is true. Table 5.1 depicts the bounds for the systems failure probability for the different systems.

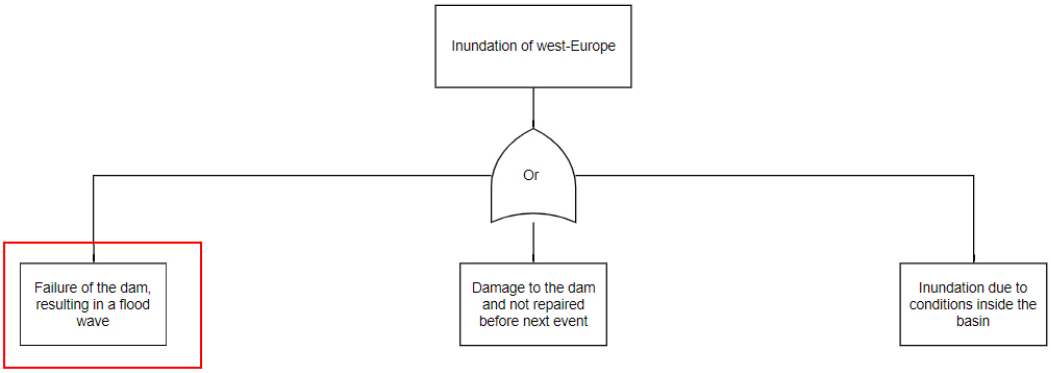

Figure 5.2: Causes of the top event inundation of west Europe.

This thesis focuses on the failure of the dam section, and the associated failure tree is explained in more detail.

Earthen dam

Failure of an earthen dam section is defined as the loss of the water-retaining function of the dam. One row below is the failure of an individual section. The failure of one section leads to the failure of the system results in the OR gate connection. The next row of the fault tree is equal for each section and consists of 4 events: inner and outer slope erosion, internal erosion, and others. Examples of 'others' failures are; Human error, seismic activities, sabotage, and tsunamis. A tsunami can arise due to a break off, of part of the North pole ice cap, resulting in a flood wave. The flood wave can damage the dam and possibly result in failure. Human error can occur by ship collisions or mistakes by operating the dam.
In the last row, the events are; revetment failure, toe instability, overtopping, overflow, and the events leading to piping. These failure mechanisms are explained in section 5.2. Hydraulic structures such

as sluices, pumps, etc., are out of the scope of this thesis, and therefore the corresponding failure mechanisms are not taken into account.

Table 5.1: Summary of values for the system failure probability for various cases [29]

System	Gate	Mutually exclusive	Independent	Fully Dependent
series	OR	$\sum_{n=1}^{\infty} P_i$ (upper bound)	$1 - \prod_{i=1}^{n}(1 - P_i)$	max$\{ P_i \}$ (lower bound)
parallel	AND	0 (lower bound)	$\prod_{i=1}^{n}(P_i)$	min$\{ P_i \}$ (upper bound)

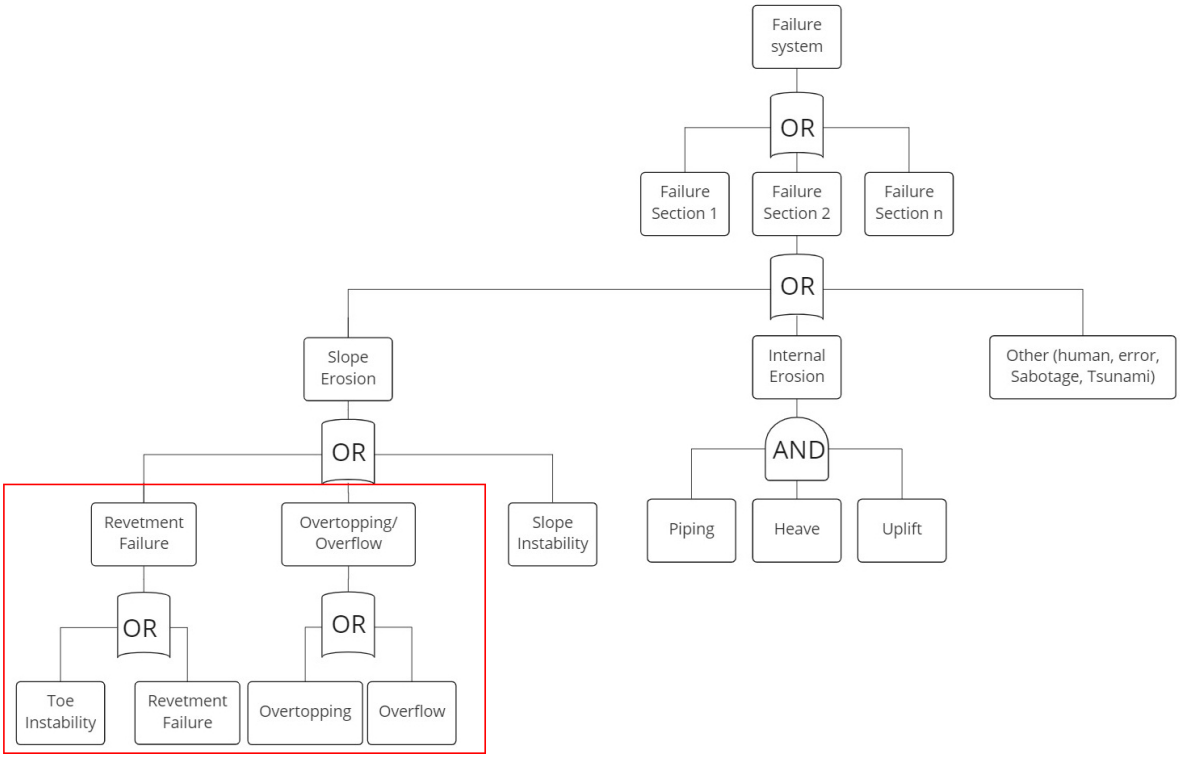

Figure 5.3: The fault tree of the earthen dam. The failure mechanisms analyzed are indicated with a red box.

Caisson

The failure mechanism leading to caisson failure differ slightly compared to the failure of an earthen dam. Extremely large overtopping volumes can result deterioration of the road structure or concrete integrity. But this probability is extremely small and therefore neglected. The availability conditions of the road connection is governing for overtopping and determined in the next section. A vital failure mechanism for caisson failure is the stability of the subsoil. Four sub failure mechanisms can lead to the failure of the caisson due to the soil stability: liquefaction, planar slip, sliding, and circular slip. Structural integrity is the ability of the caisson to withstand the load that is acted upon without failing. Due to continuous loading, small cracks can form and will result in concrete degradation. The last failure mechanism is the stability of the caisson. Due to wave loading, tide, and water level difference, the caisson can slide and tilt. Which results in the loss of the water-retaining function.

The failure of each individual section has the same cause. The cause of failure is shown for only one section to save space. The same has been done for inner and outer slope erosion. To save time and still make a reasonable conclusion about the technical feasibility, only two failure mechanisms are assessed fully probabilistically. These failure mechanisms are chosen because they depend on the governing load condition—a storm event. The locations of these failure mechanisms in the fault tree are indicated with a red box. The failure mechanisms for the earthen dam that are fully probabilistically assessed are overtopping, and revetment failure (including toe stability). For the caisson dam, the failure mechanisms are: stability (tilting and sliding), and overtopping. Piping is checked using a deterministic calculation.

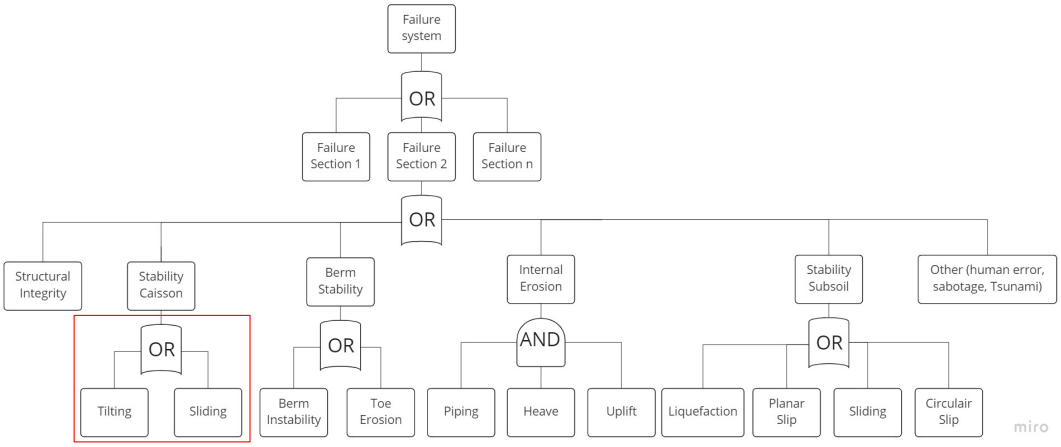

Figure 5.4: The fault tree of the caisson dam. The failure mechanisms analyzed are indicated with a red box

5.2.2. Overtopping/Overflow Earthen Dam

When the still water level is higher than the dam's crest, water flows over the dam—overflow results in damage to the inner slope of the dam. The damage is caused by the pressure difference over the revetment or due to erosion(grass or other material). The revetment can slide and or lift, resulting in a wash-out of material. If this process continues, the loss of material will lead to failure. The erosion process is based on the inner slope revetment. [28]
Overtopping occurs when the still water level is below the dam's crest, but the wave runs up is higher than the crest and overtops the dam. The resulting damage is for both mechanisms the same. The connection between the two failure types is an OR gate, meaning that the failure is overtopping and or overflow, as shown above.

Critical overtopping discharge

The maximum allowable overtopping/overflow depends on the resistance of the inner slope revetment and the types of waves that overtops the dam. The overtopping process is not constant but varies over space and time. Quite a lot of overtopping is allowed because the basin is vast; thus, the overtopping will not result in a drastic increase in the water level of the North sea. The limiting factor is the armor layer at the inner slope. The armor layer that protects the slope against overtopping is the part of the inner slope that lies above the influence area of the waves. A material that can withstand hugh amount of overtopping is asphalt. The maximum overtopping discharge for an asphalt revetment is equal to 100 l/s/m with a COV of 10%, based on the Europtop Manual [19].

5.2.3. Internal erosion (Piping) Earthen Dam & Caisson

This failure mechanism is assessed deterministically. Three sub mechanisms should all occur to result in the failure mechanism of internal erosion; the mechanisms are uplift, heave, and piping. If there is no impermeable layer, internal erosion is solely dependent on piping. A significant difference in water level at both sides of the dam can lead to the formation of pipes. The most crucial driving mechanism that results in piping is the groundwater flow. The pipes form just below the impermeable layer/structure and the loose material. Due to internal erosion, water can freely flow from the high waterside to the low waterside. At the downflow side sand boils up and forms little 'Sand Volcanoes.' When the scour holes grow, the stability of the structure will decrease, and eventually, the structure will fail. The empire formulas based on the research from Bligh and Lane are commonly used to describe this failure mechanism. The formula described the limit state function with the critical head difference and seepage length. The Sellmeijer equation is a more advanced method explicit estimates of the parameters are needed, Appendix H. The equation used are retrieved from the TAW Technisch Rapport Zandmeevoerende Wellen [7].

5.2.4. Revetment failure Earthen Dam

The revetment can fail under two independent conditions, the toe can fail that makes the revetment slide, or the revetment can fail due to the hydraulic loading on the revetment itself.

A hard layer protects both the outer and inner slopes of a dam against erosion due to wave run-up and wave impact. Revetment failure occurs when the forces caused by the wave attack is larger than the strength of the revetment or due to erosion caused by the run-up. The allowable damage and thus failure depend on the type of revetment. According to Schiereck [45], the placed block revetment fails if a single block is dislocated, resulting in the exposure of the sublayer. When exposed, the sublayer starts to erode. The erosion of the sublayer can trigger the dam's collapse. In Appendix H, the stability equation from Van der Meer is shown. These equations are derived for the stability of rocks and depend on the allowable damage. Depending on the loading, rocks may not be stable enough to be used in such a situation; interlocking revetment can provide a solution. A commonly used interlocking revetment is Xbloc. In Appendix H, the stability of Xblocs is demonstrated. Xblocs are interlocking elements; the stability equations for Xbloc are based on the Hudson equations. The equation is derived from the Xbloc design guide [9].

Extending the armor layer over the entire water depth is not necessary. The wave action is limited below one wave height of the lowest still water level. The toe protects the front of the armor layer from sliding and erosion. If the same rock diameter is used in the toe as the armor layer, the toe is very likely to be stable. Reducing the toe is preferable as the cost will decrease significantly. The diameter of the stones depends on the depth of the toe, wave height, and allowable damage. The equation the toe stability is shown in Appendix H.

5.2.5. Stability caisson

The stability of the caisson is a critical failure mechanism. This failure mechanism consists of two main mechanisms which are described in this report; sliding and tilting. Sliding occurs when the frictional force is less than the horizontal force acting on the caisson. Tilting occurs when the overturning moments at the heel of the structure are larger than the counteracting moment resulting from the self-weight of the caisson. Goda [21] investigated numerous vertical breakwaters to come up with a formula that concludes the stability. The equation is valid as long as breaking waves are avoided, which is the case in this project as the Caissons are placed in deep water.

All the equation to describe the failure mechanisms are explained in Appendix H.

5.3. Maximum allowable probability per failure mechanism ULS

The Ultimate Limit State (ULS) describes the dam's behavior under extreme loading [8]. The maximum allowable probability of inundation of West-Europe (the top event) is set to 1/10 000 per year, this probability is based on the flooding probability of the Dutch coast. In this thesis, we are interested in the likelihood of the event: Failure of the dam resulting in a flood wave. The connection between the different failure mechanisms leading to the inundation of West-Europe is an OR gate, Figure 5.2. As explained before, the relationship between the three events that lead to inundation is correlated. Therefore the maximum probability of dam failure is chosen to be lower, namely 1/20 000 per year.

The failure probability for each individual failure mechanisms depends on the length and contribution factor. The road-map for determining the failure probabilities of each of the failure mechanisms is shown below.

1. **Length effect**
   The dam is split into four sections to take the inhomogeneity into account. The northern dam is divided into three parts and the southern 1 part, each 10 km long. The locations of these sections are based on; the water depth, bottom composition, and hydraulic loading. The first section is at the deep trench near the Norwegian coast. The challenge for this section is to come up with an efficient material design that will satisfy the set maximum allowable probabilities. The following section is between the Norwegian trench and the Orkney Islands. The depth, bottom material, wave climate is equal over the trajectory, making that section representative for the entire distance. The last northern section is between the Scottish coast and the Orkney island. The bottom material consists of a coarse substrate, which will influence the design of the cross-section. Only one section is chosen for the southern dam, as the bottom composition, hydraulic loading, and depth are pretty homogeneous. This section is located precisely in the middle of between France and the UK. Values for the length effect are retrieved from Handreikingen ontwerpen overstromingskans [40] and are calculated using equation 5.1.

2. **Contribution factor**
   Each failure mechanism has a specific contribution to the failure of the entire dam. The factor is called the contribution factor and allows to calculate of the probability of failure of a particular failure mechanism by multiplying the total probability of failure by the contribution factor of he failure mechanism, equation 5.2.

   The different failure mechanisms for the earthen dam are: inner slope erosion, outer slope erosion and overtopping (height structure). The contribution factor for closure structure is used for the caisson failure mechanisms tilting and sliding. These contributing factors that are used are retrieved from the Handreikingen ontwerpen overstromingskans [40]. Those contribution parameters are fitted for dutch dikes and dams, however for simplicity they are also used in this thesis.

Table 5.2: Contribution factor ω per failure mechanism used for dutch flood defences [40].

Failure mechanism ω	**Dunes**	**Dikes and Dams**
Height structure	0	0.24
Internal stability	0	0.24
Macro stability inner slope	0	0.04
Grass cover outer slope	0	0.05
Other revetment outer slope	0	0.05
Closure structure	0	0.02
Dune erosion	0.7	0
Other failure mechanism	0.3	0.3

3. **Maximum allowable failure probability per failure mechanism**
   Based on the contribution factor and the length factor, the probability of failure per failure mech-

anism per year is determined, see equation 5.3 . The results are presented in Table 5.4

$$N = 1 + \frac{a * L_{section}}{b} \tag{5.1}$$

$$P_{max} = \frac{\omega P_{norm}}{N_{dsm}} \tag{5.2}$$

where:
P_{norm} is the probability of failure per year 1/20 000
a is the fraction of the length of the trajectory that is sensitive to the failure mechanism [-]
b is the length of independent, equivalent boxes for the respective failure mechanism [m]
$L_{section}$ is the length of the dike section to which the standard applies [m]

Table 5.3: Allowable failure probability ULS.

Failure mechanism	Contribution Factor ω	Length effect factor for trajectory of 10 km	Maximum allowable failure probability per year
Earthen dam			
Overtopping and overflow	0.24	3	4e-6
Toe stability	0.05	-	2.5e-6
Grass cover inner/outer slope	0.05	-	2.5e-6
Revetment failure	0.05	-	1e-6
Caisson			
Tilting and Sliding	0.02	1	2.5e-6

5.4. Maximum allowable probability of failure SLS

For the same failure modes as the ULS conditions, the criterion of the serviceability limit state are defined. The Serviceability Limit State (SLS) describes the dam's behavior under normal loading (rock manual) or, for RLS, the degree of damage that is accepted. Different assumptions have been used to arrive at the requirements, the condition are retrieved from the lecture notes of Breakwater design [50].

Overtopping and overflow
An essential function of the closure dam is to provide a road and train connection between the United Kingdom and mainland Europe. According to the rock manual, when the amount of overtopping exceeds $1 * 10^{-5}$–$5 * 10^{-5} m^3/s/m$ [8], it becomes dangerous to drive over the dam at moderate or high speed. The maximum return period of the road being closed due to the exceedance of the overtopping limit is set 1:1 per year. This is for both the caisson dam and the earthen dam.

Revetment and Toe
Some damage to the revetment is allowed as long as the dam's primary function and the structural integrity are not compromised, corresponding to intermediate damage. This also applies to the toe protection that prevents the revetment from sliding. The height of the toe depends on the allowable damage of the toe. A thorough inspection of the toe is quite expensive, leading to a 1: 50 per year return period.

For an *interlocking block revetment*, a single displacement of one block is already considered a failure, meaning there is no room for a Serviceability limit state. The ULS is therefore governing.

For *placed block revetment* consisting of multiple layers, some movement of the block and or rocking blocks depending on the block type is allowed as long as the block is repaired (table 6.3) after the event causing the damage. The length of the dam makes a thorough inspection quite expensive, so

the return period is set at 1:50 per year. The classification of damage level depends on the type of blocks that's is used and on the slope of the dam.

Quarry stone revetment some damage to the quarry stone revetment is allowed if the armor layer consists of at least two layers (intermediate damage). After an event that caused some damage to the revetment, the entire dam should be checked and repaired. This leads to a return period of 1:50 per year (The S factor depends on the slope) [50].

Table 5.4: ULS and SLS for the governing failure mechanisms.

Failure Mechanism ULS	**Maximum allowable probability Of exceedance per Year**	**Value**	**Nod**
Earthen Dam			
ULS Overtopping	4e-6	$0.1[m^3/s/m]$	-
ULS inner dike Revetment	2.5e-6	-	*
ULS Toe stability	2.5e-6	-	4
Caisson			
ULS Tilting and Sliding	1e-6		-
Failure Mechanism SLS	**Maximum allowable probability of exceedance per year**		
Earthen Dam			
SLS Overtopping	1	$1 * 10^{-5}[m^3/s/m]$	-
SLS Revetment	0.02	Depends	1
SLS Toe Stability	0.02	-	1
Caisson			
SLS Overtopping	1	$1 * 10^{-5}[m^3/s/m]$	-

- The value corresponds to the resistance of the systems.
- N_{od} is the character of damage, which is 0.5 for the start of damage, 1 for acceptable damage and 4 for failure. For interlocking revetment no damage is allowed.
- For rock revetment the damage parameter depends on the slope of the dam and the damage level. The table containing different slopes and damage parameters for quarry stone is shown in Table 5.23 of the Rock Manual [8].

5.5. Probabilistic method

A reliability calculation will conclude if all the above-mentioned safety criteria are met. A simple way to check this is by using the limit state function; the limit state function is described in equation:

$$Z = R - S \tag{5.3}$$

The R is the strength of the system's resistance, and the S stands for the load or solicitation. The system fails if the resistance is smaller than the load.

Most systems have multiple failure mechanisms, and each failure mechanism has multiple load and resistance parameters. For overtopping, a load parameter is the water level, wave loading, the resistance is the revetment, height of the dam, etc. The equation that describes the failure mechanisms has also an uncertainty. There is no single value representing the load or resistance of a system; a distribution is used to take the uncertainties into account. The distribution has a mean value μ representing the value with the highest probability; the mean has some deviation. This deviation is called the standard deviation σ. The part where the resistance and load distribution overlap is called failure.
There are four levels of probabilistic approaches that can be used to calculate the total probability of failure[29].

- Level 3 method. This level consists of fully probabilistic methods and can calculate the probability of failure precisely. A commonly used way is the Monte Carlo analysis; the MC analysis uses random variables (from distributions) for all the parameters and checks whether it fulfilled the limit state function. This process is repeated many times, increasing the accuracy of the failure probability. Other methods such as numerical integration become more difficult as the function becomes complex.
  The number of steps required to get a good approximation of the failure probability increases exponentially for the number of variables .
- Level 2 This level is less accurate compared to the level three methods. For the probabilistic analysis, only the mean values and the first and second-order moments are used. An example of a first-order method is the FORM analysis. The FORM analysis linearised the limit state function in a point with the highest probability density, the design point. A conclusion about the failure probability can be made using the design point.
- Level 1 consists of semi-probabilistic methods. The uncertainties of the different variables are incorporated in the characteristic values. The 95 percentile is used for the load parameters, and the resistance, the 5 percentile. The characteristic value for load is then multiplied by the safety factor; the characteristic value for resistance is divided by a safety factor. These values are then put into the limit state function to check the failure of the system.

This MSc thesis aims to verify the cross-section using a fully probabilistic method, level III. The probability of failure is assessed using the crude Monte Carlo method. For all variables, a random vector is created using the distribution functions; these vectors are input for the limit state function. By repeating this process many times and saving the number of failures, the probability of failure can be estimated using the following formula:

$$p_f = n_f/n \tag{5.4}$$

The greater the number of realizations of the limit state function, the more reliable the probability of failure. The reliability of the Monte Carlo run can best be described using the coefficient of variation. For small values of p_f the coefficient of variation can be written as [46]:

$$V_{P_f} \approx \frac{1}{\sqrt{z * p_f}} \tag{5.5}$$

For example, if a small COV is required, eq 10%, and the probability of failure is $p_f\ 10^{-4}$, it results in 10^6 Monte Carlo Runs [46]. This process is programmed using Python. The amount of runs needed to get a reliable answer for each of the failure mechanisms can be determined using equation 5.5.

For all Monte Carlo simulations, the minimum amount of runs is calculated. The coefficient of variation is set to 30 percent; this value is chosen to give a reliable conclusion about the feasibility and ensure that the calculation time is not much longer than an hour. When higher accuracy is selected, the number of runs increases with the coefficient of variation squared.
A method that can be used to improve the efficiency of the Monte Carlo simulation is importance sampling. Importance sampling decreases the number of runs significantly by using a distribution that overweights the critical region. This is done by shifting the density function to the failure domain [49]. This technique is advantageous with a limited amount of variables. For this thesis, the method is too complex and is therefore not used. Another approach to decrease the computational time is using multiple core processing. Depending on the number of cores, various calculations are performed simultaneously. Table 5.5 gives the minimum amount of runs for all failure mechanisms, both SLS and ULS. The amount of runs differ per location as explained in appendix G.

Table 5.5: Number of Monte Carlo runs per Failure Mechanism.

Failure Mechanism	Minimum amount of run
Earthen Dam	
ULS Overflow/Overtopping	2.8e6
SLS Overflow/Overtopping	11
ULS Revetment	4.5e6
SLS Revetement	1.9e6
SLS Toe Stability	1.9e6
ULS Toe Stability	4.5e6
Caisson	
ULS Internal Stability	12e6
ULS Tilting and Sliding	12e6
SLS Overflow/Overtopping	11

5.6. Conclusion

This chapter assessed the safety norm that is assigned to the enclosure dam. The safety norm of the dam was determined based on the top failure event, the inundation of West-Europe due to failure of the dam. This chapter considered two different types of closure dams: the earthen dam and the caisson dam. A fault tree was constructed for both types. From this fault tree, the most critical sub failure mechanisms were further analyzed. The Dutch guidelines were used to resolve the failure probabilities of the essential sub mechanisms. The maximum allowable failure probability of these sub failure mechanisms provides tools to determine the dimensions of both dam types. These steps were taken for both ULS and SLS conditions, where ULS stands for the ultimate limit state and SLS the serviceability limit state. It was concluded that the fully probabilistic approach was most appropriate to assess the dam types. The fully probabilistic method is used in the next chapter called ‘Crude Monte Carlo.’ The Monte Carlo method needs the number of runs evaluated in the last section of this chapter. This chapter formed the basis for the design process; this knowledge is applied in the next chapter: the design of both types of dams.

6

Cross-section Design

The primary purpose of this chapter is to develop a design that satisfies the safety criteria set in the previous chapter. The design steps are performed for both the caissons and the earthen dam. The following steps are used to come up with a good design for four different locations along the NEED.

- The important input parameters are fitted to various distributions, see section 6.1.
- An overview of the general input of the Monte Carlo Analysis is shown. For each failure mechanism, a Limit State Function is described to determine the probability of failure, see section 6.2.
- The dimensions of both concepts (caisson and earthen dam) are determined by changing it for each Monte Carlo test until resulting probability of failure is lower than the criterion. The results are shown in section 6.3

Aspects of the dam that are not parts of the probabilistic method but are essential for the design are determined deterministically
The two design concepts (caisson and earthen dam) are compared based on the feasibility, and the best design is chosen.

6.1. Data Analysis

In this section, the wave data along the dam is being analyzed by an extreme value analysis to derive the wave conditions. A hindcast model provides the wave data of the past forty years. This model is retrieved from the Copernicus observation program. The data from the hindcast model is based on several wave-buoys, wind observation points, and geological information. The hindcast model provides 116800 observations per point, with a resolution of 3 hours per day for the past forty years. The model has a resolution of an aspheric cell of 3 by 1.5 km, stretching the entire North Sea and English channel. The observations are wave height, wave direction, and wave period. Four points along the length of the dam are chosen to be analyzed. Three points are located at the northern dam and one at the southern dam, see figure 6.1. The locations of these points depend on the hydrodynamics and geographical features, as explained in chapter 3. The dominant parameter that is used for the analysis is the wave height.

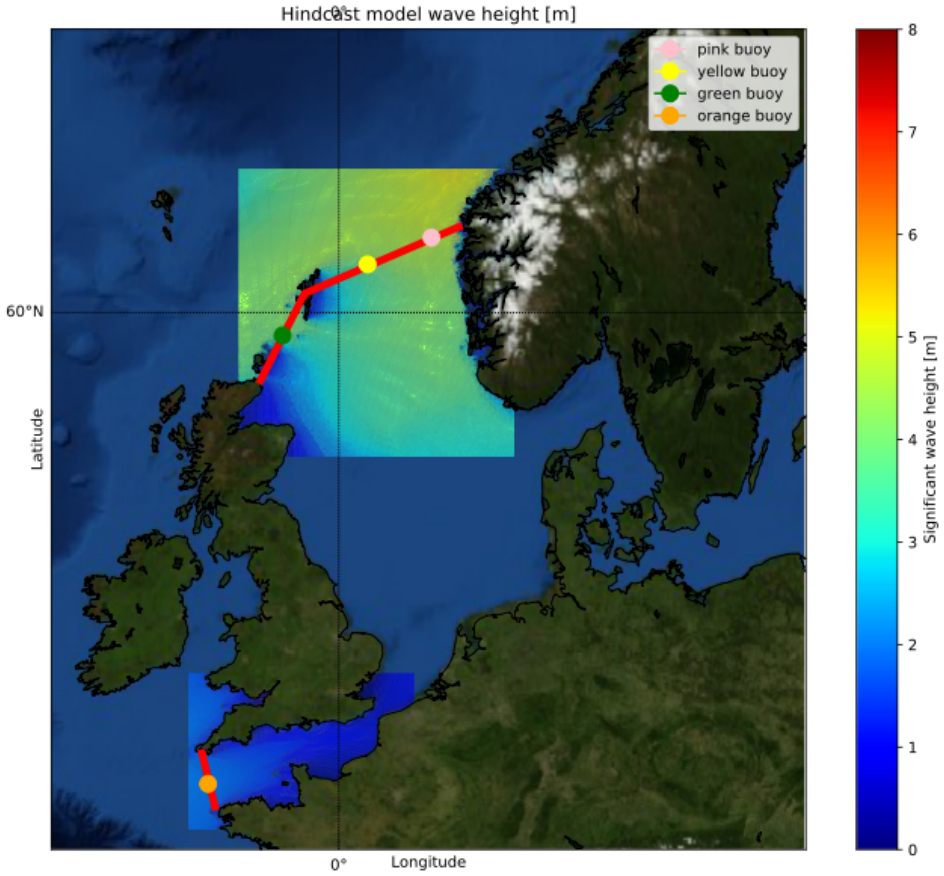

Figure 6.1: Location observation buoys retrieved from hindcast model.

The data per wave buoy is split into two sections to consider the two sides of the dam (the Basin side and the Ocean side).

6.1.1. Extreme Value Analysis

Extreme value analysis is performed to get a better insight into the reliability of the extreme values—the data from the hindcast model is used for this simulation. The extreme value analysis focuses on the tail of the distribution and is essential as it mostly influences the dam's design. The best method to determine the extreme analysis model is the so-called Peak over threshold method (POT) with the Generalized Pareto Distribution. This method separated the normal sea condition from the storm waves. It has a slight advantage over the other method, the block maxima, as the latter disregards a lot of information (the maximum value in a particular block represents all the extreme events in that block) [42] .

For the POT method, a reasonable threshold should be determined. First the data is declustered to be used for the analysis. Declustering is performed to ensure that these values are independent and identically distributed which is required for the corresponding limit distribution to be applicable.
High wave occurs mostly in groups during storm events; declustering makes the extreme events more independent. The declustering is based on the duration of storms; according to Holthuijsen [24], the average time of a storm is 6- 12 hours, but sometimes it could last a day. Daily maxima wave height is a commonly selected time lag used as the minimum distance between 2 peak events. In Figure 6.2, the data and declustered data is presented with an arbitrary threshold.

Next, the threshold is selected; the selection of the threshold is essential as it significantly influences the results of the extreme value analysis. A higher threshold will result in less extreme values leading to a large variance in the outcome (a large confidence interval). A smaller threshold will lack accuracy resulting in a less approximation of the Generalized Extreme Pareto distribution. The most optimal

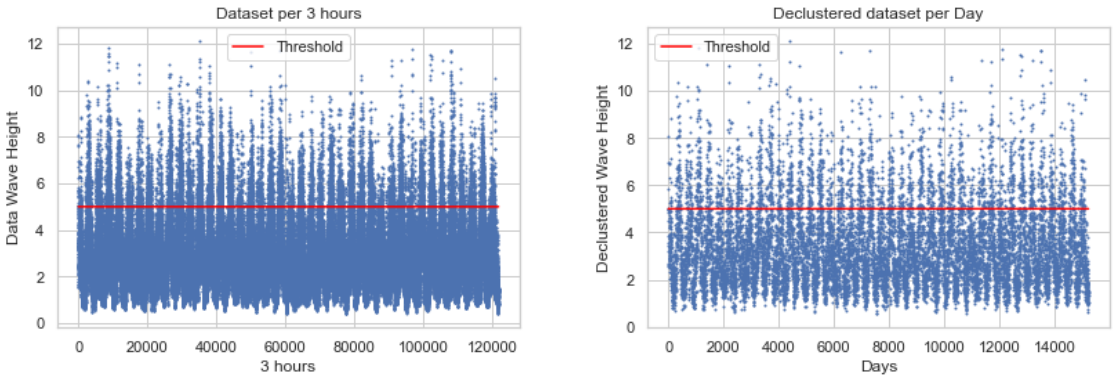

(a) Clustered Data, pink wave buoy 1

(b) Declustered Data, pink wave buoy 2

Figure 6.2: Data waveheight, clusered every 3 hour period, declusterd 6-12 hours.

threshold is the smallest threshold that produces the most optimal GDP. The threshold is chosen at the point where the estimated values of the parameter converge, and the parameter is relatively stable. Two methods are generally used to determine the threshold: the Mean Residual Life and the Stability of the Parameter.

Mean Residual Life

The mean Residual Life plot calculates the average excess value for a given threshold. This process is repeated for different thresholds. The mean residual life plot is approximately linear until it reaches values above a threshold for which the Generalized Pareto Distribution is not valid anymore. The maximum threshold is used.

The stability of the parameter

The stability of the parameter shows how the scale parameter ζ and the shape parameter σ^* of the Generalized Pareto Distribution change the threshold values. The parameter should be relatively stable and vary only a small amount within the threshold.

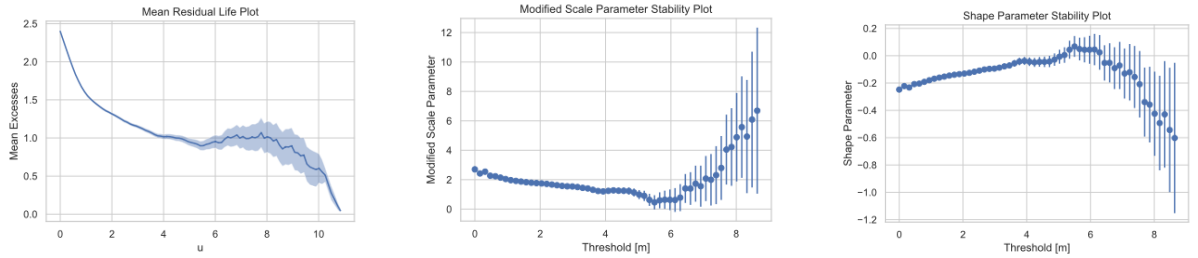

(a) Mean Residual Life Plot

(b) Stability scale parameter

(c) Stability shape parameter

Figure 6.3: Mean Residual Life plot and the Stability of the Parameter Plot.

Both analyses determine the selected threshold for the four-wave buoys and two directions; the thresholds and number of peaks can be found in Appendix G. Next the extreme value distribution GDP is used to analyse the return value. The 1 in m year return period is given as:

$$z_m = \begin{cases} u + \frac{\sigma_u}{\xi}\left\{(\lambda_u m)^{\xi}, \text{ for } \xi \neq 0\right\} \\ u + \sigma_u \log\left(\lambda_u m\right), \text{ for } \xi = 0 \end{cases} \tag{6.1}$$

Equation 6.1, is solved using python. The maximum likelihood estimator is used to determine the μ location, α scale and ξ shape parameter. The resulting return value plot of the Generalized Pareto Distribution is presented in Figure 6.4. The GDP plots for all location and directions can be found in Appendix G and corresponding wave height in Table 6.1.

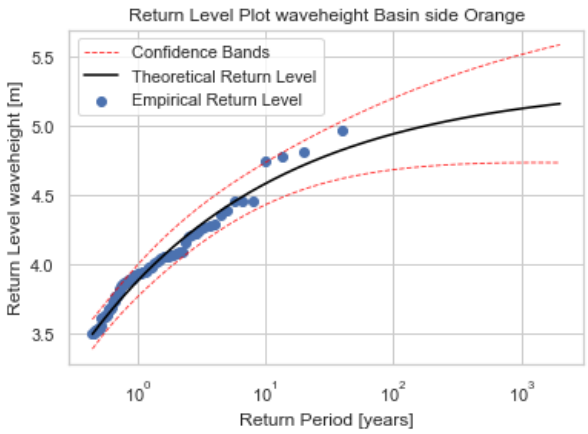

Figure 6.4: Extreme value analysis (GDP), Period in years, Return level (waveheight [m]), for Orange buoy Basin side.

Table 6.1: 1:20 000 per year Siginificant Wave Height per direction and trajectory

Dam Section	Ocean Side	Basin Side
Orange [m]	13.2	5.2
Green [m]	14	9.2
Yellow [m]	11.9	9.9
Pink [m]	11.9	10

6.1.2. Bi/Multivariate Copulae

The best way to describe a joint distribution function of two or more dependent stochastic variables is with Copulae [20]. Different dependence patterns can be induced while keeping the marginal distributions equal. Copulae are an essential feature and highly suitable for Monte Carlo simulations. A copula is a distribution on the unit square, meaning that its support is in [0,1], [0,1], with uniform marginal distributions [20]. The joint distribution can be written as:

$$H(x, y) = C\{F(x), G(y)\}, \quad x, y \in \mathbb{R} \tag{6.2}$$

Where $F(x)$ and $G(y)$= marginal distributions; and $C : [0, 1]^2$.

The main advantage of a copula is that it can represent every continuous bivariate distribution. The corresponding Copula can constantly be retrieved if the joint distribution and the margins are known. Traditionally, joint distributions were modeled using bivariate distribution; their behavior must be characterized by the same univariate distribution family and limited dependencies. These restrictions are avoided by using copulae.
For more than two dependent variables, a multivariate copula should be used. Two distribution functions implement the multivariate distribution by combining the marginal univariate distributions of Gaussian and Student-t. A distribution fit can be executed for three-dimensional cases using the Python class Multivariate distributions. There are other multivariate distribution functions, but determining the necessary parameters takes a lot of computational time and is quite tricky. Therefore only these two multivariate copulae are used.

A more elegant approach is to implement a multivariate distribution using Vine Copulae. This is a different approach for getting a higher-dimensional multivariate distribution. A vine copula is a d-dimensional copula consisting of d(d-1)/2 bivariate copulas. It is a nested set of trees consisting of n elements. An edge joins the edges of the tree j in tree j+1 if they share a common node [27]. The most commonly used type of vine is a regular vine. A regular vine is a particular case where the constraints are all 2-dimensional or conditional 2-dimensional. There are two subtype structures of a regular vine (R-vine), the C- Vine (canonical) and D-vine (drawable). The canonical vine has a central node that connects all the other nodes; the central node is the dominant variable. The drawable vine has only one path with no side branches. In this thesis, the maximum correlated parameters are three, namely wave height,

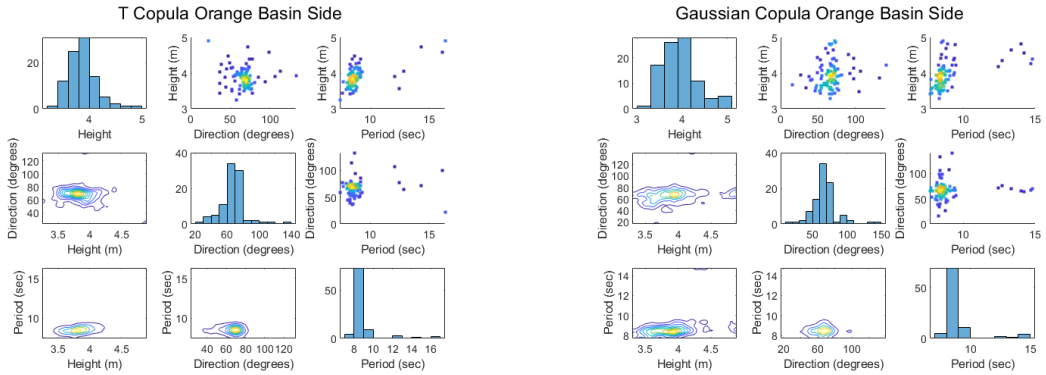

(a) T Copula, orange buoy.

(b) Gaussian Copula, orange buoy .

Figure 6.5: T and Gaussian copula Basin side orange buoy..

wave direction, and wave period, and therefore the C-Vine and D-vine have the same structure as the R-vine. The first tree of the vine, the dependence of the first and second variable, the second and third, and so on is modeled using paired Copula (1,2), (2,3), (3,4) [44]. The second tree consists of the conditional dependence of the first and the third note. The second mode is modeled as (1,3|2) etc. The following tree layer is then given as (1,4|2,3), and this is repeated until only two nodes are left.
The number of vine structures that can be formed depends on the number of variables (nodes) in the systems. Using equation below, the number of possible structures based on the number of nodes can be calculated.

$$\text{number of regular vines } = \begin{pmatrix} n \\ 2 \end{pmatrix} \times (n-2)! \times 2^{(n-2)(n-3)/2} \tag{6.3}$$

6.1.3. Modeling vine copula

The vine copula is computed using the MatVine tool of MATLAB. This program uses four different steps to complete the multivariate distribution. Wave data (Period, height, and direction) is used to construct the vine.

- Tree structure
  First, the structures of all possible combinations of nodes are constructed. Based on equation 6.3, the number of possible structures is three, consisting of two trees. The first tree is modeled with pairwise dependency, as shown in figure 6.6. The edges of each tree represent the bivariate distribution. The values in the figure corresponds to the data, where 1 is the wave height, 2 is the wave direction, and 3 is the wave period: the following step of the tree model is the conditional probability of the pairwise dependencies concerning the second variables. The tree structure can be rewritten in a matrix form and input in the MATvine Matlab tool.

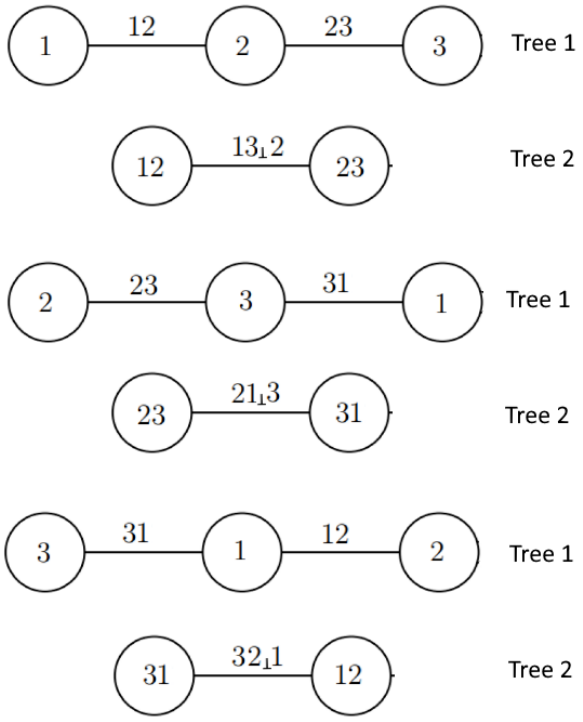

Figure 6.6: Regular vine, for three nodes, edges are bivariate copula.

- Copula selection and estimation
  The next step is the copula selection; 15 different kinds of Copula are fitted. MATvines uses the Maximum Likelihood estimator to determine the copulas for all the edges defined in the tree structure.
- Model evaluation
  After all the copulas are fitted, the combined distribution is compared to the data. This is performed using the AIC method (Akaike Information Criteria) [13]. The AIC used the likelihood estimator and the number of parameters to conclude the best model. A problem with such fitting models is overfitting, resulting in a less reliable model. Overfitting is prevented by assigning a penalty when the model uses too many parameters. The model with the lowest AIC score is considered best fitting. The AIC score depends on the likelihood estimator, which gives the probability that the parameters could be estimated from the distribution model. The equation is described as follows:

$$\text{AIC} = 2k - 2\log(L) \tag{6.4}$$

  where,
  k is the number of parameters.
  L is the liklihood estimator.

The vine structure that best fit the data is the Vine structure 2. An example of the bivariate distribution at the edges are shown in the table below.

Table 6.2: Copula at the edges of the best fitting vine, orange buoy ocean side.

Vine Structure 2	Edge	Copula
Tree 1	2,3 (direction, period) 3,1 (period, height)	*Plackett* *T*
Tree 2	2,1:3 (direction, height; period)	*Amhaq*

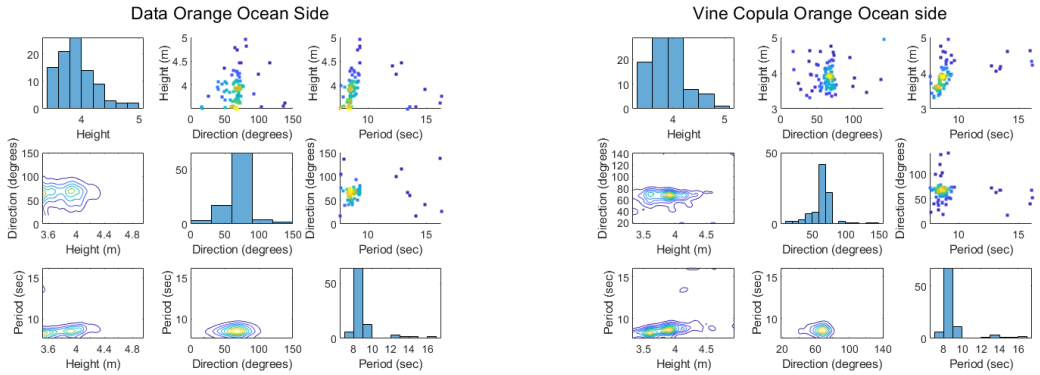

(a) Data, orange buoy.

(b) Vine Copula, orange buoy.

Figure 6.7: Data and Vine copula Basin side orange buoy.

- Verifications of the fits
  This step compares the three models (vines, T, and Gaussian) to the data. These are computed using two methods: the sum of the squared distance per cluster and the sum of the squared distances per variable. Using the sum of the squared distance, the error between the model ends the data is determined and partly determine the best model. The SSD per cluster is used to compare the 3D distribution of the models to the data. The latter will include the correlation between the variables. But first, the number of clusters should be determined. This is done using the silhouette score. The equation for the silhouette score is given below.

$$s(i) = \frac{b(i) - a(i)}{\max\{a(i), b(i)\}}, -1 \leq s(i) \leq 1 \tag{6.5}$$

  Where
  A is the intra-cluster distance, the distance between the sample point and the centroid.
  B is the distance of the sample to the nearest cluster.

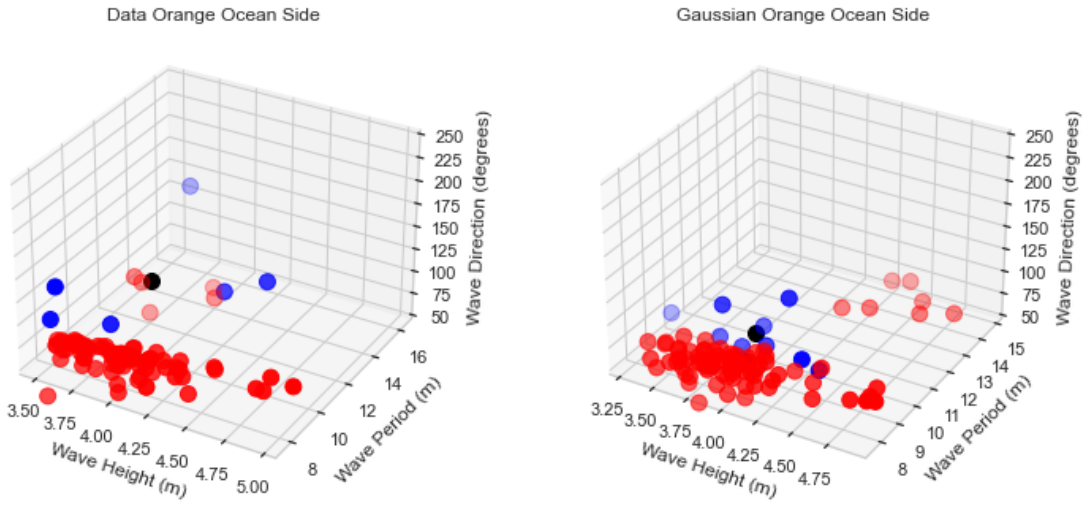

(a) Cluster Data, orange buoy.

(b) Cluster Gaussian, orange buoy.

Figure 6.8: Clusters Data and Gaussian ocean side orange buoy. The red and blue colors represent the two clusters, the centre of each cluster is indicated by a black dot.

The silhouette score ranges from 1 to -1; the optimal number of clusters is the case with the highest silhouette score. Based on the location of the centroid, the SSD is calculated for the data and all the models and compared. The scores for the fits are shown in Appendix G.

6.1.4. Wind setup/setdown

The wind setup is neglected at the basin's outer side because the wind setup is proportional to the water depth (less than 20 cm). The water set in motion in the upper layers can quickly spread out in deep water. This allows for vertical exchange, resulting in minimal wind setup [5]. The water depth is relatively deep, resulting in a maximum wind set in order of a few centimeters. At the lakeside of the dam, this effect cannot be neglected. The MDP [33], already did some calculations for the wind set up inside the basin. Wind setup is considered fully correlated with the wave data; the highest wind waves also from the direction with the longest fetch. In a closed lake, the volume is constant and, therefore, the inclination of the water level [54]. The water level tilts around its center of gravity resulting in one side of the lake to a water level increase (wind setup) and the other side in a decrease in water level (wind setdown). The MDP divided the north sea into a deep (100 meters) and shallower (40 meters)

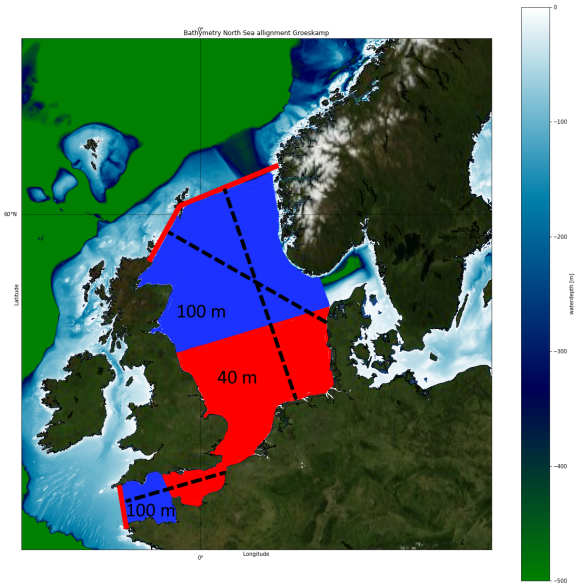

Figure 6.9: Wind setdown resulting from the dominant storm wind direction.

part and calculated the inclination for the maximum wind speed. This is only done for two-directions where the highest wind velocities (extreme storm directions), the directions are NW and SW. For the other directions, the wind setup is neglectable. From NW and SW direction results in a lowering of the water level this is called wind set down. For both direction a wind velocity of 35 m/s is taken, this results in the same inclination for both wind direction with the same depth. The set down influences the stability of the caisson and the height of the toe. The equation for wind setup/set down is given below.

$$\frac{\partial S}{\partial x} = C_2 \frac{u^2}{g \cdot d} \tag{6.6}$$

Where,
$\frac{\partial S}{\partial x}$ [-] is the horizontal bed slope.
C_2 [-] coefficient taking into account various effects (like temperature, humidity) ($3.5 * 10^{-6}$ to $4.0 * 10^{-6}$)
g [m/s2] is the gravitational constant.
d [m] is the water depth over the fetch.
u [m/s] is the wind velocity 10 m above the water surface.

The fetch length is being calculated by measuring the length of the basin perpendicular to the dam section, see Figure 6.9. The resulting set down of 1.3 meters at the innerside of the northern part and a setdown of 0.8 at the southern part

6.2. Model Setup

First the universal parameters are given in the table below. If there is no data about the distribution a representative deterministic value is used. Both sides of the dam are assessed. The reference frame

is changed to 180 degrees for the inner side, keeping the input parameters equal.

Table 6.3: General input parameters Monte Carlo analysis.

				Orange	**Yellow**	**Pink**	**Green**
Ocean Side							
Tidal Constituents	h_{tide}	Deterministic	[m]	M_2 2.6 S_2 0.9	M_2 0.6 S_2 0.2	M_2 0.6 S_2 0.2	M_2 0.8 S_2 0.3
MWL	h_{ocean}	Deterministic	[m]	100	110	395	105
Sea level rise Ocean		Deterministic	[m]	10	10	10	10
Multivariate Distribution				Gaussian μ, σ	Vine μ, σ	Gaussian μ, σ	Gaussian μ, σ
Wave Height	H_s		[m]	7.8, 0.3	7.0, 0.9	8.0, 0.8	8,8, 0.7
Wave Period	T_s	Probabilistic	[s]	14.25, 1.1	12.5, 1.2	13.7, 1.1	14.0, 1.0
Wave Direction	α		[°]	258, 54.2	300, 100.8	291, 31	287, 34
Basin Side (no tide)							
MWL	h_{basin}	Deterministic	[m]	100	110	395	105
Wind setup basin		Determinsitic	[m]	-0.8	-1.3	-1.3	-1.3
Multivariate Distribution				Gaussian μ, σ	Gaussian μ, σ	Vine μ, σ	Gaussian μ, σ
Wave Height	H_s		[m]	4.3, 0.3	6.9, 0.7	5.7, 0.6	5.7, 0.6
Wave Period	T_s	Probabilistic	[s]	9.3, 1.1	11.1 0.6	10.8, 0.8	10.8, 0.8
Wave Direction	α		[°]	77, 54	161, 23	204, 11	198, 6
Position Trajectory		Deterministic	[°]	105	40	40	60

The equations below highlights all simplified limit-state function for each of the failure mechanisms. The other parameters and complete limit state functions are shown in Appendix H.

$$
\begin{aligned}
&Overtopping: && Z_1 = q_{crit} - q \\
&Sliding: && Z_2 = \mu(Mg - U) - 1.2p \\
&Tilting: && Z_3 = (Mgt - M_U) - 1.2M_p \\
&Revetment\ Stability: && Z_4 = d_n - d_{crit} \\
&Toe\ Stability: && Z_5 = d_{toe} - d_{crit}
\end{aligned}
$$

Table 6.4 shows the design water level and wave height used for the deterministic approach. To show the dispersion of the wave height the 1:1 per year wave height is shown. The distribution is unknown for water level, and therefore only the design levels are shown. The design water levels (DWL) are according to Chart Datum. The design water level is comprised of 4 levels.

- The mean sea level (MSL), is the average between MLWN and MHWN.
- The highest astronomical tide (MHWS)
- The wind setup.
- The sea-level rise (SLR)

Table 6.4: The deterministic values for Wave height and design water level. The distributions for design water level are unknown, and therefore only the design value is presented.

	Wave Height		Design Water Level (mCD)
Ocean Side	1:1 per year	1:20 000 per year	1:20 000 per year
Orange [m]	8.5	13.2	13.9
Green [m]	10.2	14	11.4
Yellow [m]	8	11.9	10.8
Pink [m]	8	11.9	10.8
Basin Side			
Orange [m]	3.8	5.2	-0.8
Green [m]	6	9.2	-1.3
Yellow [m]	7.3	9.9	-1.3
Pink [m]	6.5	10	-1.3

6.2.1. Overtopping Earthendam

First, the overtopping is assessed. The maximum allowable overtopping is already determined in the previous chapter for both USL and SLS conditions. The mean value probabilistic overtopping equations are retrieved from the Eurotop manual [19]. The model is made in Python, using multiple core processing, resulting in reduced computing time. In the previous chapter, the minimum amount of runs is calculated to reach a reasonable conclusion. It takes approximately three-quarters of an hour to do 1 billion iterations, which is doable. The design conditions determine the minimum height of the dam, for which all conditions are met. The equation and the variables are all elaborated in Appendix H. Some simplifications that are made are listed below.

- The wave run-up, reduction factor of the berm, and representative slope all depend on each other. An iterative approach is used to solve this. First, an initial guess is made on the wave run-up; the wave run-up is set to 1.5 times the wave height. The gamma beta, Irribaren number, representative slope, and wave run-up are calculated based on the berm location. To save computational time, this is repeated six times.
- The values for the tidal constituents and the water depth are determined deterministically.
- The berm length is a maximum 1/4 of the deepwater wavelength; otherwise, interpolation should be used. The length of the berm is determined based on extreme conditions where this condition is met.

Input

The maximum allowable failure probability is determined in Chapter 5 for the ULS and SLS cases. The slope of the berm is set to 0, which corresponds to a horizontal berm. The slope of the armor layer is set to 1/1.5, based on the supplier recommendations. The slope is for the interlocking elements. A conservative value of the friction coefficient of 0.45 is chosen, which corresponds to the interlocking revetment (Xblocs) [8]. The berm has a maximum effect when it is placed at still water level. The still water level solely depends on the tide. In Table 6.3, all other parameters are summarized.

6.2.2. Overtopping Caisson Dam

The equation or overtopping of a caisson slightly differs from the sloped dam. The steps from the Eurotop manual are followed for the wall overtopping. The simplifications that are applied are:

- Only non-impulsive conditions prevail, with a minimum water depth of 100 meters, impulsive conditions are very unlikely.
- The presence of a mound is neglected, according to the Europtop manual, if the water depth exceeds 60% of the water depth at the top influence of the mound is significant. This is clearly not the case.
- The same adjusting equation is used for oblique waves as for overtopping on a slope.

Input

The input parameters are the same as for the slope overtopping and are given in Table 6.3. Same additional parameters are the influence factor of the roughness and permeability on the slope, which is set to 1. And the slope angel $\cot \alpha = 0$.

6.2.3. Caisson Sliding and Tilting

The equations that are put into the model are all retrieved from the research by Goda [21]. Some adjustments are made to include the difference in hydrostatic pressure. In the model same simplifications and assumptions are used; these are listed below.

- The equations of wave attack on caisson from Goda are used. These equations are based on Japanese breakwater research and will need to be adjusted for the extremely deep caissons in the trench. The applicability in extreme deepwater conditions is unknown; further research is necessary when this type of construction is chosen.
- A 10-meter high sill is chosen; this value is based on the deepwater caisson at the Spanish coast.
- No adjustment factor is used for oblique waves because the change in wave height and period is already considered.
- The angle foreshore is assumed to be very small, so the water depth at 5 times the wave height is equal to the water depth at the caisson.
- Goda uses a safety factor for both sliding and tilting of 1.2. Because a fully probabilistic method is used, the safety factor is set to 1.

Input

The same parameters are used as Table 6.3. Additional parameters are the density of the concrete 2400 kg/m^3, wet sand density 1922 kg/m^3, and saltwater $1030kg/m^3$. The friction coefficient between concrete and sand is set to 0.4 [8].

6.2.4. Revetment and Toe

For the revetment, two types of equations are used; the Van der Meer and Izbash equation. First, a riprap revetment (quarry stone) is calculated, the cheapest armor layer type. If the needed nominal rock diameter is too big, an interlocking revetment is used. For the Northern European enclosure dam, Xbloc are chosen because of their proven reliability. Also, the required nominal rock diameter for the toe is calculated, the equation used in the Van der Meer. For the design of the Xblocs the Xblocs manual is used [9].

Input

The toe's location is determined iteratively; a beginning assumption is one wave height below the lowest still water level. The effect of oblique waves is taken into account, and the change in wave height is described in the overtopping manual [19]. The damage level for toe stability used is 4 for the ULS condition and 1 for SLS. For riprap, this value is 8 for ULS and 5 for SLS. And for the interlocking armor layer, no damage is allowed. For Xblocs, a correction factor should be used if one of the following criteria apply:

- Water depth is significant.
- Core permeability is low.
- The foreshore is steep.
- The armor slope is mild.

The correction factors for these local phenomena can be found in the Xbloc manual. If more of the above criteria is applicable, the largest factor should be used. For the NEED the correction factor is 2.

6.3. Results

In Table 6.5 the dimensions for both the earthen dam and the caisson dam are shown. The values are retrieved using the fully probabilistic method described in Chapter 5. The ULS state was governing for most of the failure mechanisms, except for caisson overtopping. The width and height parameters are assessed fully probabilistically by using steps of one meter until the previously set requirement are met. Smaller measures are used for the volume of rock and Xblocs. The properties of the dam that are determined deterministically and described in the section below.

Table 6.5: Main dimensions Caisson and Earthen dam, assessed fully probabilistically, using standard gradings EN133383.

	Orange	Yellow	Pink	Green
Crest Outer [m]	136	144	430	148
Crest Inner [m]	112	130	416	127
Berm Height outer wrt MSL [m]	3.5	0.6	0.6	1.1
Caisson Height [m]	127	132	420	138
Caisson Width [m]	70	70	240	80
Volume outer Xblocs [m^3]	208	176	180	144
Volume inner Xblocs [m^3]	26	90	114	82
Dn50 toe Inner [m]	1.1	1.3	1.3	1.4
Grading toe Inner [-]	HMA 3000-6000	HMA 6000-10000	HMA 6000-10000	HMA 6000-10000
Height toe inner wrt MSL [m]	8-10	16-21	16-21	14.4-19.4
Dn50 toe outer [m]	1.55	1.4	1.3	1.4
Grading toe Outer [-]	HMA 6000-10000	HMA 6000-10000	HMA 6000-10000	HMA 6000-10000
Height Toe outer wrt MSL [m]	23.5-18.5	15-20	15-20	18-23

6.3.1. Design Earthen dam

The width near the bottom of the earthen dam is more than a kilometer due to the minimum angle of internal friction of sand. The minimum angle for stable under water sand slope is 1:5. The reason for using sand as building material for the dam is that it is widely available. Sand is easily extractable as the sublayer of the North Sea bottom consists for the most part of a thick layer of sand. The width and height is slightly reduced by using a berm. The berm is placed at the maximum still water level to reduce overtopping by changing the effective slope angle (making the dam less steep) and influencing the breaking pattern.

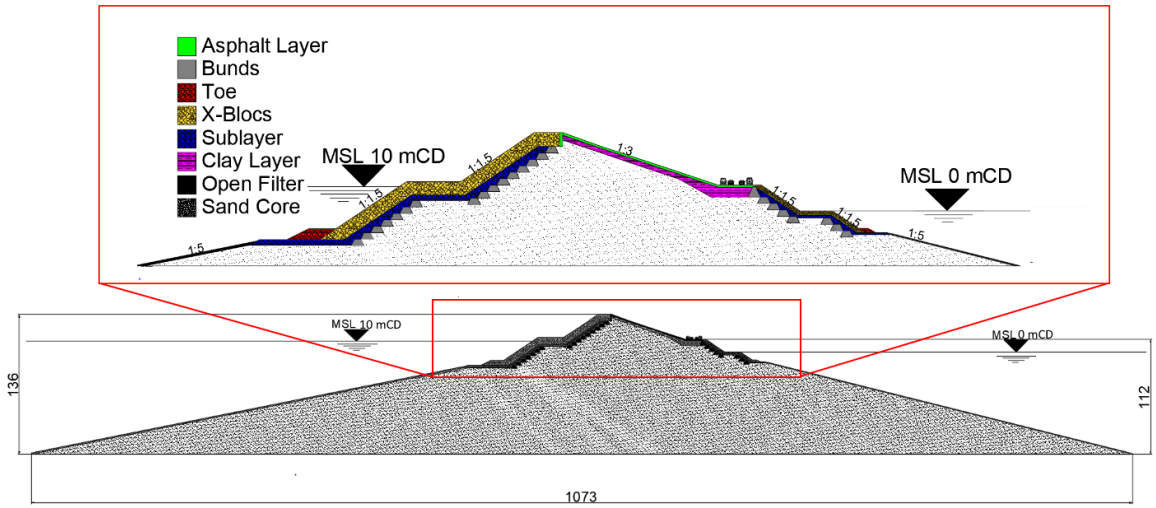

Figure 6.10: The earthen dam, units in meters.

Toe

The toe's primary function is to support the armor layer. The recommended toe location is one wave height below the lowest still water level, limiting the wave action on the toe. Below this water depth, only light protection is sufficient. According to the research by Van Der Meer and D'Angremnond [50], the height of the toe should be at least between 2-3 Dn50 of the toe.

Open Filter

The main difference between a geometrically closed and open filter is that no material can be washed out from a closed filter. To protect the sand core from eroding, a geotextile is applied to make the filter completely closed for the part above the toe. For deeper water depths constructing a geotextile is complicated; an alternative is an open filter. The filter layer is designed to minimize the hydraulic

loading onto the base layer to keep the amount of erosion within a specific range. The equations from the study by Klein Bretler and Den Adel [56] are used and explained in Appendix H.

Armor Layer
The armor layer consists of Xblocs. Xblocs are chosen for their reliability, interlocking properties and can be randomly placed. Ordinary quarry stone revetment is impossible to use because of the required stone size. Xbloc's main advantage compared to other revetment types are the interlocking properties, the porosity of the Xbloc armor layer is high, and the concrete consumption is low. The Xblock is designed to reduce the required diameter needed to be stable under severe storm conditions. Xblocs require a slope of 1:4/3 to 1:1.15, which is impossible to make with sand. Bunds are used to create this slope. Bunds are cascaded stacked to create such a steep slope. These bunds can be made out of gabions or concrete units. The latter is already applied to water depths up to 30 meters.
A road is placed on the crest of the inner side of the dam, with a width of 20 meters. The road consists of 2 lanes in both directions. There is also space to place a railway track on top of the dam.
The basin is large enough that the amount of overtopping will not significantly increase the water level. The limiting overtopping factor is the resistance to the overtopping of the dam. Usually, a dam has grass protection, which can only handle small amounts overtopping. A more expensive solution is an asphalt protection, it can resist a relatively high overtopping discharge, and is therefore used. A clay layer below the asphalt ensures that the upwards water pressure is compensated. At both ends of the asphalt layer a transition zone is created to prevent pressure from building up at the ends.

6.3.2. Design Caisson

The caisson dam consists of individual elements the caissons. Caissons are stacked on and next to each other to create an impermeable wall which has a sufficient height and length. The caissons are filled with sand to make them unmovable. A sill is designed to distribute the load onto the seabed and is made out of sand. It is also essential that the caisson is placed on a flat surface; unequal surfaces create significant stresses in the caisson. It is very costly and time-consuming to make each caisson a different height. A cheaper solution is to vary in size of the sill, making all the caisson equal height. The sill needs to be protected against the waves to prevent scour near the caisson; although the wave action is limited at such a depth, scour can still occur.

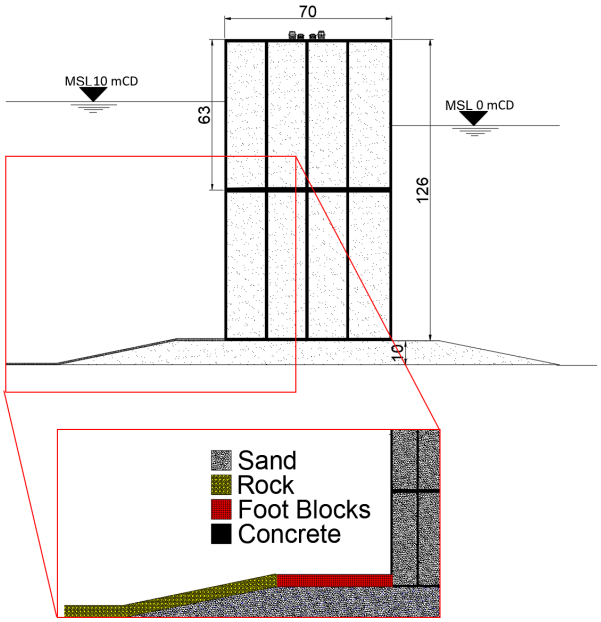

Figure 6.11: The caisson dam, units in meters.

Toe Protection and armor layer
In front of the caisson, toe scour or slope scour could occur. Foot protection next to the caisson pre-

vents toe scour and minimizes the risk of failure. Goda advised placing Japanese foot protection blocks at both sides of the caisson. The size of the block is determined by using the CEM manual [1]. Due to a lack of uncertainty, the equations are solved deterministically using extreme values given in Appendix G. The thickness depends on the ratio of the still water level on top of the sill, the still water in front of the sill and the maximum wave height, explained in Appendix H. The resulting blocks are displayed in the AutoCAD drawings. A filter is used next to the Japanese blocks based on appendix H using quarry stones. The protection consists of a layer of quarry stone revetment. The nominal diameter of the quarry stones is calculated using the equation by Tanimoto. The equations are explained in Appendix H.

Dimenions Caissons
The height of the dam is determined based on the SLS condition for overtopping. The dam shouldn't be closed many times a year due to a large amount of overtopping. Resulting in an SLS condition of 1 time per year. In this thesis, a simple box shape caisson is used. It is possible to optimize the caisson by taking the overtopping heights from both sides into account. The water level at the basin side is 10 meter lower, so there is room for optimization. By chancing the shape of the caisson, the complexity increases and has an influence on the stability of sliding and tilting.
The width of the caisson depends on the stability against tilting and sliding. The minimum width of the dam is 20 meters to place a road on top of it.

For both earthen and caisson dam the piping model from the research of Sellmeijer is used. The Sellmeijer equations calculated the point where the hydraulic head difference and the grains are in equilibrium. Due to a lack of information, the calculations are performed deterministically. An important unknown is the thickness of the sand layer. In the future location of the dam, no CPT cone penetration test or bore sample is made. Dinoloket provides CPT's and bore monsters of the entire Dutch territory, including the Dutch North sea. This provides information on the variation of the sand layer thickness. According to Dinoloket, the thickness ranges between 2 and 20 meters. These range is used, the result is that for all 4 location the risk of piping is minimal.

On scale AutoCad drawings of all design can be found in Appendix I

6.4. Difference between the two Concepts

Material
The availability of the materials will significantly impact the feasibility of the earthen dam. The main difference between the two dam types is their size. For a water depth of 100 meters, the width of the earthen dam at the bottom is more than a kilometer, and for the deeper parts, it is far wider. Erosion during construction results in a much higher production of sand to account for the losses.

The impact on the sea bottom due to the need for sand will be far less for the caisson dam than for the earthen dam. The caisson dam requires seven times less material than the earthen dam. The vertical structure needs a smaller width than the earthen dam to be stable. Furthermore, research into the costs of an earthen dam concluded that sand is the biggest expense of constructing the dam [37]—sand accounts for 95 percent of the total costs of the earthen dam NEED. Reducing the amount of material will therefore also reduce the costs. For this reason, caisson breakwaters are used for a water depth of more than 15 meters instead of a rubble mound.

Duration
The required amount of volume to construct the NEED determines the duration primarily. A significant number of dredging vessels and materials are required. When more ships are available different sections could be built simultaneously. The same is true for the production of caisson units; when there is plenty of material and labor, the units could be produced in large quantities and transported by tugboats to the location. The alignment can be subdivided into different sections placing the caissons from both sides for each section. The premanufacture of the caisson will result in a far shorter construction time of the dam compared to the earthen dam.

A great obstacle forms the manageable size of the caisson. There are no limitations for constructing a larger caisson; it is proven for caisson sizes up to 75 meters [36]. But transporting it to the final location is the bottleneck. A smaller caisson can be used, which could be stacked up to reach the required higher elevation, but this complicates the placings and makes the caisson dam more expensive. Accurate placing in deep wavy seas is complicated and hard to achieve. Stacking the caisson introduces new failure mechanisms that should be quantified to develop a good design. The deep wavy sea also complicates the transportation of the caisson as the dam's location is far from any production sites. A new method of production and transportation could be developed to make the placement and production less complicated. Nowadays, new vessels can lift entire oil platforms; these types can also be used to transport and place the caissons.

The construction of the core of the earthen dam is less complicated, although a large number of losses should not be underestimated. The seafloor consists mostly of sand reducing the transportation cost and time. Large parts of the North sea need to be dredged to collect the required amount of sand; this will harm local marine life and could be detrimental to the ecology

Adaptability
The adaptability of the dam is an important aspect as the amount of sea-level rise is quite uncertain. During the lifetime, it is possible that the height must be increased to fulfill the required safety. The caisson dam could be quite adaptable if it is considered during design. A new layer could be added to increase its size. A change in design for the earthen dam will impact the entire cross-section of the dam and is therefore far more difficult and costly.

Xblocs
The armor layer of the earthen dam is made of Xblocs. The diameter of the Xblocs becomes very large. The Xblocs needed for the NEED exceed a volume of 100 cubic meters. The current largest Xblocs have a volume of 20 cubic meters. Extensive testing is necessary to prove their stability when implementing these interlocking elements. The elements must be placed with some degree of accuracy; the on-sea conditions and the extreme weight of the elements will complicate that.

To summarize:

- The earthen dam requires seven times more material than the caisson dam.
- Sand accounts for 95% of the total costs of the earthen dam NEED [37].
- No structural limitation height caisson, transportation forms the bottleneck. Smaller caissons could be stacked to reach the required size but introduce new failure mechanisms.
- Caisson dam more adaptable in height.
- Earthen dam requires extremely large Xblocs, which are difficult to place.
- For breakwaters, caissons are used if water depth exceeds 15 m.

Based on the above arguments, it is concluded that a caisson dam is the most appropriate solution for the NEED. Further research should conclude whether this is the more feasible solution or a combination of both concepts is possible.

6.5. Conclusion and Feasibility

This chapter proposes two different designs, the caisson dam, and the earthen dam. First, the data is analyzed and fitted using multivariate copula. These copulae are then used for the fully probabilistic analysis. The criteria that are assessed fully probabilistically are: overtopping earthen and caisson dam, stability revetment and toe, caisson sliding, and tilting.
The remaining failure mechanism: piping, open filter revetment, and the toe protection caisson, are assessed deterministically. Lastly, the two dam designs are compared; based on this comparison, the caisson dam is more technically feasible.
The caisson dam comes with different challenges. The enormous size has never been built before. Although there is no structural limit for the size of the caisson, extensive testing is necessary to investigate the behavior under wave exposure. The bottleneck that limits the caissons' size is the transportation from the building site to the final location. This could be solved by building smaller caissons stacked to

reach the necessary height. The stacking of caisson poses new failure mechanisms, which should be tested.
The foundation is fundamental due to the immense weight of the caisson. For the deepest part, the pressure on the seafloor due to the dam is 4000 kN/m^2. This is more than four times the pressure under the great pyramid of Khufu. The immense weight can result in subsidence of the caisson leading to pressure built up and cracks in the concrete—an investigation into the bearing capacity of the soil essential. If the bearing capacity of the bottom is not adequate, a soil improvement method or a reinforcement foundation could turn out to be necessary.

7

Project Execution Plan

This chapter provides an initial estimation of construction times based on key figures and traditional construction methods for the caisson dam. In reality, multiple work fronts and innovative execution methods will increase efficiency and reduce execution times. The material used and main production stages are explained, and the duration is estimated.

7.1. Production Calculation

In this section, calculations are made for the material use of the NEED. The main dimensions of different components of the NEED are based on to the technical drawings in Appendix I, the material volume calculations are performed for the four sections.

7.1.1. Sand Sill

The caissons are founded on a sand sill; the shape of the sill is trapezoidal, with the dimensions determined according to the technical drawing. Only the width of the sill is different over the sections. In the deep trench, the first layer of the subsoil needs to be removed and replaced by a sand layer. The thickness of that layer is unknown and disregarded for this thesis.

7.1.2. Japanese foot block

The dimensions of the foot block protection are determined in Chapter H. Standard dimensions were used, which resulted in the same sizes for each of the sections. The dimensions l x b x t are, 2.5, 1.5, 0.8 respectively. That means that the cross-section consists of 8 foot blocks on each side of the caisson. Below the foot block, a small layer of rubble mount is necessary to prevent erosion. The need for blocks differ per section and side of the caisson.

7.1.3. Scoure Protection and Geotextile

The the scour protection extends to 1/4 of the wavelength. The protection layer protects the sill from eroding. The needed diameter and thickness depend on the location of the protection layer. A geotextile is present to prevent the sand layer from eroding. The geotextile can be placed using a fascine mattresses and should cover the entire area of the protection layer. The geotextile is a woven type which allows the connection to the faggots. Typical dimensions of a fascine mattrasses are 100 meter long an 16-20 meter wide [45]. The total required volume of the protection layer per median rock diameter differ per section.

7.1.4. Caissons and fill

The caissons consist of a wall thickness of 1 meter with the crown on top. Multiple 1 meter thick walls support the crown. The following concrete masses are based on the dimensions found in Chapter 6. The amount of rebar inside the concrete is disregarded. The sand filling inside the caissons is calculated per compartment inside the caissons. Multiplying by the total section length, the total volume of the

sand filling is calculated. The resulting volumes for each component and section are shown in the Table below.

Table 7.1: Production most important materials caisson dam.

	Orange	Green	Yellow	Pink	Total
Dimension caisson LXBXH [m]	50X70X63	50X80X69	50X70X67	50X60X53	-
Total caissons [-]	6440	5800	7240	96 000	115 480
Length Section [km]	161	145	181	150	637
Japanese foot Blocks [-]	0.9E6	1.5E6	2E6	-	4.4E6
Sand Sill [m^3]	226E6	218E6	254E6	456E6	1154E6
Grading inner Slope	-	LMA 40-200	LMA 40-200	-	-
Volume Armor inner Slope [m^3]	-	2.7E6	4.6E6	-	-
Grading outer Slope	LMA 15-300	LMA 60-300	LMA 40-200	-	-
Volume Armor outer Slope	9.2E6	6.6E6	6.2E6	-	-
Concrete Caisson [m^3]	146E6	146E6	172E6	1530E6	1994E6
Sand Fill [m^3]	1299E6	1561E6	1552E6	12096E6	16508E6
Scour Protection [m^2]	19E6	31E6	40E6	-	90E6

The main construction components are the caissons and the Japanese toe protection blocks. These will be manufactured near the site to reduce the costs. Temporary dry docks can be constructed in sheltered estuaries to minimize transportation costs. After completion of the caissons the dry dock can be filled with water to transport the caisson to its final destination. The Japanese toe protection blocks can be manufactured at the existing factories. The quarry stones are obtained from the mines in Norway, and sand can be dredged nearby the dam.

7.1.5. Material feasibility

Table 7.1 shows the volume of materials used to construct the NEED. The quantities of a project of this magnitude are difficult to visualize; therefore, the amounts are compared to the world wide production capacity. The most used construction material is sand. In total, 25 billion tons of sand (density 1400 kg/m^3) are needed to fill the caissons and construct the sill. The volume of sand required is approximately equal to half the world's yearly production [38]. The bottom of the North Sea consists of more than 80% of sand, with a total surface area of 575.000 km^2, only a layer of 4 cm needs to be dredged to fill the caissons and construct the sill.
The caissons are made out of concrete; concrete is made out of cement 15%, sand 30%, gravel 45%, and water 10%. The total amount of concrete used for the NEED is about the world's total yearly production [38].
The rocks and concrete blocks needed for the armor layer is less of a problem; wider grading could increase the availability.
The amount of material required for the NEED is enormous, this has a effect on the environment. The concrete industry is responsible for 8% of the yearly global CO2 emissions. The dam will therefore contribute significantly to global warming. The extraction of the materials also damages ecosystems. All these effects will have to be included in further research into he effects of the NEED.

7.2. Production Planning

In the following section, a rough estimation is made for the total duration of constructing the NEED. First, the construction phases are analyzed. Based on the steps, an estimate is made for the total time.

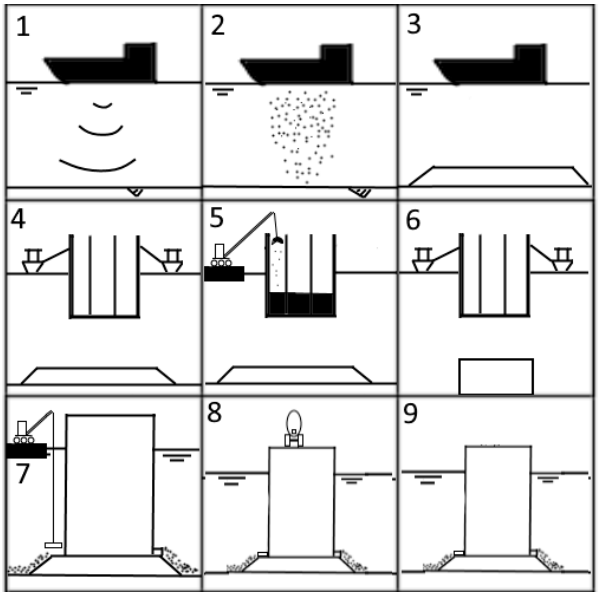

Figure 7.1: Phases of construction execution.

1. A **bottom survey** is executed to obtain information about the geotechnical properties. Many data are already available, so the survey should focus on the less analyzed areas. The survey consists of bottom samples to determine the grain size distribution, bathymetry and CPT's. The estimated time to collect and analyze all the data is in the order of a year. The duration may differ based on the findings.

2. The next step is to prepare the bed by **removing irregularities** and weak layers.

3. Next is **constructing the sand sill**. Hopper dredgers suck relatively loose bed material and load it inside the vessel. This material is then dumped at the location. The average hopper dredger has a capacity of 2.44 m^3/s [53]. The capacity is reduced to 1.95 m^3/s (construction nearby the source), when considering the overflow and erosions losses. The four largest dredging companies, Van Oord(22), Boskalis(17), DEME (21), and De Nul(30), have a combined capacity of 175 m^3/s. Most dredgers have a wave height restriction of 3 m high waves. This resulted in a 65 % workability for the Northern part of the NEED and 60 % for the southern part. Figure 7.2 shows the distribution of the daily maximum wave height of the different months. The wave climate is milder during the summer months, resulting in higher workability. With the brightest scenario and continuous dredging (day and night), the entire sill could be constructed in half a year.

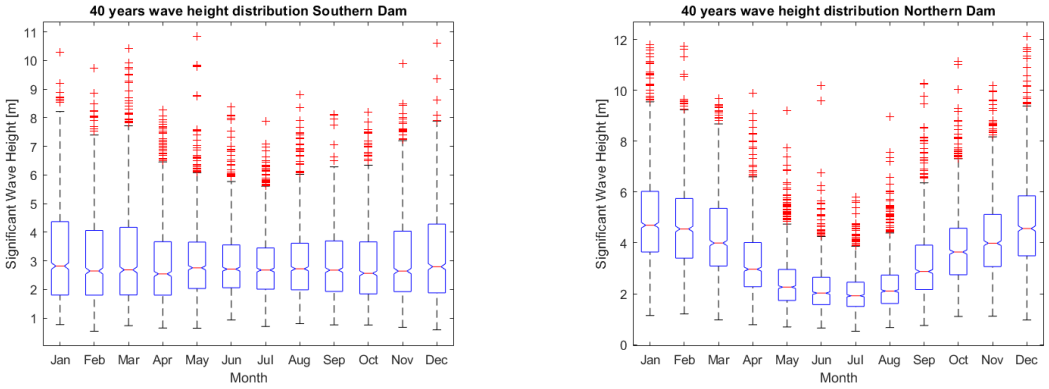

(a) Wave height distribution Southern dam 1

(b) Wave height distribution Northern dam 2

Figure 7.2: Boxplot of the 40 years wave height distribution per month.

4. When the sill is constructed, the **caissons can be placed on top**. Steps 2 and 3 can occur almost simultaneously, reducing the total construction time. Two massive dry docks are used to construct the caissons; these are located at the southern and the northern dams. After completing the caisson, they need to be transported to the dam location. The required power to transport the caisson to its final destination depends on the size of the submerged part of the caisson. To transport the caisson, the center of buoyance plus the metacenter height should be above the center of mass; this results in the caisson being in a stable equilibrium. A minor disturbance will result in a return in the original position [52]. Stable equilibrium can be reached by placing a mass (sand) inside the caisson. This increases the metacenter height and thereby its stability. For the largest caisson, this results in a draught of the governing caisson (green) 20 m.
   The total pulling force required is 560 000 kN (666 666 kW) velocity 5 m/s and drag coefficient 4 [52]. The current most powerful tug boat is the Island Victoria (42 880 HP); it requires 12 tugboats to transport the caissons to their final destination. A more realistic scenario is to develop a construction vessel that can move and place the caissons. The current largest construction vessel is the Pioneering Spirit; it can lift 75% of the largest caissons used for the NEED. Improvement of the design of this ship will allow the transportation and placement of the caissons. The duration of the placings of the caisson depends on the available ships. In the scenario where enough transportation capacity is available and working from both sides for each of the four sections, the duration solely depends on the weather conditions and the sinking procedure. Using the Veerse Gat closure as a reference and extrapolating the sinking and connecting process, the duration of placing is about 1/2 a day (positioning, sinking, and connections).

5. The **caisson is filled with water to let it sink** to the sill in a controlled way. When the caisson is in the correct position, it is filled with sand. A large part of the worldwide dredging capacity is already needed to build the sill. The volume of sand to fill the caissons is much larger. As a result, it can be concluded that the current dredging capacity is not sufficient to close the dam within the foreseeable future.

6. Depending on the depth, another **caisson is placed on top**. Placing a caissons takes approximately 12.5 hours as explained in the chapter 8. This results in the total construction time (step 4, 5,6) for the Orange, Yellow, and Green section closure of approximately 15 years each. The pink section will take 146 years to complete. Larger caissons and subdivisions into smaller sections could decrease the time. The downside is that it will increase the costs and is sensitive to errors.

7. The next step is to **sink the fascine mattresses**. On top of the mattresses, a protection layer and Japanese toe protection blocks are placed at both sides of the dam. This can essentially take place during the placement of the caisson. A sinking beam is used at the end of the fascine mattress to cause the mattress to sink. A side stone dumper is used to drop the stones on the mattress to give it stability. If the mattress is entirely on the bottom, the sinking beam is disconnected and used for the next mattress [45]. Cranes are used to place the **foot protection blocks on the sill**. The duration depends on the number of vessels and cranes used. The protection layer and foot blocs are relatively thin, hardly affecting the project's total time. The placings can be done simultaneously with other phases.

8. After the caissons and protection has been completed. The necessary **infrastructure is installed**, and the connections of the caisson are checked.

9. **Continuous monitoring** during the lifetime of the caisson is essential to minimize the risk of failure.

7.3. Conclusion

The duration of the project is highly uncertain. The type of transportation and the number of vessels used positively influence the duration of this phase. Estimates of the duration per phase are made

based on current techniques. The most time-consuming phase is the placements of the caissons especially for the deep trench section.

8

Design of the final Closure

This chapter explains the final closure of the NEED. The closure procedure for both the southern and northern parts of the NEED are analyzed. An overview is made of the models used to determine the flow velocity through the final gaps. A procedure is proposed based on the model results.

8.1. Closure

There are generally three different closure types: rock, sand, and caissons. The most technically feasible dam design discussed in the previous chapter is a caisson structure. Therefore, the apparent closure structure is also the sudden caisson closure. A sand closure is impossible due to the losses, and a rock closure will require a tremendous amount of rock to create the closure.
The flow inside the closure gap depends on the height of the tide outside the basin. A favorable location for the final closure is where the tidal amplitude is lowest; this results in the lowest velocities during closure. Other aspects that should be considered include the availability of materials and equipment. It is assumed that the material and equipment needed do not constitute an obstacle. Figure 8.1, shows a model of the tide, including a cross-section of the average flow velocity at the location of the dam. The vertical tide near the Norwegian coast is minimum. In the English channel, the largest tidal amplitudes are present.

8.1.1. Phasing of the closure

The flow velocity through the Strait of Dover is relatively low, ranging from 1 to -1 m/s [51]. The cross-sectional area of the Strait is also very small; therefore, the basin can be seen as two independent parts. The two parts consist of The English Channel part and the North Sea, as shown in Figure 8.2. The English Channel is blocked first from the Atlantic ocean, further decreasing the discharge through the Strait as modeled by Groeskamp et al. [22]. After the southern closure, the northern part of the NEED is closed, completing the dam.
The closure of either of the two parts can be distinguished into three different phases. These phases are based on the water depth at the dam. The phases are: closing the shallow area first, closing the deep area first, and a simultaneous closure (a horizontal or vertical closure over the entire length). The phasing is essential as it influences the flow conditions through the gap. The advantage of closing the shallow area first is that the flow velocities will not increase that much, making it relatively easy to close the gap. The limited flow results in smaller and lighter bed protection needed to prevent scour. When closing the deep part first, the flow velocity on the shallow area will increase. This increase results in erosion over the entire length of the site. To minimize erosion, bed protection is needed over a wider area. The advantage is that generally, the closure costs are less when the deep parts are closed first [25].
For the northern part of the NEED, it is preferred to closure the shallow parts first. The reason is the lower tidal amplitude and flow velocities. Figure 8.1 clearly shows that the flow velocities in the shallow part of the dam location are minimum. This makes placing the caisson in those parts relatively easy. The southern part of the NEED has no deep parts; the phasing does not matter much.

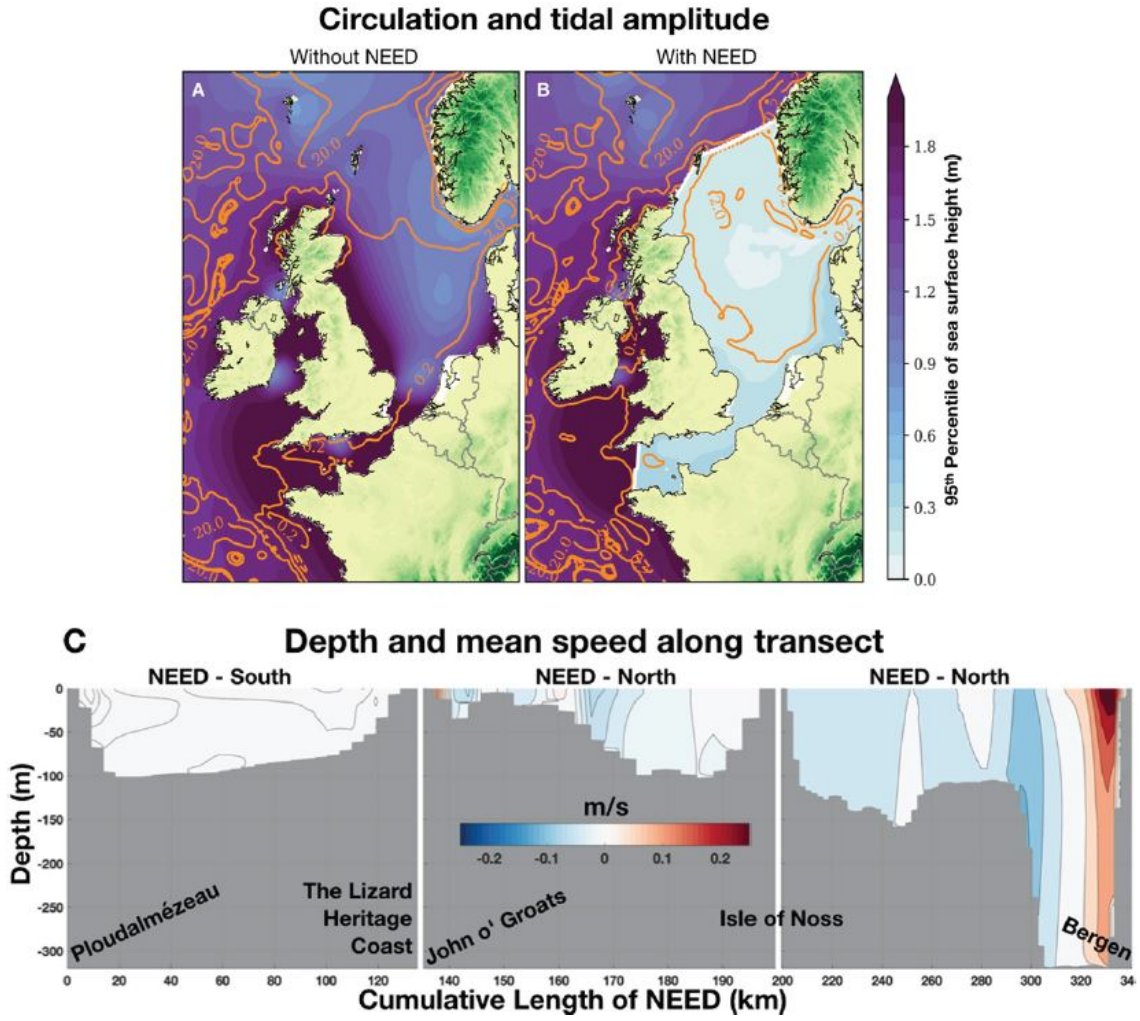

Figure 8.1: The bathymetry of the cross section traversed by NEED, split into its southern and northern components [22].

8.1.2. Overview

The two sections are considered separately as two enclosed areas, meaning that only at the final gap can water flow into the ocean and discharge through the Strait.

Northen Basin

The northern storage basin is best defined by neglecting the discharge through the English Channel (southern dam is constructed first) and the Kattegat. A rectangle is formed with the dimensions 625 km by 825 km [33]. The depth varies along the length of the basin. It ranges between 20-40 meters below sea level near the Dutch coast and 100 – 140 meters near the dam. The difference in depth can only be considered in 1 direction because of the 1D numerical model, explained in the section below. The difference in depth is taken by averaging three cross-sections of the North Sea. Further investigation using a 3d model should quantify the effect of the difference in depth.

Southern Basin

The southern part of the north sea (the English channel) is schematized as a rectangle of 500 km by 100 km, with a linear water depth starting at 100 meters near the dam and less than 40 meters at the Strait. A limited amount of water can flow through the Strait. The discharge through the Strait will decrease during the closure procedure. This decrease is not considered in the model as the effect is negligible.

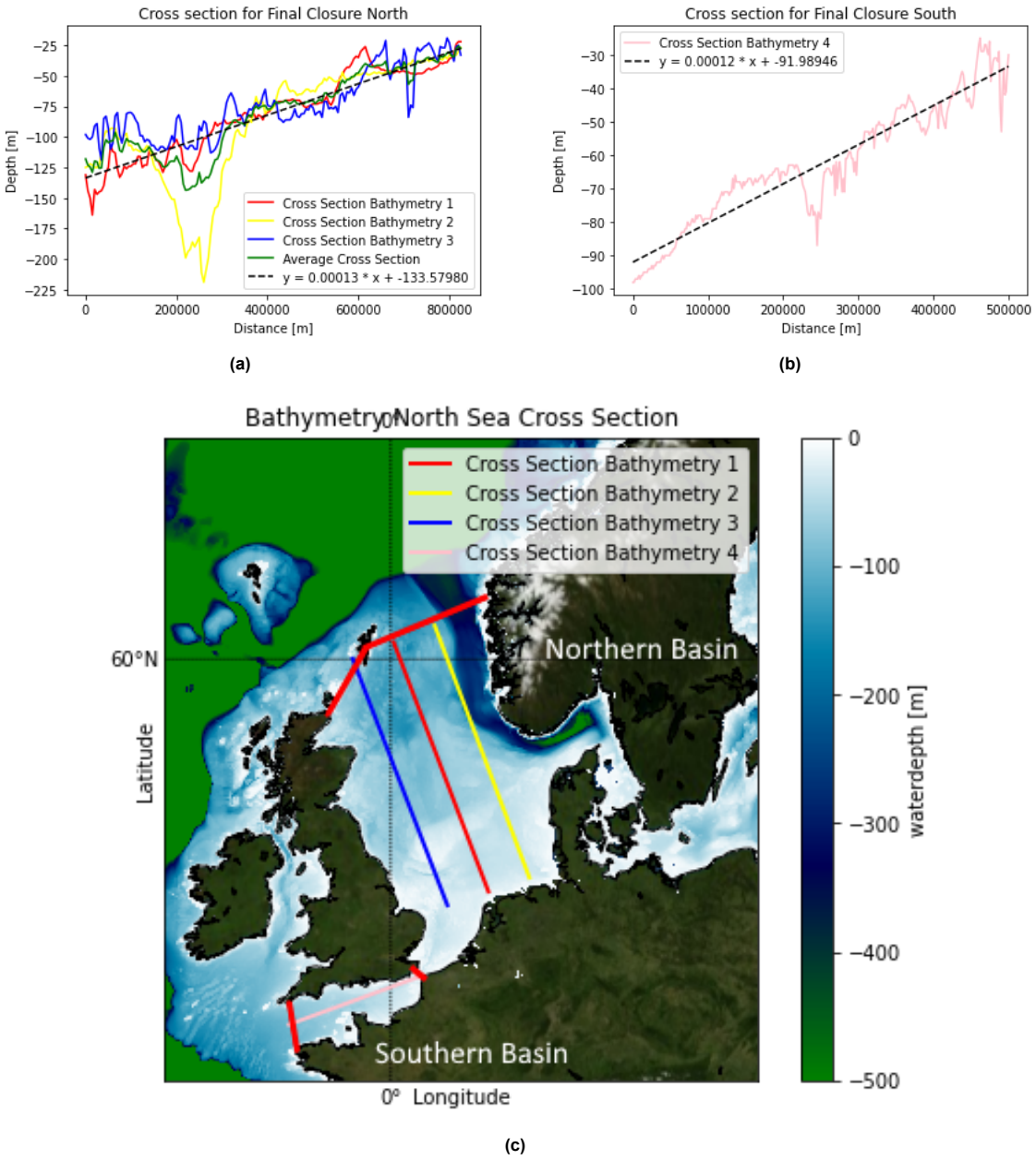

Figure 8.2: Location cross-section and bathymetry, the red line at Dover separating the two enclosed areas .

The bathymetry is retrieved from GEBCO bathymetry chard. For the northern part of the North Sea, a linear line is fitted through the average bathymetry of the three lines, stretching from the northern dam to the southern North Sea. This is a simplification of the bathymetry and will influence the results. The resulting bed level over the basin's length is shown in Figure 8.2. The same procedure is executed for the English channel part.

The ocean side boundary is the dam splitting the North Sea and the Atlantic Ocean with a gap in the middle. The water level outside of the dam constantly changes due to the tide. This tidal difference causes a head difference between the water level inside the basin and the ocean.
The other boundary conditions is formed by the discharge through the strait of Dover, only for the southern closure model. Groeskamp [22] concluded that the discharge through the Strait of Dover decreased drastically after closure of the southern part of the NEED. As the southern part is closed first the second boundary condition for the northern closure model is a closed boundary.

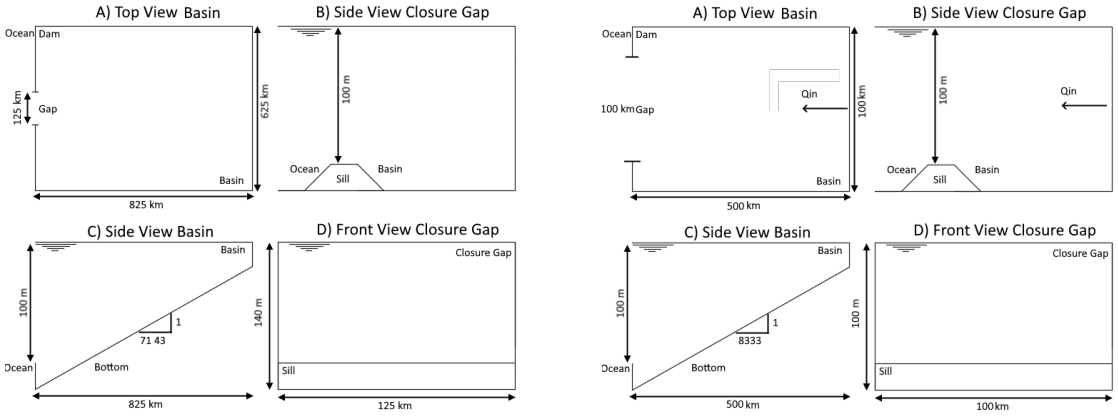

(a) Model North Sea (southern basin) **(b)** Model English Channel (northern basin)

Figure 8.3: Overview of the closure models.

8.1.3. Numerical Method

A set of differential equations can describe the motion of water flowing through the final closure gap. The differential equations used to get insight into the occurring flow velocities in the gap is the shallow water equation. The shallow water equation is a hyperbolic equation consisting of the continuity equation 8.1 and the momentum equation 8.2. The continuity equation is derived from the mass balance, simplified to the volume balance assuming that water is incompressible. The momentum is a balance between inertia, forcing, and resistance [4].

$$B_s \frac{\partial h}{\partial t} + \frac{\partial Q}{\partial s} = 0 \tag{8.1}$$

$$\frac{\partial Q}{\partial t} + \frac{\partial}{\partial s}\frac{Q^2}{A_s} + gA_s\frac{\partial h}{\partial s} + c_f\frac{Q|Q|}{A_s R} = 0 \tag{8.2}$$

Where:
B [m] is the conveyance cross-section
h [m] is the mean depth
Q [m^3/s] is the discharge through the gap
A_s [m^2]is the cross-sectional area
R [m] is the hydraulic radius.
cf [-] friction coefficient.

Equations 8.1 and 8.2, form the shallow water equation which is sometimes called the Navier Stokes equation and is only valid for shallow water conditions. The condition for shallow water waves (tidal waves) is $H/L < 20$. Due to the considerable period of the tidal wave, namely 12.5 hours, the condition is always met. This means that the Navier Stokes equation can be used for this situation. There is no real solutions for the Navier Stokes equations and can therefore only be solved by using an approximation or by a numerical method. The Navier Stokes equation can be simplified to the small basin equation if the ratio between the basin length and the wave length is small. Unfortunately the basin is too large and therefore the small basin approximation is not valid. Another way to describe the flow velocity inside the gap is by using a numerical method. The numerical model that is used is retrieved from Battjes et al. [4]. The equations 8.1 and 8.2 can be discretized in time and space, and the corresponding water level and discharge can be calculated. The formulas described below formulate a semi-implicit method where the water level using the continuity equation and then the discharge using the momentum equation is updated.
First, the continuity equation is approximated. The numerical methods used are the forward Euler method for the time discretization and the central differencing method for the space discretization. This leads to the following approximation for the continuity equation[4]:

$$h_m^{n+1} = h_m^n - \frac{\Delta t_n}{\Delta S_m} \frac{Q_{m+1}^n - Q_m^n}{B_m^n} \tag{8.3}$$

Where,

$$\Delta S_m = \frac{1}{2}(\Delta S_m + \Delta S_{m+1}) \tag{8.4}$$

To update the discharge for each time step, the momentum equation is discretized. The advection term can be neglected for low waves propagation in stagnant water. The momentum equation is discretized in time through the backward Euler method; central differences then evaluate the water level gradient [4].

$$Q_m^{n+1} = Q_m^n - \frac{\Delta t_n}{\Delta s_m}(gA_m^{n+1} - h_{m-1}^{n+1} + \chi_m^{n+1} \frac{|Q_m^{n+1}|Q_m^{n+1}}{A_m^{n+1}}) \tag{8.5}$$

Where,

$$\chi_m^{n+1} = \frac{c_f \Delta s_m}{R_m^{n+1}} \tag{8.6}$$

χ is the dimensionless bed resistance coefficient.

Unfortunately, the advection term cannot be neglected, the term must be included in the momentum equation. This is done by discretizing the momentum flux; the formulation for the momentum flux is presented in equation 8.8 [4].

$$\frac{\partial}{\partial s}(\frac{Q^2}{A}) \approx \frac{F_m - F_{m-1}}{\Delta s_m} \tag{8.7}$$

where

$$F_m = \begin{cases} \frac{Q_m^2}{A_m}, & \text{if Q}_m > 0 \text{ and } Q_{m+1} > 0, \\ \frac{Q_{m+1}^2}{A_{m+1}}, & \text{if Q}_m < 0 \text{ and } Q_{m+1} < 0, \\ 0, & \text{otherwise.} \end{cases} \tag{8.8}$$

8.1.4. Boundary conditions

Two boundary conditions are needed to solve the numerical problem. The landside boundary condition differs per part; the boundary condition for the southern basin is the discharge through the Strait. And for the northern basin, a closed boundary is used (both the discharge through the Strait as the river discharge is negligible compared to the bain size). At the dam, the boundary condition is the discharge through the gap caused by the difference in water level.

Boundary Condition Gap

The caissons should be placed on a sill to spread the forces evenly to the subsurface and keep the water depth on top of the sill equal for the sections. During the closure, the flow over the sill acts as a weir. The energy head and impulse balance determine the discharge over a weir. The total discharge through the gap depends on the water level in the ocean, the water level in the basin, and the geometry of the gap. There are three types of flow; free flow, submerged flow, and intermediate flow. The discharge through the opening depends on the upstream water level for free flow. When the water level downstream exceeds a certain level, the flow becomes submerged. The difference between the two types of flow is intermediate flow. The flow type over the crest can be calculated using the Froude number. The Froude number is the ratio between the kinetic force and the gravitational force , equation 8.9 [17].

$$Fr = \frac{u}{\sqrt{2 * g}} \tag{8.9}$$

If the Froude number is smaller than one, the flow is subcritical. For a Froude number larger than one, the flow is supercritical.

Based on the flow condition upstream and downstream of the weir, the discharge through the weir can be calculated for both the sub-critical equation 8.10 and supercritical situation equation 8.11. An overview with the definitions of the weir is presented in figure 8.4

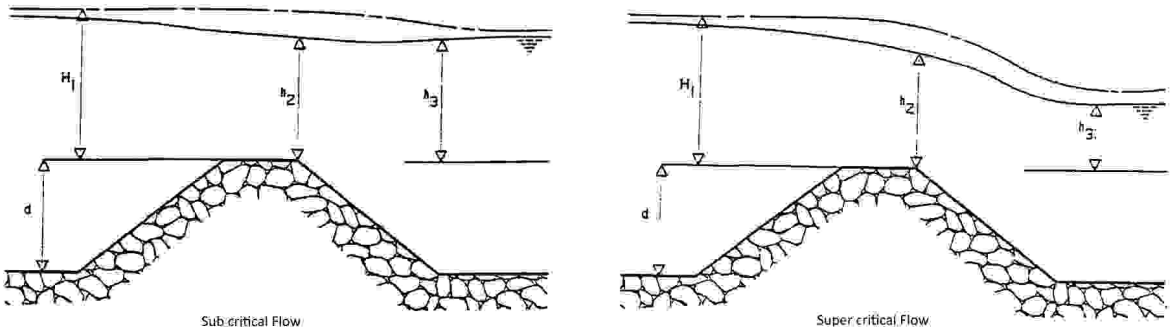

Figure 8.4: Sub and supercitical flow over a weir [34].

Sub-critical flow conditions:

$$Q_s(t) = \mu * b * h_2 * \sqrt{2 * g * (H_1(t) - h_2(t)} \tag{8.10}$$
$$h_2 = h_3 \text{ for } h_3 > \tfrac{2}{3} H_1(t)$$

Super-critical flow conditions:

$$Q_s(t) = \mu * \frac{2}{3} * b * h_2 * \sqrt{\frac{2}{3} * g * H_1(t)} \tag{8.11}$$
$$h_2 = \tfrac{2}{3} \mathrm{H}_1 for \mathrm{h}_3 < \tfrac{2}{3} H_1$$

Where:
B [m] is the width of the gap.
H_1 [m] upstream energy level.
μ [-] discharge coefficient 0.8 sub-critical flow, 0.9 super-critical flow. [8].
Q is the discharge through the gap.
h_2 [m] downstream water level.

Another flow regime is through-flow, this type of flow occurs if the sill (plus the concrete caisson) is permeable enough to allow water to flow through it. For this thesis the sill assumed to be impermeable, meaning that the flow regime can be ignored.
The discharge through the closure gap can be calculated using these two relations for a specific time period. This discharge is then used as sea side boundary condition for the numerical model.

Land side boundary condition
For the southern closure the landward boundary is equal to the discharge through the Strait of Dover. After the southern closure this discharge is negligible therefore the land side boundary condition for the northern closure is equal to zero.

Other conditions
The truncation error for this scheme is second-order in space and first-order in time. The method is called semi-implicit and is conditionally stable. The condition that needs to be full-filled is the CFL condition. The CFL condition is given in equation 8.12.

$$c\frac{\Delta t}{\Delta s} \leq 1 \tag{8.12}$$

Spin-up time
In Figure 8.7, the velocity inside the gap over time is shown. The first iteration steps quite wiggly due to the initial conditions, but after a few iterations, the wiggles vanish due to the friction in the system. The time it takes that the initial condition does not affect the discharge is called the spin-up time. This should be considered for analyzing the flow velocities because the initial wiggles are part of

the numerical scheme and not reality. After a particular iteration step, the largest velocity of a specific gap cross-section can be calculated.

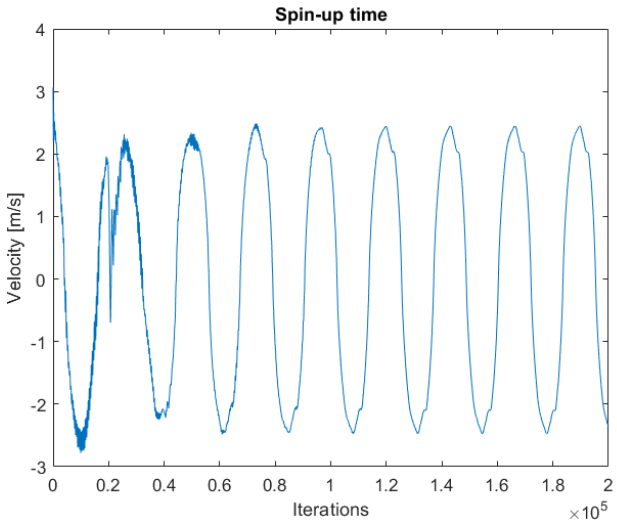

Figure 8.5: Spin-up time velocity graph for a certain gap area.

8.1.5. Model Results

The velocities can easily be computed for different gap sizes based on the above conditions and models. The models are programmed in MATLAB. In Figure 8.6, the results for both the southern and northern closure (a velocity design graph) are shown. A velocity design graph quickly shows the occurring flow velocities inside the closure gap from which the closure strategy can be determined. The model is verified using example 5.2 of Verhagen [52]. The value on the x-axis is the water level on top of the sill, and the y-axis is the width of the gap. A side note is that these graphs are only valid for rectangular cross-sections. A single run of a particular gap size results in multiple flow velocities inside the gap due to the tidal difference inside and outside the basin. The maximum flow velocity for each specific gap size is pointed as a color of the plane. Due to the number of iterations needed to develop a reliable answer, the computation time is quite long. The number of steps is 20 making the last couple of kilometers during closure unreliable. The logarithmic step size is used in the next section, where the closure procedures are analyzed in more detail.

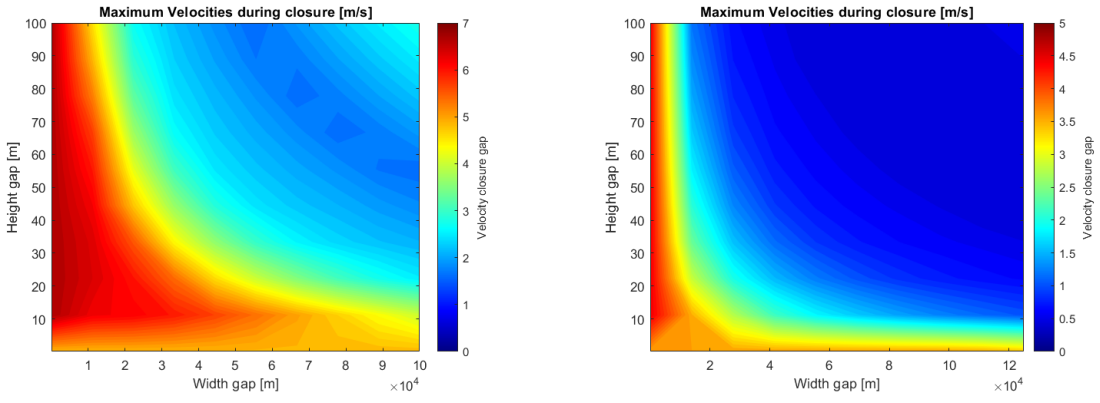

(a) Velocity design graph Southern Closure.

(b) Velocity design graph Northern Closure.

Figure 8.6: Velocity design graphs both closures, maximum velocities.

8.2. Closure Procedure Southern NEED

For this part, the studies on closure dams of Huis in 't Veld [25], and Konter [34] have been extensively used. First, the steps taken to closure the southern dam are discussed. A infographic of the closure procedure is shown in Figure 8.11.

- The first step of the closure is the construction of the 10-meter high sill; the sill hardly changes the flow velocity. The sill serves as the dam's foundation; it distributes the pressure evenly to the bed. The sill also reduces the irregularities and keeps the water level above the sill constant over distance. The main advantage of the sill is to reduce the number of different caisson sizes. Noteworthy is that the sill crest must be extremely level; otherwise, the caisson cannot be attached to each other to create an impermeable closure. The flow velocity on top of the sill is less than 2.5 m/s, meaning that no bed protection is needed to protect the sill.
- Normal caissons are stacked and placed at both sides of the gap, reducing the width of the gap to 50 kilometers. The flow velocity in the remaining gap does not increase significantly.
- Next, normal caissons are placed in the remaining gap on top of the sill to reduce the water depth at the final closure gap to 50 meters. This reduces the sinking time of the final closure caissons. Figure 8.7 shows that lowering the water depth to 50 meters results in a maximum tidal flow velocity of 1.7 m/s .

Table 8.1: Minimum time required for caisson placement [52].

	Time before slack water	**Velocity above sill**
- sailing in the caisson	- 70 min	
- positioning caisson above sill	- 55 min	
- connect caisson to already placed ones	- 30 min	< 0.75 m/s
- sinking down of caisson	- 15 min	< 0.30 m/s
- caisson on sill	- 5 min	
- moment of slack water	0 min	
- removal of wooden floating planks	+ 10 min	
- dumping of extra stone ballast	+60 min	

The caisson needs to be transported to the final destination. If the caisson is in position, the sinking process can start. This is performed during low, slack water because the flow velocity and water depth on top of the sill are minimal. The procedure can begin when the maximum flow velocity is lower than 2.5 m/s [52]. When an M-2 tide is dominant, placing the caissons is only possible for a maximum flow velocity that does not exceed 2.5 m/s. During the sinking process, which lasts approximately 15 minutes, the flow velocity should not exceed 0.3 m/s. Placing during slack water is preferable because the sinking time is less.

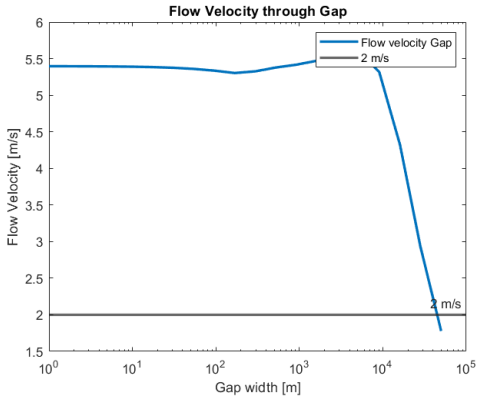

(a) Occurring flow velocities during vertical closure.

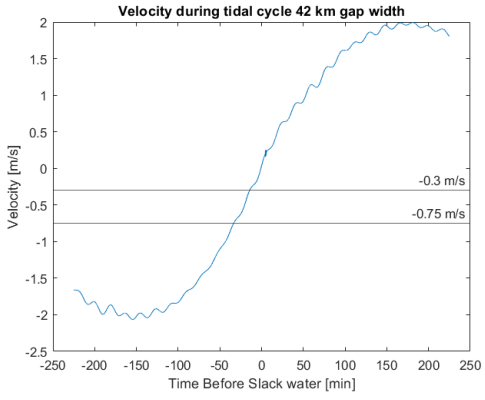

(b) Flow velocities during Caisson closure 3.2 km point, half a tidal cycle.

Figure 8.7: Flow velocities during southern vertical closure 50-meter flow depth.

- It is possible to close the entire section using sluice caisson, but this method is very costly. Therefore a horizontal caisson closure is performed until the maximum flow velocity in the gap exceeds 2 m/s. The sluice caisson decreases the cross-sectional area, increasing the flow velocity to 2.5 m/s. Sluice caissons reduce the head difference over the caisson until the caissons are placed and ballasted. Figure 8.7 starts with a gap size of 50 km with a flow depth of 50 meters. A horizontal closure is used until the flow velocities inside the gap reaches 2 m/s. This is reached by a gap length of 42 000 m. For the last part of the closure, sluice caissons are used. The sluice gate is positioned in the final gap to finish the closure. The gates are closed during sinkage and immediately opened after it is correctly positioned [45].
  The flow velocities during one tidal cycle for when the last caisson and the last sluice are placed are analyzed in further detail. Figure 8.8 shows the flow velocities during 1/2 a tidal cycle. It concludes that the maximum velocities during the sinking procedure, according to Table 8.1, are not exceeded.

- The last 42 km is closed during one tidal cycle, a sudden closure. The caisson sluices partly close off the gap for the sudden closure, reducing the cross-sectional area. An reduction of 20% is used to check the feasibility. This result in Figure 8.8

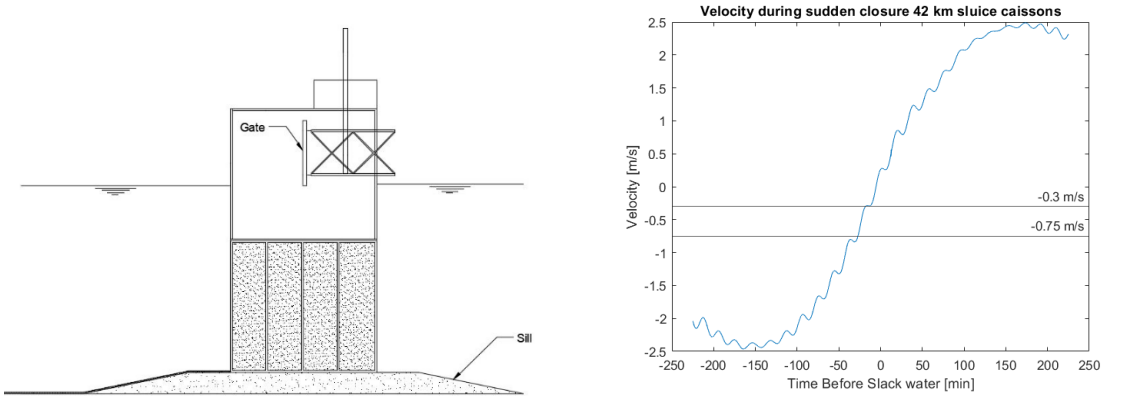

(a) Sluice caissons.

(b) Occurring flow velocities during placements sluice caissons, half a tidal cycle.

Figure 8.8: Sluice caisson and flow velocities during placement sluice caissons.

8.3. Closure Procedure Northern NEED

Figure 8.9 concluded that the discharge through the Strait of Dover is negligible, resulting in a closed boundary condition at the right side of the model. The Figure shows that closing the southern part of the NEED results in minimal tidal elevation inside the basin. This consequently leads to little flow velocities. The same closure procedure is applied for the southern closure of the northern part of the NEED. First, the cross-section is reduced to 70 á 80 percent of its original size. The cross-section is narrowed by closing the shallow area first, by placing caisson on top of the sill.

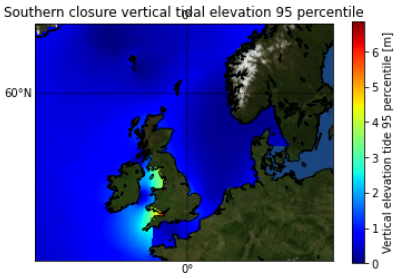

Figure 8.9: The vertical tidal elevation after closure of the southern NEED [22].

The remaining closure area forms the main channel where water can flow in and out depending on the tide [25]. The bed of the deep trench consists mainly of mud that should be dredged to make the bed suitable for the dam's foundation. A 10-meter height sill is constructed where the caisson can be placed on. The flow depth in the deep trench is decreased to 50 meters to make the sinking procedure feasible. Next, the remaining gap is reduced in width until the flow velocity of 2 m/s is exceeded (at 15 km gap length). The remaining gap is closed using sluice caissons. The flow velocities for the final gap with a flow depth of 50 meters is shown in Figure 8.10.

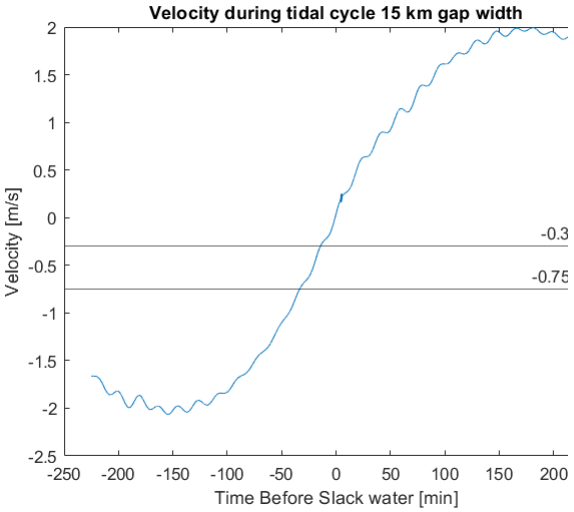

(a) Flow velocities during half a tidal cycle , gap size 15 km by 50 meters.

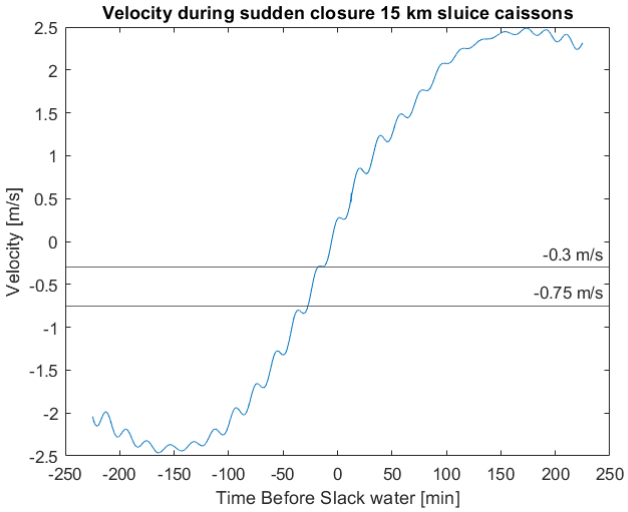

(b) Flow velocities during half a tidal cycle, gap size 15 km by 50 meters with sluice caisson placed in the gap.

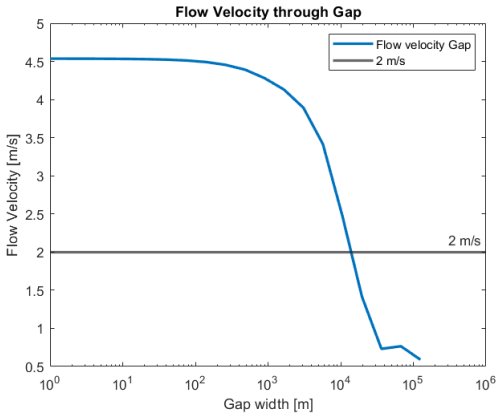

(c) Flow velocities as function of the gap width for horizontal closure with a water depth of 50 meters.

Figure 8.10: Maximum occuring flow velocities through gap and the flow velocities at 15 km gap width 50 meter flow velocity height for with and without caissons during one tidal cycle.

To summarize the closing procedure
First the southern dam is closed.

1. Placing a sill over the entire alignment.
2. Reduce the cross-section to 50 km using normal caissons.
3. Decrease the flow depth to 50 meters by placing caissons underwater.
4. Place caissons on either side of the gap, reducing the gap width to 42 km.
5. Place the sluice caissons in the remaining gap.
6. Close the sluices between one tidal cycle.

Next the northern part is closed.

1. Placing a sill over the entire alignment
2. Reducing the flow depth by closing the shallow area first.
3. Reducing the flow depth to 50 m by placing caissons underwater.
4. Placing caissons on either side of the final gap to reduce the 15 km.
5. Place the sluice caissons in the remaining gap.
6. Close the sluices between one tidal cycle.

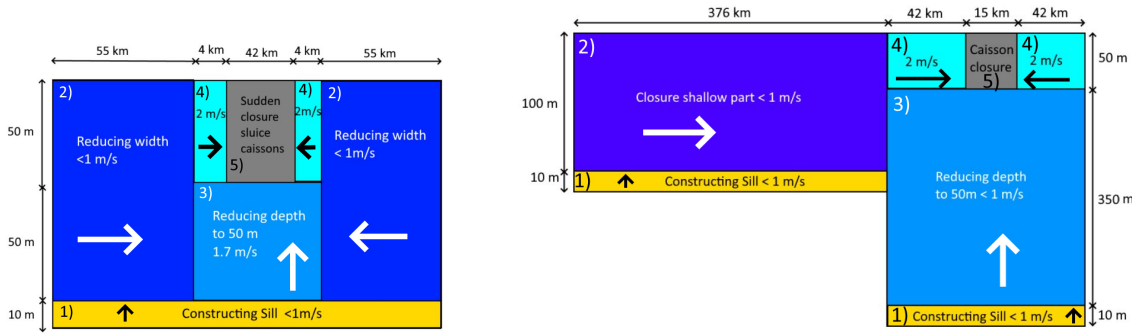

(a) Cross-section of the gap for the southern Closure.

(b) Cross-section of the gap for the Northern Closure.

Figure 8.11: Overview closure procedure with steps and the maximum occurring flow velocity during closure. The arrows indicate the direction of closure.

8.4. Conclusion

This Chapter showed the principles regarding the flow velocities during a closure procedure. The calculation results have shown that a caisson closure is possible for both dam locations. In the southern part of the NEED, the final gap is 42 km long (50 meters deep) and should be closed using sluice caissons. The gap size is enormous and, therefore, difficult to achieve. The final gap of the northern part that needs to be closed using sluice caissons is only 15 km long (50 meters deep). More advanced calculations are required to derive the complete picture. The duration of placement of the caissons is essential because the sinking process can only take place during limited flow.

9 Discussion

This chapter highlights the primary assumptions made during this project.

Background
The sea-level rise used for this thesis is based on extreme sea level situation (10 m according to KNMI scenario SSP-8.5 H++ in 2300). This is based on te KNMI model of the sea level rise in 2300. The sea-level rise is highly uncertain; changes in the sea level rise consequently result in a different dam design. Nota concluded in his thesis that for sea-level rise larger than 5 m, the NEED is the favorable solution, compared to adapting current flood defense systems. At the basin side of the NEED, the water level is kept equal to the current average water level in the North Sea. It is very likely that when the NEED is constructed, the water level in the basin will have changed. The definitive water level inside the basin will have to be aligned on many aspects. The choice has little effect on the dam's design and planning.

Location
The location of the dam is based on the models made by Groeskamp. This differs slightly from the description given in the paper. The map projection used for plotting the model results magnifies this difference. Fortunately, the result obtained in this thesis will not be significantly affected by the slight change of the location as only rough calculations are made. The choice of using the location of the alignment according to the models instead of the description is so that the model data can be used for this thesis. The weighting criteria are selected and valued from the floodrisk engineer's perspective to value the technical feasibility. This view only considers a small part of the overall feasibility of the dam. The effects on ecology, the financial feasibility, socio-economical impact, etc., should be thoroughly investigated to get a complete overview and determine the feasibility of the projects. For example, the dam will impact the connectivity of the biggest port in Europe. Furthermore, the North Sea switches from salt to fresh water, inducing significant environmental changes. It is therefore advised to investigate the impact of the NEED in detail.

Probabilistic Design Condition
The top event failure of the NEED is set to 1:20000 years. This value is derived from the old safety norms in the Netherlands for the primary flood defenses. A risk-based approach will be more appropriate, considering the consequences of the dam's failure. The probability per failure mechanisms are based on the Dutch guidelines; the contribution between the failure mechanisms could be different for the NEED.
Only two failure mechanisms are taken into account to determine the probabilistic design condition. The failure mechanisms are based on the governing conditions, which are storm conditions. Perhaps the governing condition is overestimated, and other failure mechanisms can be more normative.
This aspect will influence the final design and the technical feasibility.

Cross section Design
The most important parameters used to determine the dimensions of the dam are wave height, period,

and direction. The KNMI predicts that these conditions will change due to global warming. Storms intensify, resulting in higher waves higher wind setup. These changes are not included in the probabilistic model due to a lack of information about the increase. The KNMI state that it is difficult to predict how much these parameters will change. The wave data used is obtained from a hindcast model of the past 40 years. The parameters from the hindcast model are fitted to a multivariate distribution, disregarding the future increase.
The foundation is fundamental due to the immense weight of the caisson. The immense weight can result in subsidence of the caisson leading to pressure built up and cracks in the concrete—an investigation into the bearing capacity of the soil essential. If the bearing capacity of the bottom is not adequate, the feasibility of the plan decreases significantly.
The caisson is too large to be transported to the site. Smaller caissons should be used that are staked to reach the necessary height. The stacking of caisson poses new failure mechanisms, decreasing the technical feasibility.
In this thesis, the earthen dam and the caisson dam are compared to conclude which design is more technically feasible. Further research is necessary to investigate the feasibility of combining these two methods; it could be more technically feasible to increase the sill height and place a small caisson on top.

Closure
A 1D model is used to calculate the flow velocity through the gap, disregarding the effects of the deep trench and the shape of the North Sea basin. These aspects will influence the closure behavior. The 1D model ignores any turbulence which will change the flow pattern and closure feasibility. The turbulence could affect the closure and result in considerable erosion downstream. A more sophisticated model should be used to consider the hydrodynamical effects, including the morphodynamical aspects.

Project execution
The duration highly depends on the availability and type of tug boats or construction vessels. The caisson sizes are based on the current maximum units. Future development in material technology, vessel sizes, and larger caissons will result in a shorter construction time.
The construction time can be further reduced by working on multiple sections simultaneously. This requires a lot of labor and a high degree of accuracy to precisely connect the caissons. For this thesis, only sections are used where for each section, the caissons are built from the sides inwards. Optimization is possibly provided that enough caissons and equipment are available.

10

Conclusion and Recommendations

This thesis investigates the technical feasibility of the North European Enclosure Dam (NEED). This dam protects large parts of northwest Europe if the most severe Climate change scenarios occur, and sea-level rise will exceed 10 m.

10.1. Conclusions

The dam was proposed by Groeskamp et al. [22] and was based on several assumptions to provide a first estimate of the location and effectiveness. This thesis studied more in detail the location and layout of this dam, the favorable cross-section of the dam, and the most likely closure scenarios. The layout from Groeskamp has been compared and evaluated to a proposed location based on the area most prone to flooding. The layout has been weighed at four different criteria being:

1. The total length and maximum depth of the alignment.
2. The difference in the number of people that the dam will protect by the dam.
3. The constructability of the damper alignment, based on the loads (tide and wave).
4. The geotechnical stability based on the requirements by Huis in 't Veld

The result is that the alignment of Groeskamp scores best. This is mainly due to the second criteria, the difference in protection. Although the flooded area (due to the 10-meter sea level rise) is small, many cities are affected, especially France and Norway. The optimized alignment does not protect these areas. This is heavily charged because the primary purpose of the NEED is the protection of the low-lying regions.

The most optimum cross-section was based on a comparison between two typical cross-sections. Two different types of the main dam cross sections have been compared, the caisson and the earthen dam. The main dimensions of the two concepts have been determined using a fully probabilistic approach, the Monte Carlo method. The allowable probabilities per failure mechanisms are subdivided into ULS (ultimate limit state) and SLS (serviceability limit state) conditions. The total length of the dam is subdivided into four sections; per section, a caisson and an earthen dam are designed. The earthen dam needs a mild slope to be stable; therefore, the construction requires a tremendous amount of material. The required volumes for the caisson dam are far less (1/7 of the earthen dam), resulting in the caisson dam being the more feasible option. The final design is a caisson dam consisting of foot protection blocks, sand sills, and protection layers to prevent erosion. The caisson type results in a large structure, which is difficult to transport. Multiple smaller structures could be stacked to create an impermeable barrier.

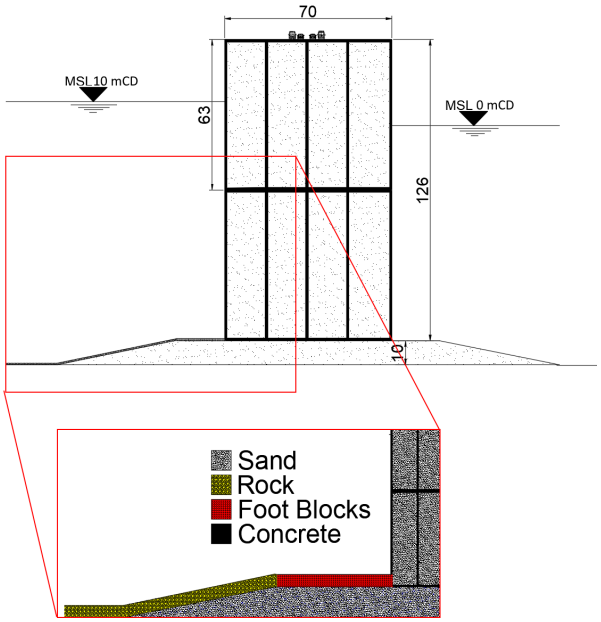

Figure 10.1: The caisson dam, units in meters.

The most likely closure scenario is the caisson closure. The closure procedure depends on the flow velocities inside the closure gap. The basin is split into two sections the English channel section and the North Sea section. First, the southern dam is closed, and then the northern dam. The occurring flow velocities during the closure determine the feasibility. These velocities are calculated using the shallow water equation. A numerical model of the shallow water equation is used by discretizing it in time and space. This numerical model is programmed in MATLAB as a 1D model. The 1D closure simulation gives the maximum flow velocity for a specific gap width. The model offers an excellent estimation of the feasibility stage, with a short computation time. A critical boundary condition for the caissons closure is that the maximum flow velocity in the gap is less than 2.5 m/s. Based on the model, a closure procedure is proposed in which this essential condition is met. The most likely closure scenario is that first, the Southern dam needs to be closed to ensure that the flow velocities do not exceed the critical value. The next step is to fulfill the Northern dam closure. The closure sequence proposed in chapter 8 ensures that the maximum flow velocity is 2.5 m/s.

The answer to the main research question is that the NEED is expected to be technically feasible. The most important conclusions are summarized below.

- The current alignment proposed by Groeskamp scores best in an MCA.
- The caisson type seems to be the best option for the NEED, as it makes optimal use of the material to create the required height.
- The individual caisson units are large structures and need a tremendous amount of material.
- The first estimation of construction time resulted in around 150 years to complete the NEED, based on the currently available equipment. Improved construction methods are required to make the project feasible.
- First, the southern dam is closed and then the northern dam. Sluice caissons have been proposed for the final gap to keep the maximum flow velocity during closure below 2.5 m/s.

10.2. Recommendations

Further research is needed to investigate the effect and implications of the NEED in further detail. The recommendation based on the discussion are presented below:

- Multiple sea level rises for both inside and outside the basin should be considered to evaluate the effects of the dam's design. It could even be possible to assess the degree of uncertainty of the sea level rise predictions.

- Detailed information on the wave climate was scarce, and most data from wave buoys were not publicly available. The hindcast model obtained from Copernicus should be corrected by using Quantile mapping. For quantile mapping, real wave data is needed. Therefore, it is advised to try to get real wave data to correct the hindcast model. For further analysis, it is recommended to gather more information about the grain size distribution, accurate water levels, borings, and CPTs.
- Using a risked-based approach to determine the maximum allowable probability of failure of the dam.
- The hydraulic loads and depths at the described location of the NEED should be compared to the model location of Groeskamp's Alignment.
- Different views should be used to determine the NEED's location; this is to take all effects into account.
- All the primary failure mechanisms should be checked to determine the safety of the NEED.
- The dam should be modeled in a 3D model such as Delft 3D. This is especially necessary to further investigate the flow velocities during the final closure and optimize the closure procedure. Turbulence, for example, is not described in a 1D model but will affect the closure behavior drastically.
- Constructive analysis of the caisson dam.
- Investigate the feasibility of combining the earthen and caisson dam.

References

[1] Coastal Engineering Research Center (US). *Shore protection manual*. Vol. 1. US Army Coastal Engineering Research Center, 1973.

[2] European Environmental Agency. *Coastal flood damage potential, European Environmental Agency*. URL: https://www.eea.europa.eu/data-and-maps/figures/coastal-flood-damage-potential/cci136_map2-6.ep.

[3] Paola Arias et al. "Climate Change 2021: The Physical Science Basis. Contribution of Working Group14 I to the Sixth Assessment Report of the Intergovernmental Panel on Climate Change; Technical Summary". In: (2021).

[4] J.A. Battjes and R.J. Labeur. "Unsteady flow in open channels". In: (2017).

[5] Judith Bosboom and Marcel JF Stive. *Coastal dynamics I: lectures notes CIE4305*. 2012.

[6] Corinna Buder. "Impact of a Northern European Enclosure Dam on North Atlantic Climate". PhD thesis. Christian-Albrechts-Universität zu Kiel, 2020.

[7] EOF Calle, MT Van der Meer, and J Niemeijer. "Technisch rapport zandmeevoerende wellen". In: *TR15* (1999).

[8] La mobilité et l'aménagement Ceremea Centre d'études et d'exertise sur les risques l'environnement. *). The Rock Manual: The use of rock in hydraulic engineering*. CIRIA, London, London, 2nd edition, 2007.

[9] Delta Marine Consultant. "Guidelines for Xbloc concept Design". In: ().

[10] OpenStreetMap contributors. "Population retrieved from OpenStreetMa". In: (2020).

[11] EU Copernicus. "Copernicus-Marine environment monitoring service". In: *URL https://marine.copernicus.eu* (2020).

[12] John Lloyd Davies and Keith M Clayton. *Geographical variation in coastal development*. Longman New York, 1977.

[13] Jan De Leeuw. "Information theory and an extension of the maximum likelihood principle by hirotogu akaike". In: (2011).

[14] Robert M DeConto and David Pollard. "Contribution of Antarctica to past and future sea-level rise". In: *Nature* 531.7596 (2016), pp. 591–597.

[15] Frederik Michel Dekking et al. *A Modern Introduction to Probability and Statistics: Understanding why and how*. Springer Science & Business Media, 2005.

[16] Sybren Drijfhout and Dewi Le Bars. "KNMI Klimaatsignaal'21, Hoe het klimaat in Nederland snel veranderd". In: (2021), p. 72.

[17] D.F. Elger et al. "Engineering Fluid Mechanics". In: (2010).

[18] NOAA National Centers for Environmental Information. *State of the Climate: Global Climate Report for Annual 2019*. 2020. URL: https://www.ncdc.noaa.gov/sotc/global/201913. (visited on 03/15/2021).

[19] II EurOtop. "Manual on wave overtopping of sea defences and related structures: An overtopping manual largely based on European research, but for worldwide application". In: *European Overtopping Manual* (2018).

[20] Christian Genest and Anne-Catherine Favre. "Everything you always wanted to know about copula modeling but were afraid to ask". In: *Journal of hydrologic engineering* 12.4 (2007), pp. 347–368.

[21] Yoshimi Goda. *Random seas and design of maritime structures*. Vol. 33. World Scientific Publishing Company, 2010.

[22] Sjoerd Groeskamp and Joakim Kjellsson. “The Northern European Enclosure Dam for if climate change mitigation fails”. In: *Bull Am Meteorol Soc. https://doi. org/10.1175/bams-d-19-0145.1. https://jou rnals. ametsoc. org/doi/pdf/10.1175/BAMS-D-19-0145.1. Accessed* 24 (2020).

[23] M Haasnoot et al. “Adaptation to uncertain sea-level rise; how uncertainty in Antarctic mass-loss impacts the coastal adaptation strategy of the Netherlands”. In: *Environmental Research Letters* 15.3 (2020), p. 034007.

[24] Leo H Holthuijsen. *Waves in oceanic and coastal waters*. Cambridge university press, 2010.

[25] J.C. Huis in ’t Veld. “The closure of Tidal Basins, Closing of Estuaries, Tidal Inlets and Dike Breaches”. In: (1984).

[26] JM Huthnance. “Physical oceanography of the North Sea”. In: *Ocean and shoreline management* 16.3-4 (1991), pp. 199–231.

[27] Harry Joe and Dorota Kurowicka. *Dependence modeling: vine copula handbook*. World Scientific, 2011.

[28] SN Jonkman and T Schweckendiek. “Flood Defences, Lecture notes CIE5314”. In: *Delft University of Technology: Delft, The Netherlands* (2017).

[29] SN Jonkman et al. “Probabilistic design: risk and reliability analysis in civil engineering”. In: *Collegedictaat CIE4130* (2015).

[30] Anu Marii Kaskela et al. “Picking Up the Pieces—Harmonising and Collating Seabed Substrate Data for European Maritime Areas”. In: *Geosciences* 9.2 (2019). ISSN: 2076-3263. DOI: 10.3390/geosciences9020084. URL: https://www.mdpi.com/2076-3263/9/2/84.

[31] Caroline A Katsman et al. “Climate scenarios of sea level rise for the northeast Atlantic Ocean: a study including the effects of ocean dynamics and gravity changes induced by ice melt”. In: *Climatic Change* 91.3 (2008), pp. 351–374.

[32] Chul-hwan Koh, Jong-Seong Ryu, and Jong-Seong Khim. “The Saemangeum: history and controversy”. In: *Journal of the Korean Society for Marine Environment & Energy* 13.4 (2010), pp. 327–334.

[33] Freek Kollaard et al. “The Northern European Enclosure Dam: A multidisciplinary project on the effects of the NEED”. In: (2021).

[34] JLM Konter, HE Klatter, and RE Jorissen. “Afsluitdammen: Regels voor het ontwerp”. In: *Rijkswaterstaat* (1992).

[35] Anders Levermann et al. “The multimillennial sea-level commitment of global warming”. In: *Proceedings of the National Academy of Sciences* 110.34 (2013), pp. 13745–13750.

[36] NJ Nederstigt. “The Deep Water Breakwater: An investigation of possibilities”. In: (1996).

[37] H. K. Nota. “Financial feasibility of large-scale adaptation strategies for future SLR in Northern Europe: NEED vs Dike Reinforcement”. In: *Repositoy, Delft University of Technology, Delft* (2022).

[38] Pascal Peduzzi. “Sand, rarer than one thinks”. In: *Environmental Development* 11 (2014), pp. 208–218.

[39] Rijkswaterstaat. *Nieuwe gemalen voorkomen overstroming*.

[40] ministerie van infrastructuur en milieu Rijkswaterstaat. “Handreiking ontwerpen met overstromingskansen”. In: *RWS rapport, door Deltares* (2013).

[41] Joeri Rogelj et al. “Paris Agreement climate proposals need a boost to keep warming well below 2 C”. In: *Nature* 534.7609 (2016), pp. 631–639.

[42] Soheil Saeed Far et al. “Evaluation of peaks-over-threshold method”. In: *Ocean Science Discussions* (2016), pp. 1–25.

[43] Andy Saulter. “North West European Shelf Production Centre NWSHELF$_{R}EANALYSIS_{W}AV_{0}04_{0}15$”. In: *Quality Information Document* (2021).

[44] U Schepsmeier and EC Brechmann. “Modeling dependence with C-and D-vine copulas: The R package CD vine”. In: *J. Stat. Software* 52.3 (2013), pp. 1–27.

[45] Gerrit J Schiereck. *Introduction to bed, bank and shore protection*. CRC Press, 2003.

[46] Jörg Schneider. *Introduction to safety and reliability of structures*. Vol. 5. Iabse, 2006.

[47] Paolo Scussolini et al. “FLOPROS: an evolving global database of flood protection standards”. In: *Natural Hazards and Earth System Sciences* 16.5 (2016), pp. 1049–1061.

[48] J Th Thijsse. “Een halve eeuw Zuiderzeewerken”. In: (1972).

[49] Surya T Tokdar and Robert E Kass. “Importance sampling: a review”. In: *Wiley Interdisciplinary Reviews: Computational Statistics* 2.1 (2010), pp. 54–60.

[50] JP Van den Bos and HJ Verhagen. “Breakwater Design”. In: *Lecture Notes CIE5308* (2018).

[51] LG Van der Linden. “A modelling study on the residual circulation in the North Sea, with the focus on water fluxes through the Strait of Dover”. In: (2014).

[52] H.J Verhagen. “Closure works, Interactive professional course”. In: (2016).

[53] WJ Vlasblom. “Designing dredging equipment”. In: *Lecture notes, TUDelft* 5 (2003), p. 24.

[54] M Vooredndt and W Molenaar. *Manual Hydraulic Structures*. TU Delft, 2021.

[55] Waterveiligheidsportaal. *Nationaal Basisbestand Primaire Waterkeringen*. URL: https://waterveiligheidsporta
nl/#/nss/nss/norm.

[56] Guido Wolters and Marcel RA Van Gent. “Granular open filters on a horizontal bed under wave and current loading”. In: *Proc. Coastal Eng* 1.33 (2012), pp. 10–9753.

A

Reliability data

A.0.1. Quality of the hindcast model

The data is retrieved from the hindcast model; the data represent the past wave climate but has a certain margin of error. The quality of the model is assessed by comparing the underpinning wave model(WAvEWATCH III) to the actual data [43]. The results of this assessment by Copernicus are summarized per variable of interest below.

Significant wave height

The difference between the model and the observation (satellite and in situ) falls within 15-35% of the observed standard deviation. The correlation between the model and the observations ranges from 0.95 to 1. There is a slight underprediction of the wave height ranging from 0.0 and -0.2. The corresponding standard deviations between the model and the observations are approximately 30-50% of the observed standard deviation. The difference is minimal; the mean error is -0.07 meter and standard deviation 0.33.

Peak wave period

This variable of interest presents the observed data poorest. The correlation between the observation and the model ranges from 0.71-0.86. This difference is amplified in the Bristol channel due to the strong tidal influences. The location exposed to the swell events from the Atlantic ocean (southwest UK and the English channel) scores worse due to the presence of multiple spectral peaks. The biases vary between -0.1 and 0.4 sec. The standard deviation of the difference between the model and the data vary between 47 and 88%. However, the model is sufficient during peak conditions, where the sea is dominated by one wave component. The mean error in open waters is 0.36 sec with a standard deviation of 1.6.

Average wave direction

Regional model biases range from +/- 10 percent due to the lack of platform direction wave data. The mean error is equal to -0.5, with a standard deviation of 28.72 degrees near the coast. In open water conditions, this difference is more negligible.

The extreme conditions are pretty well modeled. The observations quantile-quantile comparisons suggest that the model is in good agreement up to the 99.9th percentile. Although for extreme value analyses, Copernicus recommends taking the uncertainty into account in the upper tail.

B

Hydraulic Method

B.1. The Hydraulic Engineering Design Method

To determine the best design for the closure dam, the Hydraulic Engineering Design Method is used. Different variants are developed based on the location, material use, gap closure, and cross-section. These different aspects of the closure dam are interlinked; by investigating the whole system, a complete assessment can be made. The type of assessment that will be used is multicriteria analysis. The most suitable design is determined using different weights and scores for the items. The different design steps are based on the Civil Engineering design method as explained in the lecture notes from Hydraulic Structures 1. The method consists of 7 steps and is further explained below. Parts of the design steps are already discussed in the problem analysis and will be referred to when addressed. The main goal of the thesis is to determine the technical feasibility of the dam. The technical part of the design process is most important and is extensively analyzed. The method is a mean to get a good design which can be tested on the feasibility. The steps that lead to the final design are shortly treated below.

The first phase is the **analysis of the problem**, the causes, effects, and the desired function of the project is stated. In the problem analysis, a description and motivation of the project is given. It includes the implications, background, and opportunities. Research question and different sub questions are proposed to help solve the problem stated.

The next phase is the **design definition**; every part of the design phase is defined quantitatively; this makes it easy to adapt it at a later stage. A design objective is formulated based on the problem statement. The requirement for the design is categorized into three parts: functional requirements, aspects requirements, and internal and external requirements. .

- The functional requirements describe the different functions of the dam, such as discharging water to the sea, protecting the surrounding countries against sea-level rise, make a road connection between England and France and Scotland and Norway, etc
- The aspects requirements includes safety, sustainability, reliability, etc.
- The internal and external interface, forms the boundaries between elements within the system.

The most stringent safety requirement will be determined by the three criteria: Individual risk, societal risk, and economic risk. A fault tree or event tree can be drawn with the corresponding safety barriers to clarify all the types of failure and the systems itself. Also, the boundary conditions are determined in this phase. The boundary conditions consist of: natural boundary conditions, e.g., loads due to wind and waves, soil properties, and artificial boundary conditions such as traffic. An other type of boundary condition is laws and regulations. This parts of the thesis aims to develop a suitable design for the NEED and focus on the structural aspects; therefore, laws and regulations are out of scope. The boundary conditions are essential for the study of technical feasibility. In order to make a good analysis for the boundary conditions, it was decided to make it a separate section in the thesis.

The third phase is **developing concepts**; integrated designs are created based on the design objective. The components that are selected; are the closure type, location, and cross-section. The projects's most important criteria is that it needs to fulfill the primary goal of protecting west-European counties against sea-level rise. Reference projects with the same objectives should be investigated to see how the problem is solved. A sketch can help to observe the consequences of a design and how to mitigate the occurring problems.
After the idea is elaborated, a spatial-functional design can be created. In a spatial-functional design, the components and dimensions are determined, and key elements are listed.

The fourth phase is **verification of the concepts**; the concept has to be verified based on: functionality, structural safety, serviceability, durability, constructability, and maintainability. During this step, the design could slightly change to fit the boundary condition.

The fifth phase is the **evaluation and selection of alternatives**.The multicriteria analysis is a method to compare the alternatives by ranking different aspects of the project. Another method is a cost-benefit analysis, it is a balance between the costs of the project and the benefits it produces compared to strengthening existing sea dikes, including the revenue it will produce. The latter will be too complicated to use as an evaluation model and is therefore out of scope. The multicriteria analysis uses different weights to indicate the importance of the criteria. The best design is the one with the highest score.

The sixth phase is the **integration of subsystems**, a detailed analysis of a specific subsystem is developed. This analysis is the main focus of this thesis and will conclude the feasibility. The three aspects are the closure procedure, a detailed cross-section including safety calculation of the dam, and research on the availability of resources of the dam and the total costs. The approach is explained in more detail in the methodology.

The last phase is the **validation of the results**. This phase checks whether all previous phases have been completed successfully and whether the system fulfills the requirements. This part forms the conclusion of this thesis.

C

De Afsluitdijk

In this section an overview of important concepts about closure dam are briefly discussed. Using this literature review an optimal design for the NEED can be created. The literature review first discusses the the reason for building the Afsluitdijk, the design, and the consequences of the construction.

C.1. The Afsluitdijk

This overview about the afsluitdijk is written using the book 'Een halve eeuw Zuiderzeewerken' by Prof Thijsse [48]. Prof. Dr. Ir. Thijsse was engineer with the Zuiderzee project department and member of the Delta committee. He was also head of the Delft Hydraulics Laboratory.

C.1.1. Motives for the Afsluitdijk

The Afsluitdijk is a 32.5-kilometer long flood defense, protecting the coast surrounding the former Zuidersea against floods. The building of the Afsluitdijk started in 1927, and the final gap was closed in 1935. Thousands of men worked daily on the Afsluitdijk. It separates the Waddenzee from the Ijsselmeer through a dam creating a non-tidal lake which is not influenced by storm surges.

The plan of constructing the dam was based mainly on three different aspects. The first aspect was that the Zuiderzee was a thread for the low-lying areas surrounding it; these areas flooded regularly. Strengthening and heightening the surrounding sea dikes was costly and complex. The foundations of the dikes around the Zuiderzee consisted of soft peat. Heightening the dikes resulted in the soil settling. This caused the loss of part of the elevation of the dike and a decrease of the structural integrity. The unreliability of the dikes caused countless dike breaches, floods, and large parts of the adjacent land to be lost to the sea. The 1916 flood killed dozens of people resulted in the acceleration of the plans for the Afsluitdijk.
The next aspect that played an essential role in constructing the Afsluitdijk was the need for fertile land. The Zuiderzee bed was very suitable for agriculture, and due to the flat and shallow seafloor with an average depth of 3 meters ideal for reclaiming large portions of land. The need for fertile agricultural land was especially during the first world war, many people suffered from famine.
The last aspect was that brackish Zuiderzee water seeped into the fertile ground in times of extreme droughts, ruining the crops. The Afsluitdijk solved this issue and created a freshwater reservoir that could be used during water scarcity, reducing the dependency on river discharge.
The combined aspects resulted in establishing the Zuiderzee commission; the Zuiderzee commission investigated the effects of the dam, including land reclamation and the safety against flooding of the Zuiderzee area.

C.1.2. Design

The building material of the Afsluitdijk consisted mainly of sand and boulder clay. These materials were chosen because of their availability and ease to process. Constructing a dam with a massive amount

of sand has two disadvantages: sand is highly permeable, making the closure dam susceptible for seepage, and due to the small size, high water velocities could quickly erode the dam. With the use of boulder clay, the permeability and stability could both be improved. Boulder clay can resists flow velocities up to 4 m/s and has a low permeability decreasing the amount of seepage through the dam. Boulder clay is particularly suitable for the core and the revetment of the sand dam, it provided stability and making the dam non-erodible. Other materials used but not widely available were quarry stone and Rijshout (often willow tree branches). Rijshout was used to construct the fascine mattresses to protect the bed against erosion. For the revetment, a combination of clay, straw, and basalt was used. This protection method had been applied for centuries making it very reliable.
The Afsluitdijk is founded on clay and sand; sand is very suitable to bear the load of the dam and to minimize the amount of squeeze. Clay on the other hand, does not have these favorable properties. Near Den Helder, the soil consists of a thick clay layer, which could not be bypassed. If nothing was done about the parts of the dam founded on this layer, it could experience large settlements and sliding planes. Therefore a significant layer of clay soil was dredged during the construction, and the remaining soil was improved by compacting. However, the permeability of sand was still a problem; seepage could quickly occur, which could result in the failure of the dam. Luckily, the water level difference between the two sides of the dam was limited. Therefore the amount of seepage is small, and no protective measures needed to be implemented. Also, the hydrodynamic effects of the Afsluitidijk were investigated, this was done by the Staatcommissie-Lorenz. The committee investigated the influence of the Afsluitdijk on the neighboring dikes. The Staatscommissie determined the best location of the Afsluitdijk, intending to minimize the change of the tide in the Wadden Sea, caused by the construction of the dam. Physical models obtained the velocities during the closure; based on these models, the occurring flow velocities could be mapped very accurately. The physical modes were also used to determine the wave run-up, which was still inaccurate due to the lack of accurate data.

C.1.3. Cross-section

In figure C.1, the cross-section of the Afsluitdijk is presented. The crest of the dike is designed based on the highest storm surges level determined by the Lorenz committee combined with the maximum wave run-up. The crest height differs slightly along the length of the dam, near the Frisian coast; the height was +6.7 NAP due to the shallow foreshore. More to the west, the water depth in front of the dike increased, and therefore also the crest height. The largest crest height can be found near the coast of Noord-holland; the height of the crest is 7.4 because it crossed a trench. The difference in crest heigh showed that the length effect at the Afsluitdijk certainly played a role.
Based on the experimental test, a slope of 1:4 was deemed suitable for breaking the waves efficiently and reducing the run-up at the Waddensea side. The function of the inner dam is to provide space for traffic; a width of 34 meters was predicted to be sufficient to deal with future traffic intensity. The slope at the inner berm is a little steeper because it was projected that the waves and wind setup during storms in unfavorable conditions would not rise much higher than 3.5 meters. The material of the cross-section consist mostly of sand; only at the exterior boulder clay was used to protect the dam against liquefaction. The revetment at both sides of the dam consisted of basalt blocks and Belgian quarry stone reinforced with boulder clay to protect the dam against erosion.

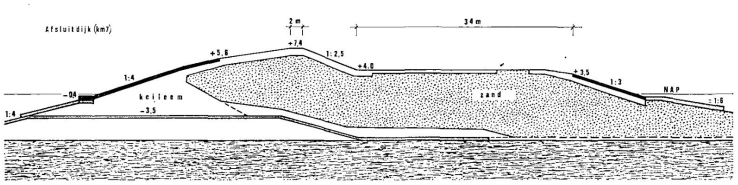

Figure C.1: Cross-section of the Afsluitdijk [48]

C.1.4. Final Closure

As mentioned before, physical models were used to give inside into the occurring flow velocities during closure. Information gathered during these experiments was used to calculate the dimensions of the bed and bank protection at the closure gap. The closure procedure was chosen in such a way that the attack on the bed was minimized. The protection consisted of zinkstukken ballasted with quarry stone from Belgium. The zinkstuk combined with ballast was tested in front of a weir in the Maas to accurate simulate the occurring flow velocities. After the test was executed, the water was pumped out and the movement of the stones was analyzed. This test was repeated in the Waterbouwkunding Laboratorium to verify the physical model that was made of the closure. Using these experiments, the Engineers were confident that the closure could be realized and it was indeed a succes.

D

Qgis Effect Different Sea Level Rise

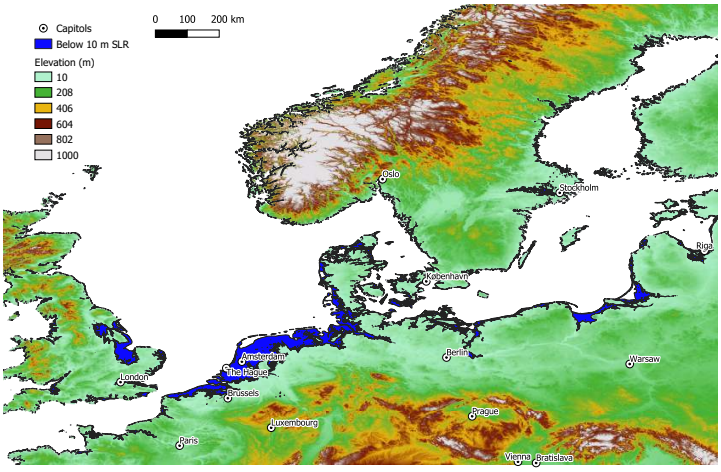

Figure D.1: Qgis Model effect of 10 meter Sea level Rise.

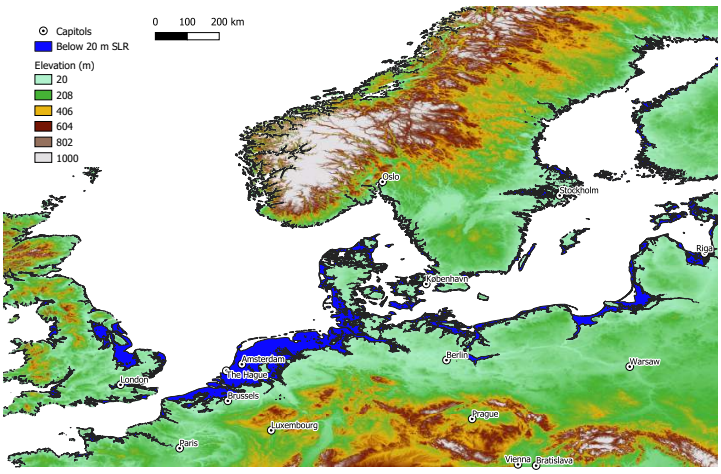

Figure D.2: Qgis Model effect of 20 meter Sea level Rise.

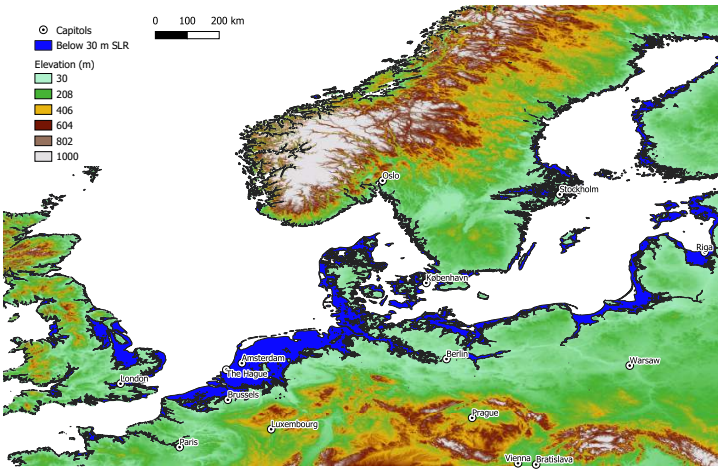

Figure D.3: Qgis Model effect of 30 meter Sea level Rise.

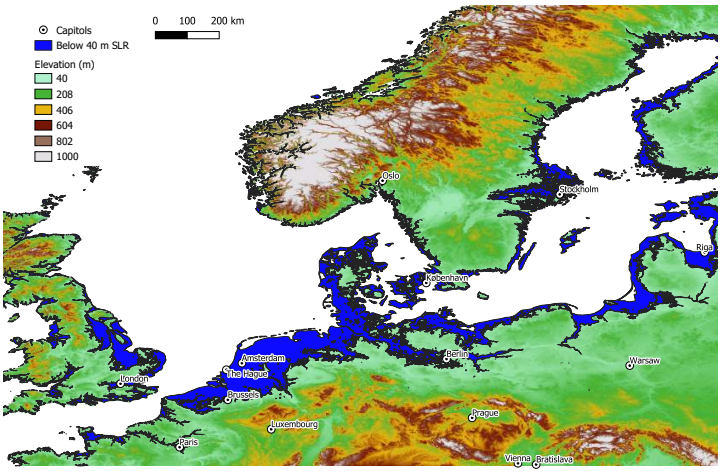

Figure D.4: Qgis Model effect of 40 meter Sea level Rise.

E

Criteria Huis in ’t Veld

Essential for determining the position of the dam are are four requirement described by Huis in ’t Veld [25], namely: Configuration of the bed in situ, the composition of the bed, the connection to the shore, and the closure method. These requirements are explained in more detail below.

E.0.1. Configuration of the Bed

For determining the most optimal position of the dam, the bathymetry of the area must be mapped. The shallow parts and deep channels should be optimally used in the configuration of the dam. Some aspects that need to be taken into account are summarized below:

- The deepest part of the area should be avoided, decreasing the cost and increasing the technical feasibility.
- Deep channels should be crossed perpendicular with respect to the channel direction and the streamlines of the flow through the channel.
- The closing gap should be far away from any confluences. A stable current pattern will make the occurring flow conditions easier to predict, and therefore the calculation during construction more precise.

E.0.2. Bed composition

The composition of the bed is essential to determine the bearing capacity of the bed and especially for the use of any building material for the dam. Weak bottom compositions should be avoided or improved by compacting the soil or replacing it with better bed materials.

E.0.3. Connection to the shores

A distinction can be made between onshore and offshore problems regarding to the shore connection. An onshore problem is a connection between the infrastructure; a poor connection between existing roads/railway will complicate the dam’s construction and thereby increase the costs. The offshore problem concerns the slope stability and disturbance to the area. Coastal outer bends and liquefaction prawn areas should be avoided.

F

Fault trees

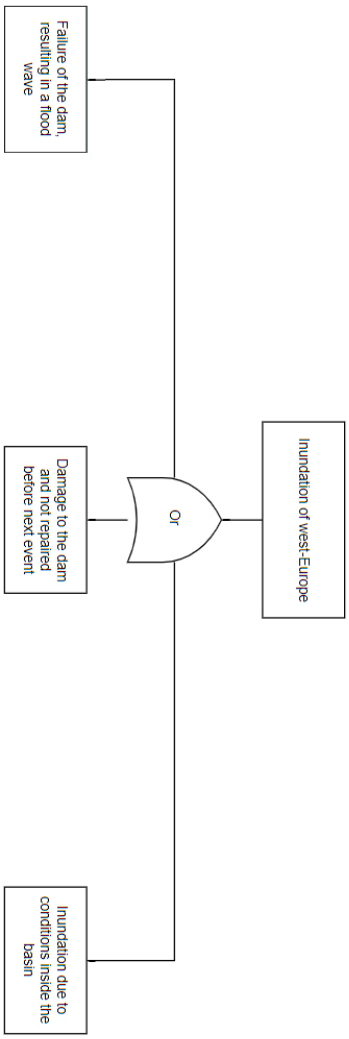

Figure F.1: Causes of the top event inundation west Europe.

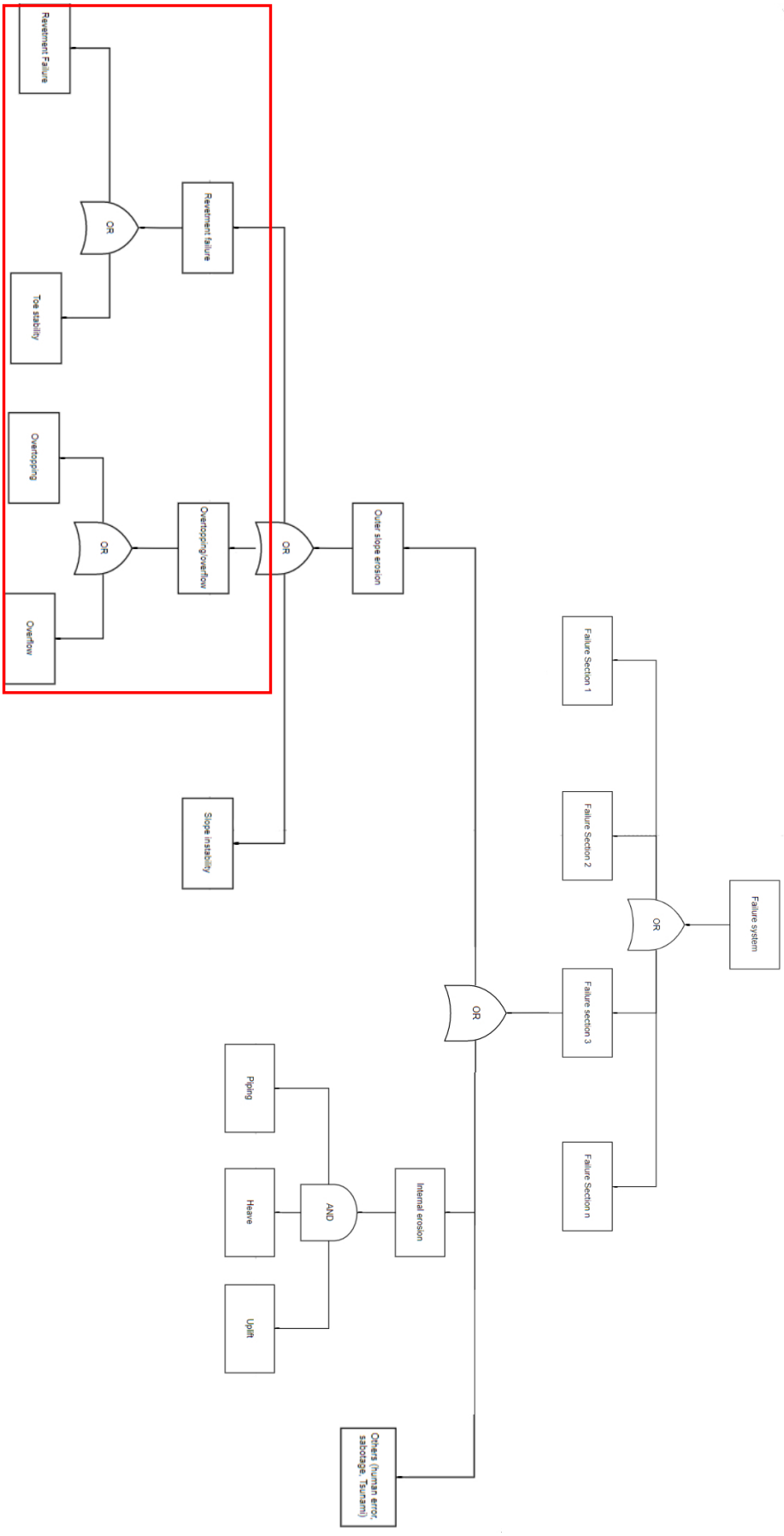

Figure F.2: Fault tree of the Earthen dam.

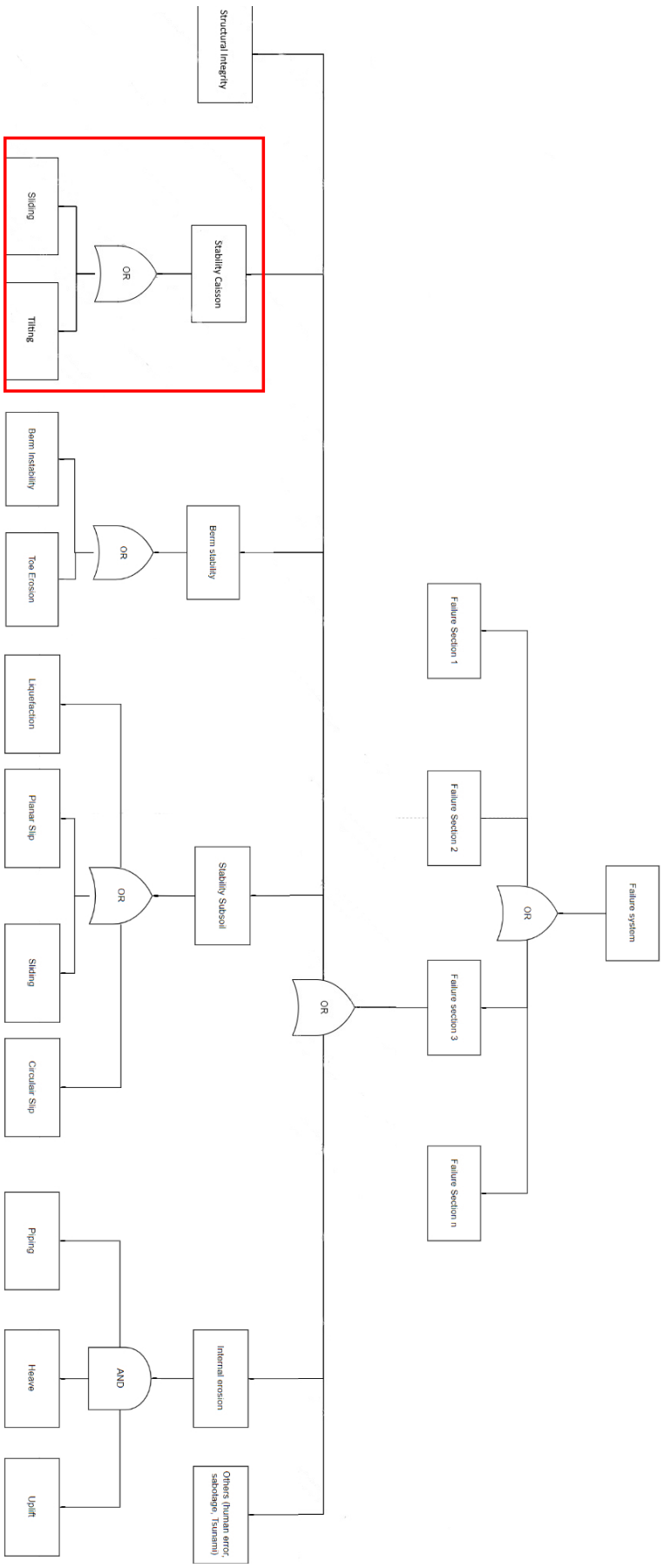

Figure F.3: Fault tree of the Caisson dam.

G

Data Analysis

G.1. Extreme Value Analysis

Table G.1: Thresholds and number of values all wave buoys Basin side and Ocean side

	Threshold	number of values
Orange Basin Side	4	161
Orange Ocean Side	7	73
Yellow Basin Side	6	92
Yellow Sea Side	6	109
Pink Basin Side	5	294
Pink Ocean Side	7	163
Green Basin Side	5	156
Green Ocean Side	8	320

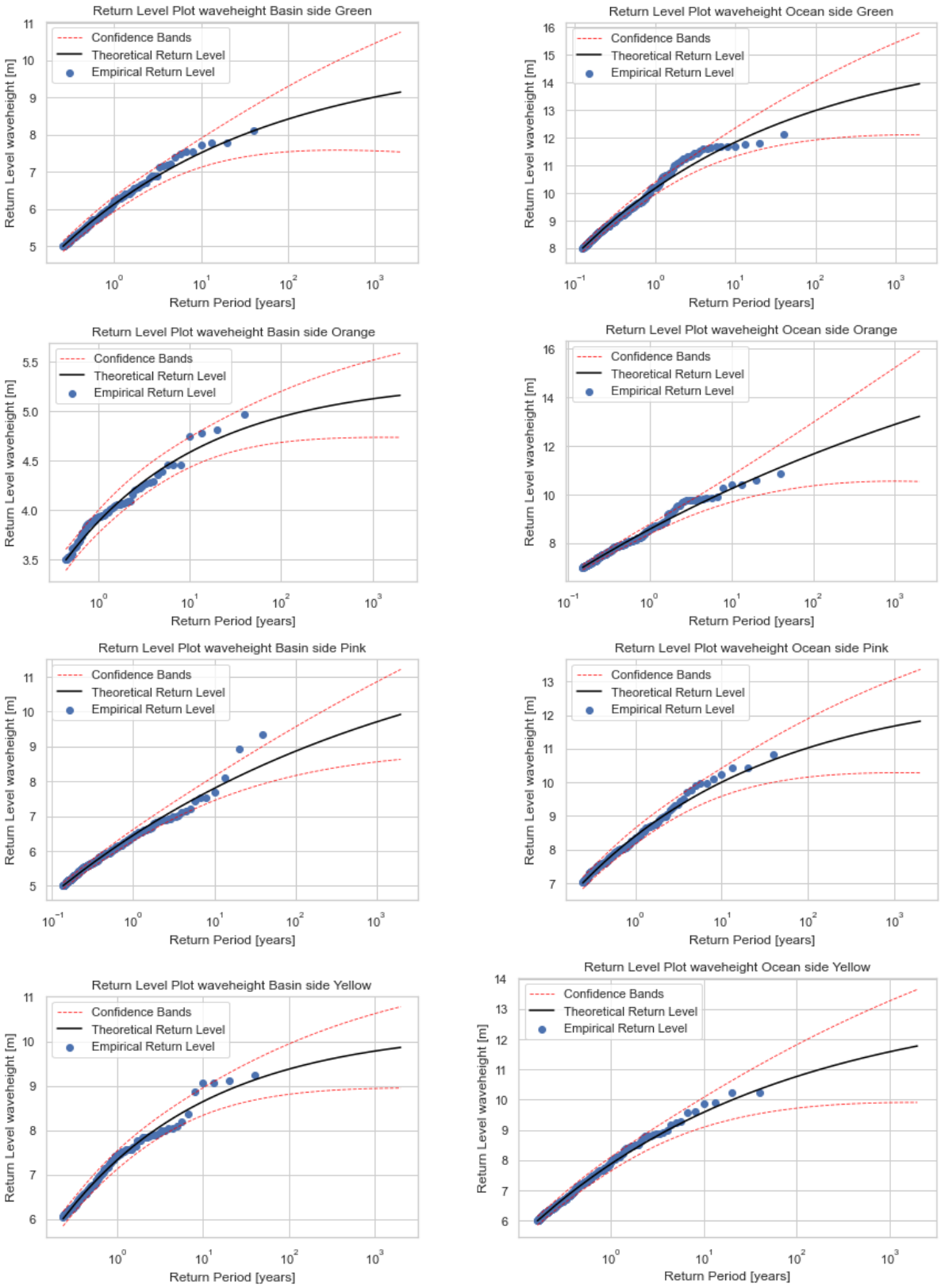

Figure G.1: Extreme Value Analysis all wave buoys inner and outer side of the dam.

G.2. Probability per event

The maximum allowable probability of failure is given per year. To calculate the probability of failure per event the Poisson distribution should be used. Because the probabilities are extremely small the following simplification can be applied:

$$p_{failureperevent} = p_{failureperyear} * \frac{L}{N} \tag{G.1}$$

Where
N [-] is the number of occurrences in the dataset.
L [years] is the length of the dataset. In the Tables below the number of events and the minimum number of runs are shown. The equation to calculate the number of runs is explained in chapter 5

Table G.2: Maximum allowable probability per event and the corresponding number of MC runs orange basin side.

Orange Buoy Basin Side 161 events per 40 years			
Failure Mechanism ULS	**Maximum allowable probability Of Failure per Year**	**Maximum allowable probability Of exceedance per event**	**Minimum number of MC runs**
Earthen Dam			
ULS Overtopping	4E-6	1E-6	11E6
ULS inner dike Revetment	2.5E-6	6.2E-7	17E6
ULS Toe stability	2.5E-6	6.2E-7	17E6
Caisson			
ULS Tilting and Sliding	1E-6	2.5E-7	44E6
Failure Mechanism SLS			
Earthen Dam			
SLS Overtopping	1	0.25	44
SLS Revetment	0.02	5E-3	2200
SLS Toe Stability	0.02	5E-3	2200
Caisson			
SLS Overtopping	1	0.25	44

Table G.3: Maximum allowable probability per events and the corresponding number of MC runs orange ocean side.

Orange Buoy Ocean Side 73 event per 40 years			
Failure Mechanism ULS	**Maximum allowable probability Of Failure per Year**	**Maximum allowable probability Of exceedance per event**	**Minimum number of MC runs**
Earthen Dam			
ULS Overtopping	4E-6	2.2E-6	5E6
ULS inner dike Revetment	2.5E-6	1.4E-6	7.9E6
ULS Toe stability	2.5E-6	1.4E-6	7.9E6
Caisson			
ULS Tilting and Sliding	1E-6	5.5E-7	20E6
Failure Mechanism SLS			
Earthen Dam			
SLS Overtopping	1	0.55	20
SLS Revetment	0.02	1E-2	1100
SLS Toe Stability	0.02	1E-2	1100
Caisson			
SLS Overtopping	1	0.55	20

Table G.4: Maximum allowable probability per event and the corresponding number of MC runs yellow basin side.

Yellow Buoy Basin Side 92 events per 40 years			
Failure Mechanism ULS	**Maximum allowable probability Of Failure per Year**	**Maximum allowable probability Of exceedance per event**	**Minimum number of MC runs**
Earthen Dam			
ULS Overtopping	4E-6	1.7E-6	5.8E6
ULS inner dike Revetment	2.5E-6	1.1E-6	10E6
ULS Toe stability	2.5E-6	1.1E-6	10E6
Caisson			
ULS Tilting and Sliding	1E-6	4.3E-7	26E6
Failure Mechanism SLS			
Earthen Dam			
SLS Overtopping	1	0.42	26
SLS Revetment	0.02	9E-3	1200
SLS Toe Stability	0.02	9E-3	1200
Caisson			
SLS Overtopping	1	0.42	26

Table G.5: Maximum allowable probability per event and the corresponding number of MC runs yellow ocean side.

Yellow Buoy Ocean Side 109 events per 40 years			
Failure Mechanism ULS	**Maximum allowable probability Of Failure per Year**	**Maximum allowable probability Of exceedance per event**	**Minimum number of MC runs**
Earthen Dam			
ULS Overtopping	4E-6	1.5E-6	7.3E6
ULS inner dike Revetment	2.5E-6	9.1E-7	12E6
ULS Toe stability	2.5E-6	9.1E-7	12E6
Caisson			
ULS Tilting and Sliding	1E-6	3.7E-7	30E6
Failure Mechanism SLS			
Earthen Dam			
SLS Overtopping	1	0.36	31
SLS Revetment	0.02	7E-3	1600
SLS Toe Stability	0.02	7E-3	1600
Caisson			
SLS Overtopping	1	0.36	31

Table G.6: Maximum allowable probability per event and the corresponding number of MC runs pink basin side.

Pink Buoy basin Side 294 events per 40 years			
Failure Mechanism ULS	**Maximum allowable probability Of Failure per Year**	**Maximum allowable probability Of exceedance per event**	**Minimum number of MC runs**
Earthen Dam			
ULS Overtopping	4E-6	5.4E-7	20E6
ULS inner dike Revetment	2.5E-6	3.4E-7	32E6
ULS Toe stability	2.5E-6	3.4E-7	32E6
Caisson			
ULS Tilting and Sliding	1E-6	1.7E-7	65E6
Failure Mechanism SLS			
Earthen Dam			
SLS Overtopping	1	0.14	79
SLS Revetment	0.02	2.7E-3	4080
SLS Toe Stability	0.02	2.7E-3	4080
Caisson			
SLS Overtopping	1	0.14	79

Table G.7: Maximum allowable probability per event and the corresponding number of MC runs pink ocean side.

Pink Buoy ocean Side 163 events per 40 years			
Failure Mechanism ULS	**Maximum allowable probability Of Failure per Year**	**Maximum allowable probability Of exceedance per event**	**Minimum number of MC runs**
Earthen Dam			
ULS Overtopping	4E-6	9.9E-7	11E6
ULS inner dike Revetment	2.5E-6	6.2E-7	18E6
ULS Toe stability	2.5E-6	6.2E-7	18E6
Caisson			
ULS Tilting and Sliding	1E-6	2.5E-7	44E6
Failure Mechanism SLS			
Earthen Dam			
SLS Overtopping	1	0.25	44
SLS Revetment	0.02	4.9E-3	2244
SLS Toe Stability	0.02	4.9E-3	2244
Caisson			
SLS Overtopping	1	0.25	44

Table G.8: Maximum allowable probability per event and the corresponding number of MC runs green basin side.

Green Buoy basin Side 156 events per 40 years			
Failure Mechanism ULS	**Maximum allowable probability Of Failure per Year**	**Maximum allowable probability Of exceedance per event**	**Minimum number of MC runs**
Earthen Dam			
ULS Overtopping	4E-6	10E-7	11E6
ULS inner dike Revetment	2.5E-6	6.4E-7	17E6
ULS Toe stability	2.5E-6	6.4E-7	17E6
Caisson			
ULS Tilting and Sliding	1E-6	2.6E-7	42E6
Failure Mechanism SLS			
Earthen Dam			
SLS Overtopping	1	0.26	42
SLS Revetment	0.02	5E-3	2200
SLS Toe Stability	0.02	5E-3	2200
Caisson			
SLS Overtopping	1	0.26	42

Table G.9: Maximum allowable probability per event and the corresponding number of MC runs green ocean side.

Green Buoy Ocean Side 320 events per 40 years			
Failure Mechanism ULS	**Maximum allowable probability Of Failure per Year**	**Maximum allowable probability Of exceedance per event**	**Minimum number of MC runs**
Earthen Dam			
ULS Overtopping	4E-6	5E-7	22E6
ULS inner dike Revetment	2.5E-6	3.1E-7	34E6
ULS Toe stability	2.5E-6	3.1E-7	34E6
Caisson			
ULS Tilting and Sliding	1E-6	1.3E-7	84E6
Failure Mechanism SLS			
Earthen Dam			
SLS Overtopping	1	0.13	82
SLS Revetment	0.02	2.5E-3	4400
SLS Toe Stability	0.02	2.5E-3	4400
Caisson			
SLS Overtopping	1	0.13	82

G.3. Results fitts

Table G.10: Goodness of fit per multivariate copula Ocean Side, bold is best fit.

		T Copula	Gaussian Copula	Vine Copula	Data
Orange				2nd Structure	
SSD	Height	2	**2**	3	
(sum of squared	Direction	1183	**632**	650	-
distance)	Period	7	**6**	8	
Silhouette Score	2 Clusters	0.5	**0.51**	0.51	0.57
SSD Clusters		14500	**13000**	17000	12500
Green				3rd Structure	
SSD	Height	3	**2**	1	
(sum of squared	Direction	1402	**1188**	1500	-
distance)	Period	14	**7**	9	
Silhouette Score	2 Clusters	0.9	**0.9**	0.9	0.91
SSD Clusters		17000	**20000**	20000	17500
Yellow				3rd Structure	
SSD	Height	3	2	**2**	
(sum of squared	Direction	513	1601	**511**	-
distance)	Period	18	20	**13**	
Silhouette Score	3 Clusters	0.91	0.91	**0.91**	0.91
SSD Clusters		32000	32000	**32000**	32000
Pink				1st Structure	
SSD	Height	3	**2**	2	
(sum of squared	Direction	1807	**1716**	1800	-
distance)	Period	21	**9**	15	
Silhouette Score	2 Clusters	0.93	**0.90**	0.9	0.91
SSD Clusters		20000	**20000**	20000	15000

Table G.11: Goodness of fit per multivariate copula Basin Side.

		T Copula	Gaussian Copula	Vine Copula	Data
Orange				1st Structure	
SSD	Height	0.4	**0.35**	0.69	
(sum of squared	Direction	268	**731**	260	-
distance)	Period	8	**20**	32	
Silhouette Score	2 Clusters	0.52	**0.77**	0.49	0.58
SSD Clusters		5700	**5500**	4800	5000
Green				3rd Structure	
SSD	Height	0.6	**0.3**	0.2	
(sum of squared	Direction	1419	**1106**	5866	-
distance)	Period	16	**26**	13	
Silhouette Score	2 Clusters	0.86	**0.89**	0.88	0.84
SSD Clusters		41000	**30000**	58000	37000
Yellow				3rd Structure	
SSD	Height	0.4	**0.1**	0.3	
(sum of squared	Direction	4788	**5868**	6625	-
distance)	Period	32	**10**	13	
Silhouette Score	2 Clusters	0.88	**0.84**	0.85	0.8
SSD Clusters		220000	**250000**	290000	240000
Pink				3rd Structure	
SSD	Height	2	5	**2**	
(sum of squared	Direction	2238	1369	**1012**	-
distance)	Period	22	55	**30**	
Silhouette Score	2 Clusters	0.62	0.65	**0.62**	0.63
SSD Clusters		210000	160000	**180000**	190000

G.4. Correlation

The last part of the analysis is the correlation between the different observation buoys. The correlation coefficient shows the coherence between the buoys. The correlation will be used in a later stage to calculate the failure probability. The Pearson's linear correlation coefficient equation G.2 is used to calculate the correlation coefficient.

$$\rho = \frac{\sum_{i=1}^{n}(X_{a,i} - \overline{X_a})(Y_{b,i} - \overline{Y_b})}{[\sum_{i=1}^{n}(X_{a,i} - \overline{X_a})^2 \sum_{j=1}^{n}(Y_{b,j} - \overline{Y_b})^2]^{1/2}} \tag{G.2}$$

A positive number means a positive correlation and vice versa. In the table, G.12 are all the possible combinations of 2 wave buoys. The table clearly shows the effect of distance on the correlation coefficient [15].

Table G.12: Pearson's linear correlation coefficient wave observation buoys.

	green buoy	**orange buoy**	**yellow buoy**	**pink buoy**
green buoy	1	0.4319	0.8406	0.8285
orange buoy	0.4319	1	0.4005	0.3710
yellow buoy	0.8406	0.4005	1	0.9399
pink buoy	0.8285	0.3710	0.9399	1

H

Equations

H.1. Overtopping

In the section below the governing overtopping equations are written out for both the caisson and earthen dam.

H.1.1. Occurring overtopping discharge Earthen Dam

The overview of the equations for overtopping and overflow are mainly based on the Eurotop manual overtopping. (bron). In equation H.1, the critical overtopping discharge as a function of the wave height for breaking waves is presented. Equation H.2, is the maximum overtopping for non-breaking waves, from the Eurotop.

$$\frac{q}{\sqrt{g \cdot H_{m0}^3}} = \frac{0.023}{\sqrt{\tan \alpha}} \gamma_b \cdot \xi_{m-1,0} \cdot \exp\left[- \left(2.7 \frac{R_c}{\xi_{m-1,0} \cdot H_{m0} \cdot \gamma_b \cdot \gamma_f \cdot \gamma_\beta \cdot \gamma_v} \right)^{1.3} \right] \tag{H.1}$$

$$\frac{q}{\sqrt{g \cdot H_{m0}^3}} = 0.09 \cdot \exp\left[- \left(1.5 \frac{R_c}{H_{m0} \cdot \gamma_f \cdot \gamma_\beta \cdot \gamma_v} \right)^{1.3} \right] \tag{H.2}$$

Where:

- q is the overtopping discharge in $[m^3/s/m]$.
- H_{m0} wave height at the toe of the dam in$[m]$.
- α is the slope angle in [°], A representative slope should be defined when a dam consists of multiple slopes or has one or multiple berms. Berms can be disregarded in the representative slope calculations because the effect of the berm is already included in the reduction factor for berms. The equation for the representative berm in equation H.3. The L_{talud} is the length of the slope, B is the berm width and $R_{2\%}$ is the 2% run-up explained later in this section.

$$\tan(\alpha) = \frac{1.5 * H_{m0} + R_{u2\%}}{L_{\text{talud}} - B} \tag{H.3}$$

- R_c is the freeboard $[m]$ which is the crest level $[m]$ minus still water level [m], $R_C = y_N - h$
- $\xi_{m-1,0}$, is the breaking parameter(the Irribaren number) in $[-]$. The dam will influence the type of wave breaking on the dam. The breaker parameter describes the type of breaking as a function of slope and the wave's steepness. The formula for the wave steepness is the wave height divided by its length which can be rewritten so that the steepness depends on the wave period.

$$\xi_{m-1,0} = \frac{\tan(\alpha)}{\sqrt{\left(H_{m0} * 2\pi\right) / \left(g * T_{m-1,0}^2\right)}} \tag{H.4}$$

- γ_b is the reduction factor of a berm. The reduction factor can be written as:

$$\gamma_b = 1 - \frac{B}{L_{\text{bem}}} \left(0.5 + 0.5 \cdot \cos\left(\pi \frac{d_h}{x}\right)\right) \text{ with } 0.6 \leq \gamma_b \leq 1.0 \tag{H.5}$$

  Where d_h is the waterdepth at the middle of the berm and x depends on the berm position. (explained in more detail (TAW TRRunupOvertopping.pdf).

-

$$\begin{array}{ll} x = z_{2\%} \text{ if } z_{2\%} > -d_h > 0 & \text{(berm above still water line)} \\ x = 2.H_{m0} \text{ if } 2.H_{m0} > d_h \geq 0 & \text{(berm below still water line)} \\ r_{dh} = 1 \text{ if } -d_h \geq z_{2\%} \text{ or } d_h \geq 2.H_{m0} & \text{(outside influence area)} \end{array}$$

- d_h is the distance between the middle of the berm and still water level.
- γ_f is the influence factor of the roughness elements. In appendix 11 of the TAW manual the influence factors of various roughness elements are shown.
- γ_v is the reduction factor for vertical wall on the dam.
- γ_β is the reduction factor due to oblique waves. In nature, almost all waves are short crested, meaning that the wave direction is scattered around the propagation direction. The reduction factor for certain wave angles can be determined using the following equations.

$$\gamma_\beta = 1 - x|\beta| \quad (0^\circ \leq |\beta| \leq 80^\circ) \tag{H.6}$$

$$\gamma_\beta = 1 - x * 80 \quad (|\beta| > 80^\circ \tag{H.7}$$

  The value for x is for 2% run-up 0.0022 and for overtopping 0.0033.
- Waves can come at an angle of more than 80 %, this reduces the run-up and overtopping. To take this effect into account the wave height and period are adjusted in stead of the influence factor.

$$H_{m0} \text{ is multiplied by } \frac{110 - |\beta|}{30} 80^\circ \leq |\beta| \leq < 110^\circ \tag{H.8}$$

$$T_{m-1,0} \text{ is multiplied by } \sqrt{\frac{110 - |\beta|}{30}}, 80^\circ \leq |\beta| \leq 110^\circ \tag{H.9}$$

  For $110^\circ < \|\beta| <= 180^\circ$ $H_{m0} = 0$ resulting no run-up and no overtopping.
- The reduction factors are determined experimentally separately from each other because of this a combination of these factors can produce a meager total reduction (e.g., rubble mount slope with a maximum reducing berm and oblique waves) therefore a minimum reduction has been proposed,$\gamma_b \gamma_f \gamma_{beta} \geq 0.4$
- $R_{u2\%}$ is the 2% wave run-up above still water level and can be calculated using the following formula:

$$\frac{R_{u2\%}}{H_{m0}} = 1.65 \cdot \gamma_b \cdot \gamma_f \cdot \gamma_\beta \cdot \xi_{m-1,0} \tag{H.10}$$

  With a maximum of:

$$\frac{R_{u2\%}}{H_{m0}} = 1.0 \cdot \gamma_f \cdot \gamma_\beta \left(4 - \frac{1.5}{\sqrt{\xi_{m-1,0}}}\right) \tag{H.11}$$

- For fully probabilistic calculations, the coefficients A and B based on the general shape; $\frac{q}{\sqrt{g \cdot H^3}} = A(\ldots) \exp -B(\ldots)^{1.3}$, should include a standard deviation. The mean and standard deviation are presented in table H.1

	A	**B**
Mean value	0.023	2.7
Standard deviation	0.003	0.2

Table H.1: Shape coefficients overtopping

The last situation is when the foreshore is very shallow, $\xi_{m-1,0} > 7$, the equation below is used.

$$\frac{q}{\sqrt{g \cdot H_{m0}^3}} = 10^c \cdot \exp\left(-\frac{R_c}{\gamma_t \cdot \gamma_\beta \cdot H_{m0} \cdot (0.33 + 0.022 \cdot \xi_{m-1,0})}\right) \tag{H.12}$$

Where, c is normal distributed with a mean of -0.92 and a standard deviation of 0.24

H.1.2. Occurring overtopping discharge Caisson

The overtopping formula for a caisson differs slightly compared to a slope. The overtopping manual from the Eurotop [19] is used to calculate the overtopping. The first step is determining the presence of a foreshore. The foreshore can influence the wave by shoaling, steepening, and breaking. The presence of a foreshore can be excluded when the waves are in deep water conditions. The equation for overtopping on a caisson without a foreshore equals the equation for steep slopes ($\cot \alpha = 0$).

$$\frac{q}{\sqrt{g \cdot H_{m0}^3}} = 0.047 \cdot \exp\left[-\left(2.35 \frac{R_c}{H_{m0} \cdot \gamma_f \cdot \gamma_\beta}\right)^{1.3}\right] \tag{H.13}$$

where

- σ(0.047) = 0.007 together with σ(2.35) =0.23.
- Rc [m]is the crest freeboard which is the difference between the still water level and the crest of the caisson. The reduction factor for the angle of attack is given by 7.17

$$\gamma\beta = 1 - 0.0062\beta \quad \text{for } 0^0 < \beta < 45^\circ \tag{H.14}$$

$$\gamma\beta = 0.72 \quad \text{for } \beta \geq 45^\circ \tag{H.15}$$

- γ_f [-] is the influence factor for the permeability and roughness of or on the slope. This value is set to zeros as the caisson has no slope.

If there is an influence of a foreshore, the next step should be proceeded. Step two considered the presence of a mound in front of the caisson. The amount of overtopping is influenced by the mound if the water depth over the mound exceeds 60% of the water depth at the toe. This is clearly not the case as the minimum water depth of the dam is 100 meters.
The following step is the likelihood of impulsive overtopping conditions. The condition for impulse and non-impulse is given below:

$$\frac{d}{H_{m0}} \cdot \frac{h}{L_{m-1.0}} > 0.65 \quad \text{Treat as non-impulsive conditions.} \tag{H.16}$$

$$\frac{d}{H_{m0}} \cdot \frac{h}{L_{m-1,0}} \leq 0.65 \quad \text{Treat as impulsive conditions.} \tag{H.17}$$

As the water depth is at a minimum of 100 meters, the impulsive situation is improbable and therefore not considered. This led to the following overtopping discharge equation for waves affected by the foreshore (non-impulsive).

$$\frac{q}{\sqrt{gH_{m0}^3}} = 0.05 \exp\left(-\frac{2.78}{\gamma_\beta} \frac{R_c}{H_{m0}}\right) \tag{H.18}$$

where σ(0.05) = 0.012 together with $\sigma\sigma$(2.78) = 0.17

H.2. Stability Caisson

The two mechanisms that determine the stability of the caisson are tilting and sliding. The equation are retrieved from the work by Goda [21]. Some adjusted are made to include the difference in hydrostatic pressure as displayed in Figure H.1.

H.2.1. Sliding

Sliding occurs when the sum of the horizontal water force (wave impact, hydrostatic pressure) is less than the balancing force (friction). The limit state function against sliding is defined as follows:

$$\text{S.F.} = \frac{\mu(Mg - U)}{p} \tag{H.19}$$

Where,

- M [kg/m] is the mass of the upright section per unit extension in still water minus the buoyancy force.
- μ [-] is the friction coefficient between the upright section and the sill, usually 0.6 for a rock berm, for a sand berm this value will be smaller. For concrete to sand the friction will be lower, e.g. 0.4 [8].
- g [m/s] is the gravitational constant.
- U [kN/m] is the Uplift force of the caisson. Which can be calculated by the following formula:

$$U = \frac{1}{2} p_u B \tag{H.20}$$

Where

$$p_u = \frac{1}{2}(1 + \cos\beta)\alpha_1 \alpha_3 \rho g H \tag{H.21}$$

Where,

- B [m] is the width of the bottom of the upright section.
- H [m] is the wave height.
- β [degrees] is the angle between the direction of wave approach and a line normal to the dam.
- α_1 [-] is the tendency of wave pressure increase with the wave period (it does not carry any theoretical significance).

$$\alpha_1 = 0.6 + \frac{1}{2}\left[\frac{4\pi h/L}{\sinh(4\pi h/L)}\right]^2 \tag{H.22}$$

- α_2 [-] not included in the stability formula against uplift, represents the tendency of the pressure to increase with the height of the sill.

$$\alpha_2 = \min\left\{\frac{h_b - d}{3h_b}\left(\frac{H_{\max}}{d}\right)^2, \frac{2d}{H_{\max}}\right\} \tag{H.23}$$

- α_3 [-] is derived on the simplification of a linear pressure variation between p_1 and p_2. α_3

$$\alpha_3 = 1 - \frac{h'}{h}\left[1 - \frac{1}{\cosh(2\pi h/L)}\right] \tag{H.24}$$

Where,

- h_b [m] is the water depth at a distance of 5 times the wave height.
- L [m] is the deep water wave length corresponding to the wave period.
- d [m] is the height of the sill.
- $h^{'}$ [m] the distance from the design water level to the bottom of the upright section.
- h_c [m] is the crest elevation of the breakwater above the design water level.
- η^* [m] is the elevation to which the wave pressure is exerted: $\eta^* = 0.75(1 + \cos\beta)H$.
- p_1, p_2, p_3, p_4 [kPa] are the different wave pressure components on the front of the caisson, the components are shown in figure H.2.

$$p_1 = \frac{1}{2}(1 + \cos\beta)\left(\alpha_1 + \alpha_2 \cos^2\beta\right)\rho g H_{max} \tag{H.25}$$

$$p_2 = \frac{p_1}{\cosh(2\pi h/L)} \tag{H.26}$$

$$p_3 = \alpha_3 p_1 \tag{H.27}$$

$$p_4 = \begin{cases} p_1\left(1 - h_c/\eta^*\right) & : \eta^* > h_c \\ 0 & : \eta^* \leq h_c \end{cases} \tag{H.28}$$

$$h_c^* = \min\left\{\eta^*, h_c\right\} \tag{H.29}$$

Based on the above formulas for wave pressure the total wave pressure equation follows:

$$P = \frac{1}{2}\left(p_1 + p_3\right)h' + \frac{1}{2}\left(p_1 + p_4\right)h_c^* \frac{1}{2}\rho_w g(h^{'2} - b^{'2} * g) \tag{H.30}$$

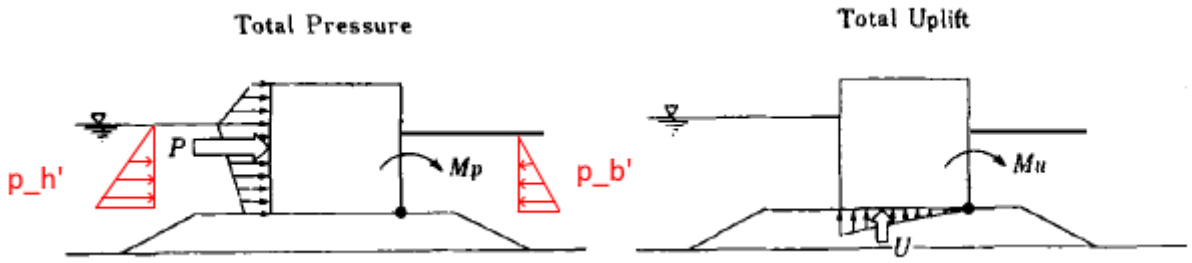

Figure H.1: Definition sketch of total pressure as well as uplift and their moment, based on research Goda [21]

H.2.2. Tilting

For tilting, the sum of the moments is calculated on the caisson. The formulas are based on the research by Goda. Also for this part a slight adjustment is made to the calculation to fit for the dam condition, the hydrostatic pressure is added. In figure xx, the hydrostatic pressure is indicated in red.

The limit state for tilting is defined as:

$$\text{S.F.} = \frac{Mgt - M_U}{M_p} \tag{H.31}$$

Most of the variables and equation are equal to the sliding equation, the ones that differ are appointed below.
Where,

- t [m] is the horizontal distance between the centre of gravity.
- M_U [kNm/m] is the moment of uplift pressure $M_U = \frac{2}{3}UB$.
- M_u [kNm/m] is the moment of wave pressure plus the hydrodostatic pressure, which can be calculated by the following formula:

$$M_p = \frac{1}{6}(2p_1 + p_3)\,h'^2 + \frac{1}{2}(p_1 + p_4)\,h' h_c^* + \frac{1}{6}(p_1 + 2p_4)\,h_c^{*2} + \frac{1}{6}\rho_w g(h'^2 - b'^2) \tag{H.32}$$

Where,

- B' [m] the distance from the design water level in the basin to the bottom of the upright section.

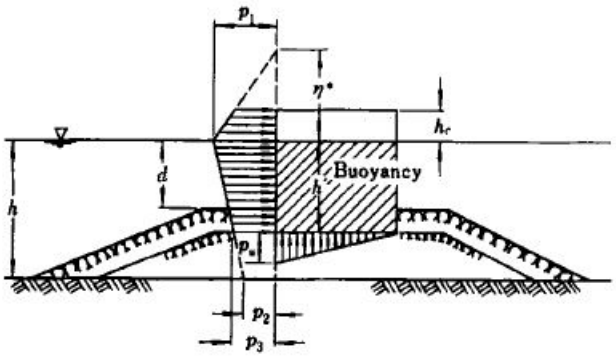

Figure H.2: Distribution of wave pressure on an upright section of a vertical breakwater [21].

H.3. Sellmeijer, Piping

The Sellmeijer equation calculates the maximum hydraulic head over a structure where the grains are still in equilibrium(Sand boils). The maximum hydraulic head calculation depends on the length of the

structure, the permeability of sand, the drag coefficient, the diameter of sand grains, and the rolling resistance. The large-scale model test validates the formula in the Delta Channel. The piping criteria can be written as:

$$(\Delta H - 0.3d) \leq \frac{1}{\gamma}\Delta H_c \tag{H.33}$$

Where:

- γ [-] is the safety factor 1.2.
- d is the crack channel length (0 if no impermeable layer)
- ΔH is the head difference at both sides of the dam.
- ΔH_c the critical hydraulic head over the flood defence.

$$\Delta H_c = \alpha c \frac{\gamma_p}{\gamma_w} \tan(\theta)(0.68 - 0.10\ln(c))L \tag{H.34}$$

Where,

$$\alpha = \left(\frac{D}{L}\right)^{\frac{0.28}{\left(\frac{D}{L}\right)^{2.8}-1}} \tag{H.35}$$

Where,

$$c = \eta d_{70}\left(\frac{1}{\kappa L}\right)^{\frac{1}{3}} \tag{H.36}$$

Where,

- γ_w [kN/m^3] is the volume weight of water.
- γ_p [kN/m^3] is the (apperent) volume weight of sand grains under water.
- θ [$degrees$] is the rolling resistance of sand.
- η [-] the drag coefficient.
- κ [m^2] is the intrinsic permeability of sand, $\kappa = \frac{v}{g}k$, v is the kinematic viscosity.
- d_{70} [m] is the 70 percent value of the grain distribution.
- D [m] is the thickness of the sand layer.

H.4. Revetment

Stability of the Revetment Earthen Dam

The revetment can be protected against waves by three main categories: Open revetment such as; rip-rap, rock, and lose grains; semi-permeable revetments such as placed blocks; and impervious such as asphalt, concrete. The difference between these types of revetment is leakage length Λ. The leakage length is the length of the protection in which the flow resistance through the top layer and the filter layer are the same. The equation is as follows:

$$\Lambda = \sqrt{\frac{k_F d_F d_T}{k_T}} \tag{H.37}$$

Where k_F and k_T are the permeability of the top layer and filter layer, respectively, d_F and d_T are the thickness of the layer. When the wavelength is much larger than the leakage length, there is almost no head difference between the top and filter layers. If the wavelength is much smaller than the leakage length, then the head difference is significant.

Stability of rock revetment

Van der Meer developed a formula to calculate the stability of a rock revetment based on the Hudson equation. He created two formulas, one for plunging and the other for surging waves.

$$\frac{H_s}{\Delta D_{n50}} = c_{pl,d} P^{0.18}\left(\frac{S_d}{\sqrt{N}}\right)^{0.2} \xi_m^{-0.5} \quad \text{for plunging waves} \tag{H.38}$$

$$\frac{H_s}{\Delta D_{n50}} = c_{s,s} P^{-0.13}\left(\frac{S_d}{\sqrt{N}}\right)^{0.2} \sqrt{\cot\alpha}\,\xi_{m-1,0}^{P} \text{ for surging waves} \tag{H.39}$$

Where,

- P [-] is the notional permeability coefficient. The notional permeability coefficient depends on the structure of the sub layers. The P parameter should lay between between 0.1 and 0.6. Figure 5.39 from the Rock manual shows the different sublayer with the corresponding P value.
- D_{n50} [m] is the nominal median block diameter, or equivalent cube size, $d_n = (M/\rho_s)^{\frac{1}{3}}$.
- N [-] is the number of waves during a storm.
- ξ_m [-] is the breaking parameter see section xx.
- H_s [m] is the significant wave height.
- T_m [sec] is the mean period of a wave.
- Δ [-] is the relative mass density $\frac{\rho_s - \rho_w}{\rho_w}$.
- S [-] is the damage level. The damage parameter depends on the slope of the dam and the damage level. The table containing different slopes and damage parameters for quarry stone is shown in table 5.23 of the Rock Manual.
- α [degrees] is the angel of the slope.
- C_{pl} & C_s [-] are the model constant which have a mean of 6.2 and 1 and a standard deviation of 0.4 and 0.08 respectively.
- The difference between plunging and surging waves can be determined by calculating the critical breaking parameter using the following equation:

$$\xi_{cr} = \left[\frac{c_{pl}}{c_s} P^{0.31} \sqrt{\tan \alpha} \right]^{\frac{1}{P+0.5}} \tag{H.40}$$

- If $\xi_m < \xi_{cr}$ waves are plunging and the other way around, the waves are surging.

The above formula is only valid for deepwater conditions, where the waves are Rayleigh distributed. The Van der Meer formula is tuned for the use Of H_s , meaning it is only applicable for deepwater conditions. Therefore the equation is slightly modified for shallow water conditions. The rock manual presents equation xx, using the Van der Meer equation with some adjustments based on model test data, especially for shallow water conditions by Van Gent.

$$\frac{H_s}{\Delta D_{n50}} = c_{pl} P^{0.18} \left(\frac{S_d}{\sqrt{N}} \right)^{0.2} \left(\frac{H_s}{H_{2\%}} \right) (\xi_{s-1,0})^{-0.5} \text{ for plunging waves} \tag{H.41}$$

$$\frac{H_s}{\Delta D_{n50}} = c_s P^{-0.13} \left(\frac{S_d}{\sqrt{N}} \right)^{0.2} \left(\frac{H_s}{H_{2\%}} \right) \sqrt{\cot \alpha} \, (\xi_{s-1,0})^{P} \text{ for surging waves} \tag{H.42}$$

H.5. Stability Placed Block Revetment

Placed block revetment or interlocking elements can be used when the median diameters of the quarry stone revetment become unrealistically large. The stability equations of the armour units have been developed for different types. Steep slopes are preferred to increase the interlocking strength. The equations are retrieved from the Rock Manual [8].

xbloc

For this thesis only the xbloc is analyzed, produced by BAM. Xbloc are single elements and are developed by Delta Marine Consultants. The storm's duration does not influence the performance of the xbloc and therefore is not part of the stability formula. For an xbloc no movement or damage is allowed, meaning that there is also no damage parameter in the formula.

The best design formula is the Hudson equation as given below.

$$\mathrm{V_{Xbloc}} = \left[\frac{H_\mathrm{s}}{2.77 \times \Delta} \right]^3 Xcorrectionfactor \tag{H.43}$$

where

- V [m^3] is the unit volume.
- Δ [-] is the relative concrete density 1.33.

The underlayer of an xbloc consists of a rock layer of 1/6 to 1/15 of unit mass of the x bloc.

H.6. Toe

It is not necessary to extend the armor layer over the entire water depth. Below one wave height of the lowest still water level, the wave action is limited. The toe protects the front of the armor layer from sliding and erosion. If the same rock diameter is used in the toe as the armor layer, the toe is very likely to be stable. Reducing the toe is preferable as the cost will decrease significantly. The equations for the stability of the toe are shown below.

If the water depth is more than three times the wave height is can result in a negative number, the boundary condition is, resulting in the condition, $\frac{h_t}{H_S} < 2$.

$$\frac{H_s}{\Delta d_{n50}} = \left(0.24\frac{h_t}{d_{n50}} + 1.6\right) N_{od}^{0.15} \quad 3 < h_t/d_{n50} < 25 \tag{H.44}$$

$$\frac{H_s}{\Delta d_{n50}} = \left(6.2\frac{h_t}{h} + 2\right) N_{od}^{0.15} \quad 0.4 < h_t/h < 0.9 \tag{H.45}$$

Where

- h_t [m] is the distance between the top of the toe and the still water level.
- N_{od} [-] is the character of damage, which is 0.5 for the start of damage, 1 for acceptable damage, and 4 for failure.
- h [m] is the distance between the bottom of the toe to the still water level.

H.7. Open filter Design

The main difference between a geometrically closed and open filter is that no material can be washed out for a closed filter. For sand, as core material, a geotextile is applied to make the filter completely closed. For deeper water depths constructing a geotextile is complicated; an alternative is an open filter. The filter layer is designed to minimize the hydraulic loading onto the base layer to keep the amount of erosion within a specific range. For this thesis, the study from Klein Bretler and Den Adel is used [56]. The critical hydraulic gradient is given as:

$$i_{cr} = a_f \cdot u_{f,cr} + b_f \cdot u_{f,cr}^2 \tag{H.46}$$

Where

- $a_f = \frac{160 \cdot v_w \cdot (1-n_f)^2}{g \cdot n_f^3 \cdot D_{f,15}^2}$ and $b_f = \frac{2.2}{g \cdot n_f^2 \cdot D_{f,15}}$ [s2/m2]

The critical filter velocity is given as:

$$u_{f,cr} = \left[\frac{n_f}{c}\left[\frac{D_{15,f}}{v_w}\right]^m \sqrt{\psi \cdot g \cdot \Delta \cdot D_{50,b}\frac{sin(\phi-\alpha)}{sin\phi}}\right]^{1/(1-m)} \quad \text{for } 0.1 \text{ mm} < D_{50,b} < 1 \text{ mm} \tag{H.47}$$

Where,

- Uf_{cr} [m/s] = critical filter velocity, where uf is the averaged velocity over the cross-section of the filter
- Δ [-] = relative submerged density of base material.
- Ψ [-] = Shields parameter for base material.
- m,c [-] = constants, dependent on $D50_b$, see Table 1.
- ν_w [m2/s] = kinematic viscosity of water.
- α [degrees] = slope of the dam.
- ϕ [degrees] = angle of internal friction base material.

- n_f [-] is the porosity of the filter layer.
- For xblocs, a correction factor should apply one of the following criteria apply: Water depth is significant. Core permeability is low. The foreshore is steep. The armor slope is mild. The correction factors for these local phenomena can be found in the xbloc manual. If more of the above criteria is applicable, the largest factor should be used.

The occurring hydraulic gradient near the bed is calculated from the linear wave theory.

$$i_{max} = \frac{kH}{2 * cosh(kh)} \tag{H.48}$$

The criterion for an open filter design is given as:

$$z_{acc} < (d_{tot} - 2D_{n50,a}) \tag{H.49}$$

- H [m] is the wave height.
- k [rad/m] is the wave number.
- h [m] is the water depth.
- The accretion area divided by the total filter layer thickness is $\frac{A_{\text{acc}}}{d_{tot}^2} = \left(0.042 \cot\alpha \frac{i_{\|,2\%}}{i_{cr}}\right)^3$, $i_{2\%}$ = 2% occurring critical gradient.
- $\frac{z_{acc}}{d_{tot}} = 0.31 \left(\frac{A_{acc}}{d_{tot}^2}\right)^{0.5}$, Z_{acc} = accretion height.

H.8. Toe Protection Caisson

Figure H.4 shows a diagram from Takahashi for determining the necessary block thickness t' as function of the wave height H, and the ratio's water depth h_b/h_s. Where h_b is the water depth on top of the sill and h_s the water depth in front of the sill [1].

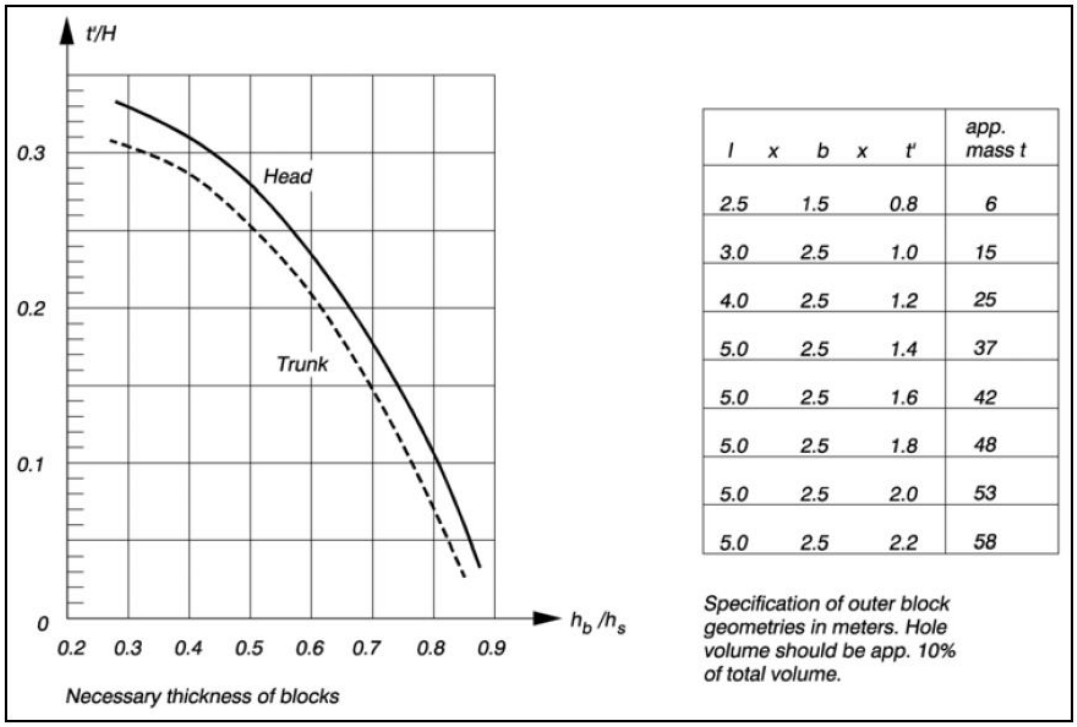

Figure H.3: Design of foot protection blocks according to Japanese practice [1].

H.9. Caisson Berm

Tanimoto [1] developed an equation to determine the rock size to prevent toe scour. Figure XX shows the berm protection with the corresponding symbols. The following set of equations gives the median stone diameter of the revetment. The minimum layer thickness is equal to $1.5d_{n50}$, with a minimum of 20 cm [45].

$$\frac{H_s}{\Delta D_{n50}} = \max\left\{1.8, 1.3\frac{1-\kappa}{\kappa^{1/3}}\frac{h'}{H_s} + 1.8\exp\left(-1.5\frac{(1-\kappa)^2}{\kappa^{1/3}}\frac{h'}{H_s}\right)\right\} \tag{H.50}$$

$\kappa = \kappa_1\kappa_2$

$\kappa_1 = 2kh'/\sinh(2kh')$

$\kappa_2 = \max\left\{0.45\sin^2\theta\cos^2(kB\cos\theta), \cos^2\theta\sin^2(kB\cos\theta)\right\}$

Where:

- H_s [m] is the significant wave height in front of the caisson.
- Δ [-] is the relative rock density.
- D_{n50} [m] is the equivalent cube length of a median stone.
- h' [m] is the water depth on top of the sill.
- B [m[is the width of the sill berm (1/4 L0).
- k [rad/m] wave number.
- θ incident wave angle deterministic $\theta = 0$.

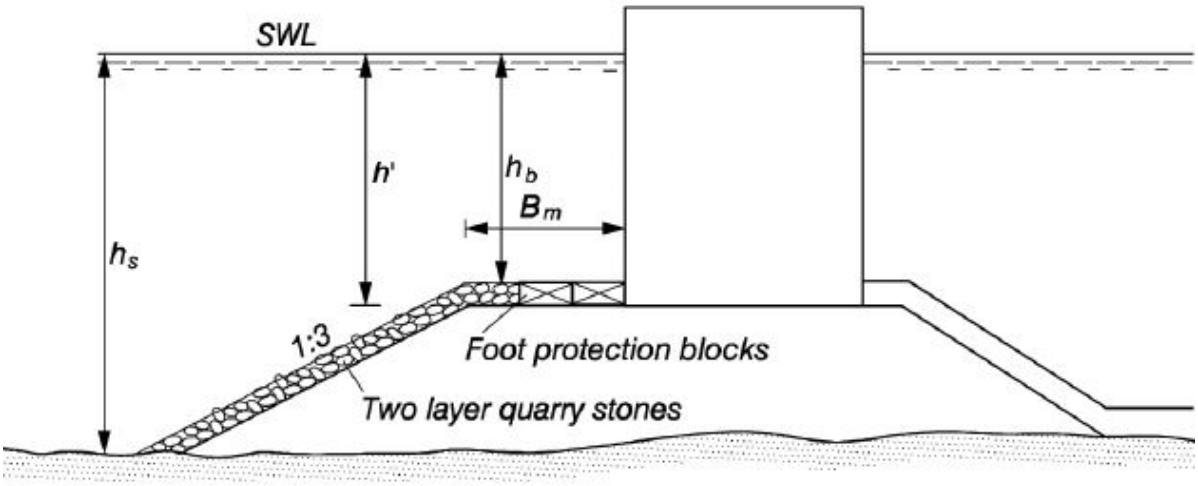

Figure H.4: Illustration of foot protection blocks for vertical structures [1].

Cross-section

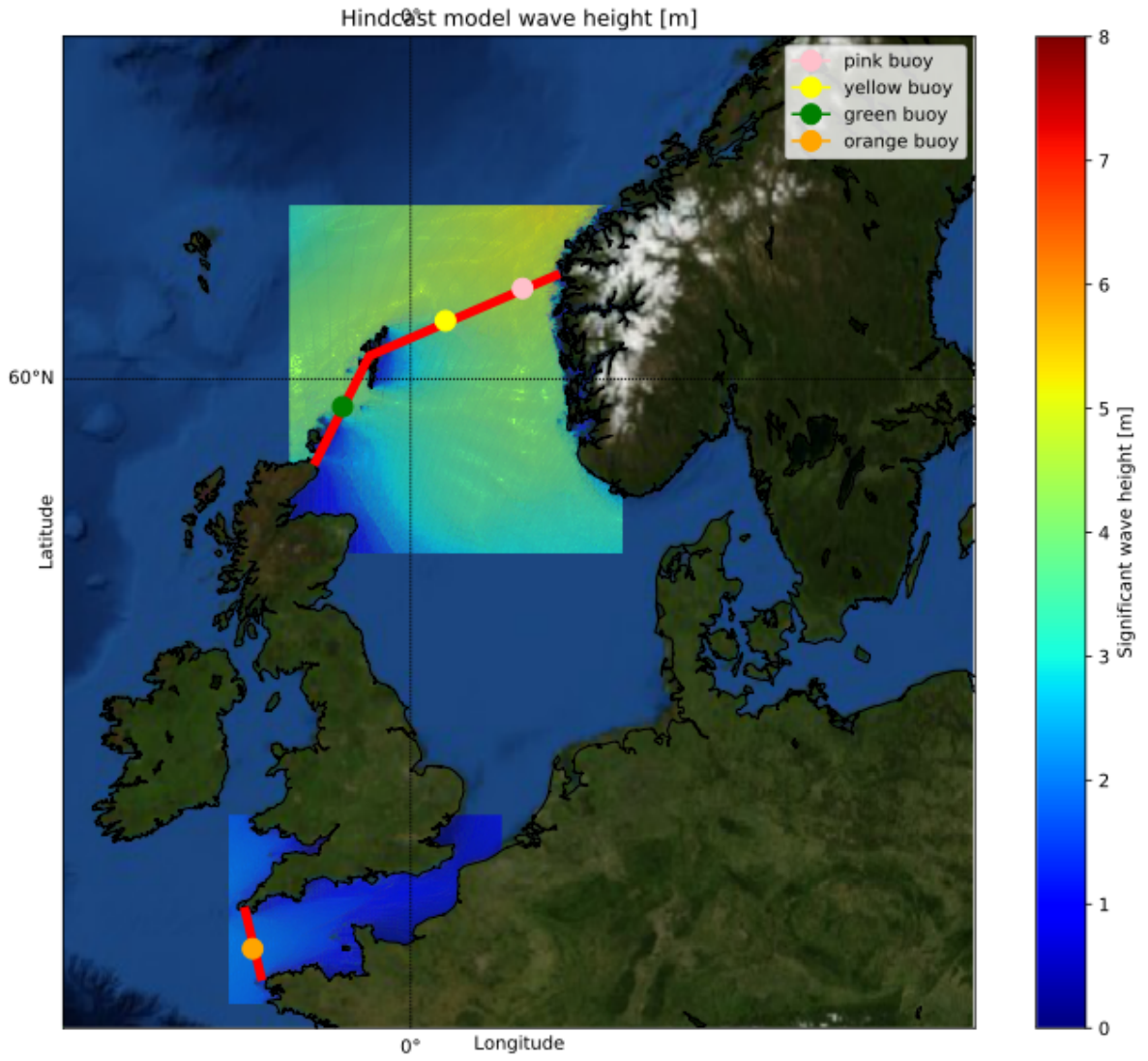

Figure I.1: Location observation buoys retrieved from hindcast model.

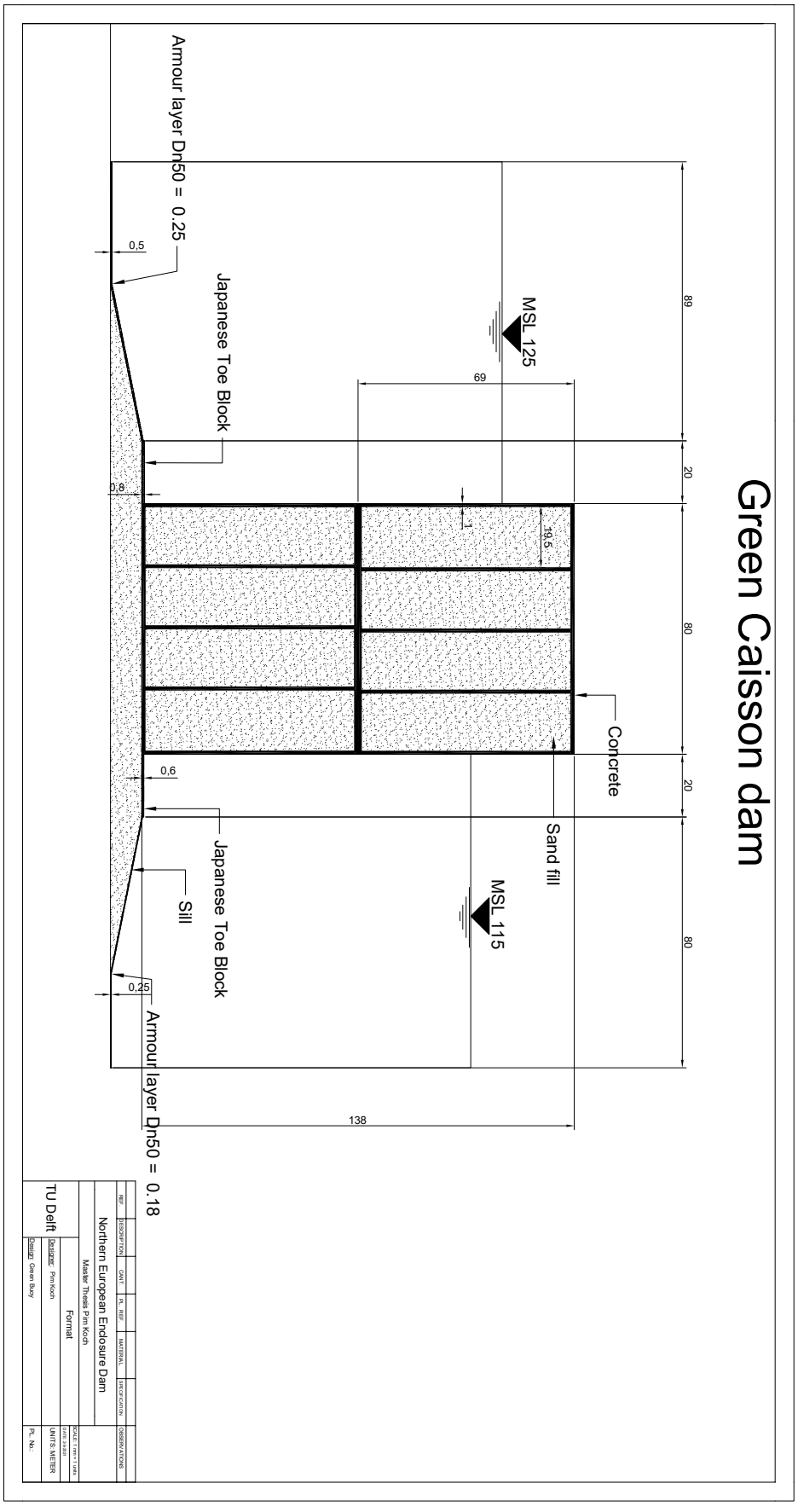

Figure I.2: Autocad drawing Green Caisson Dam.

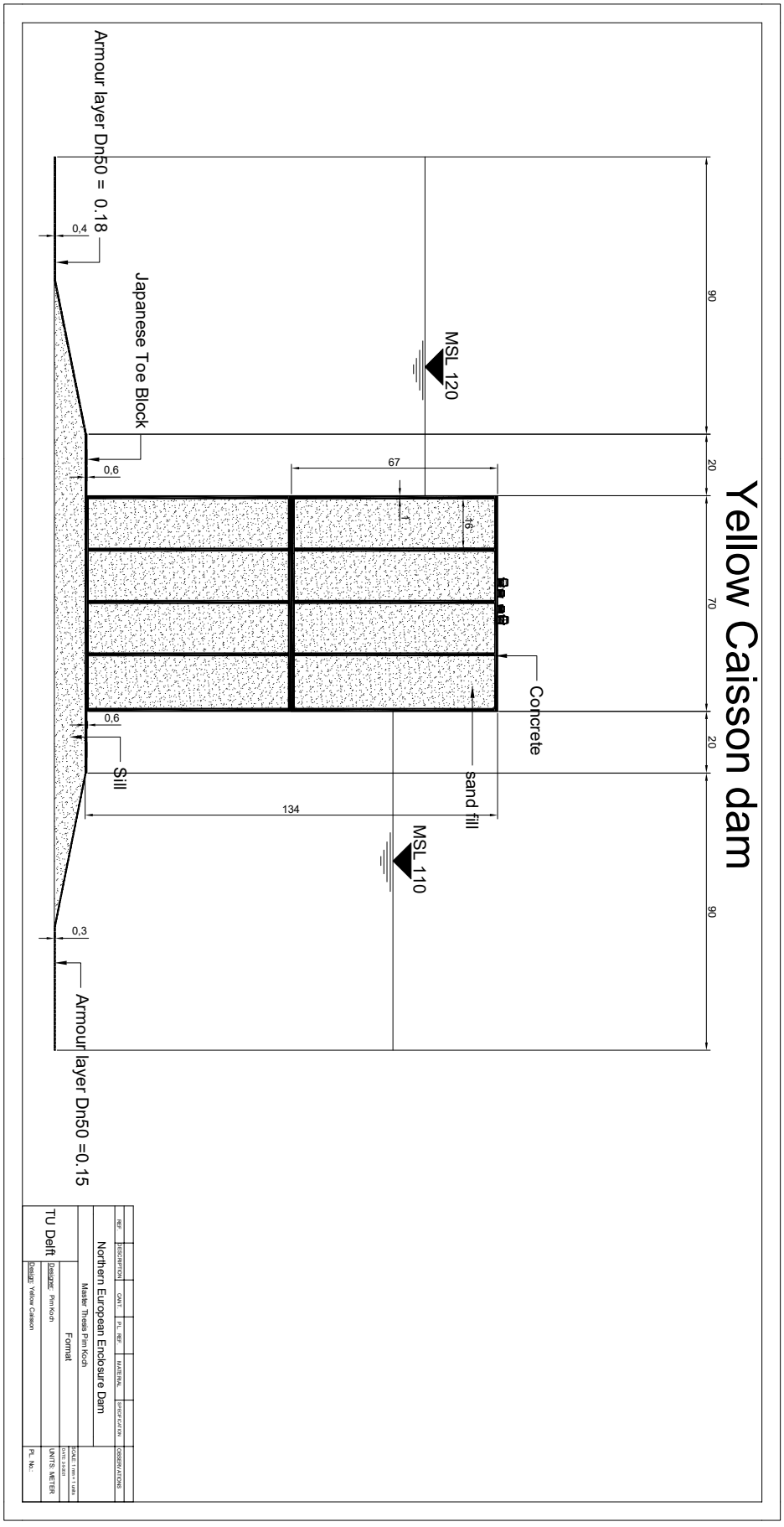

Figure I.3: Autocad drawing Yellow Caisson Dam.

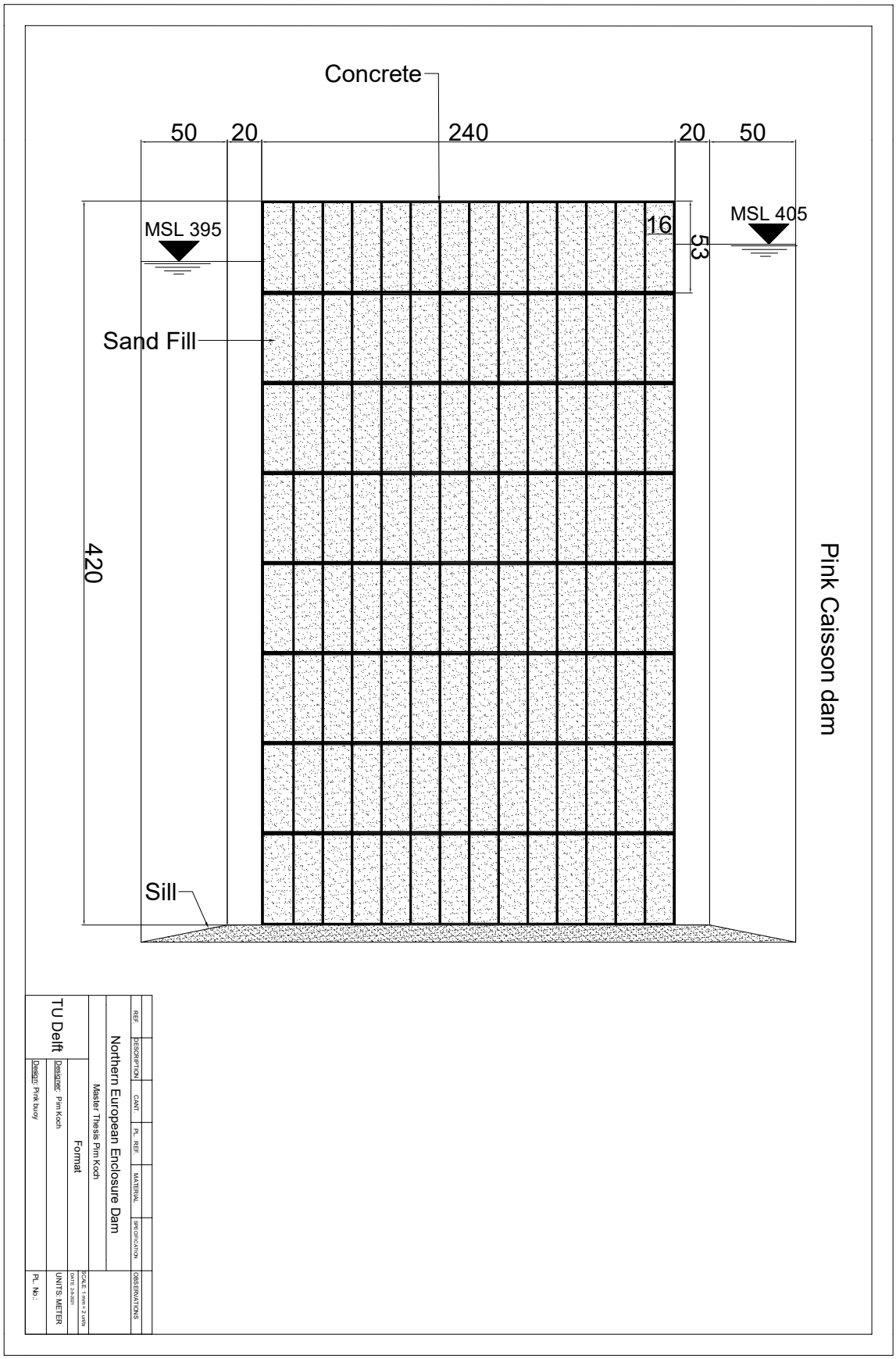

Figure I.4: Autocad drawing Pink Caisson Dam.

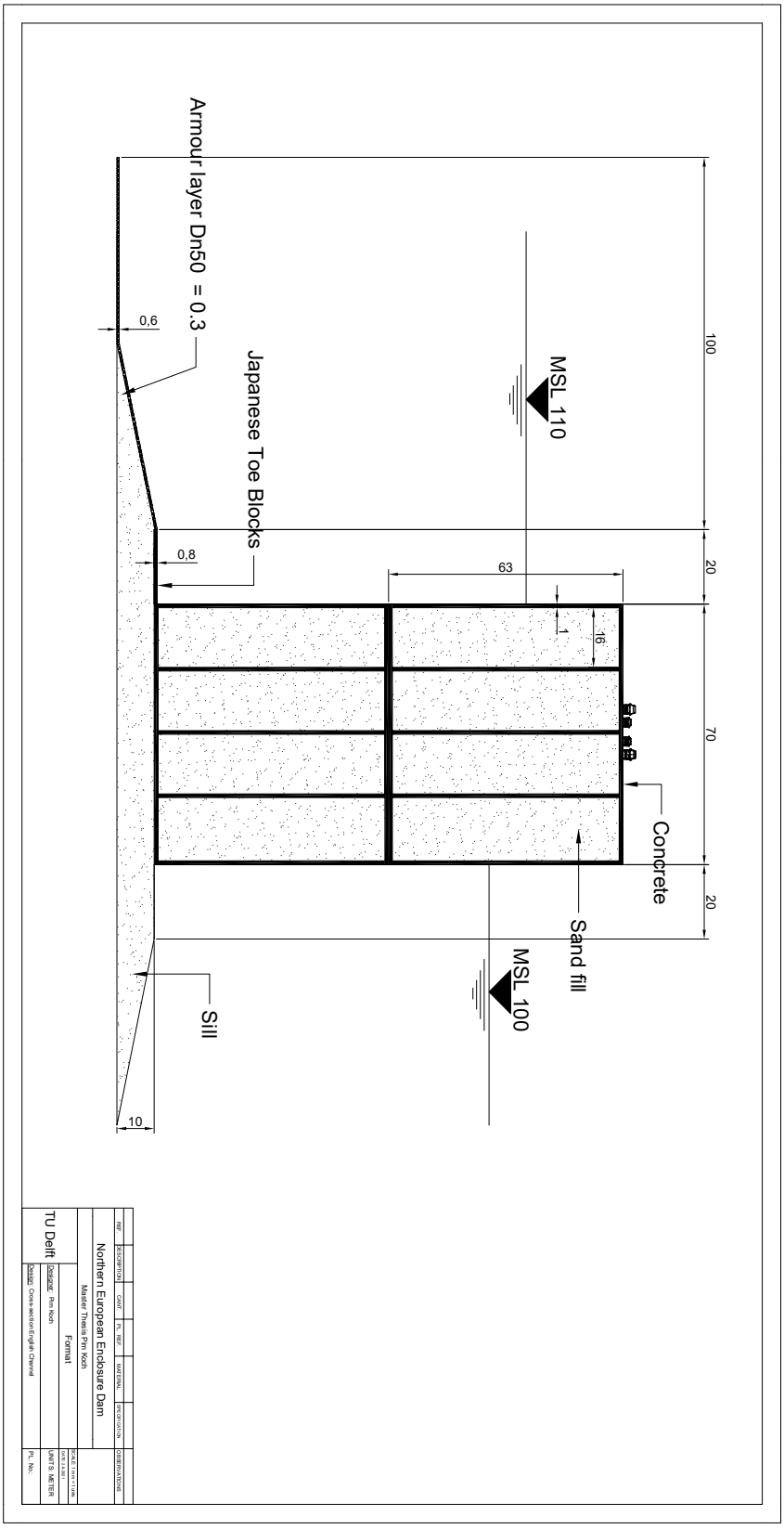

Figure I.5: Autocad drawing Orange Caisson Dam.

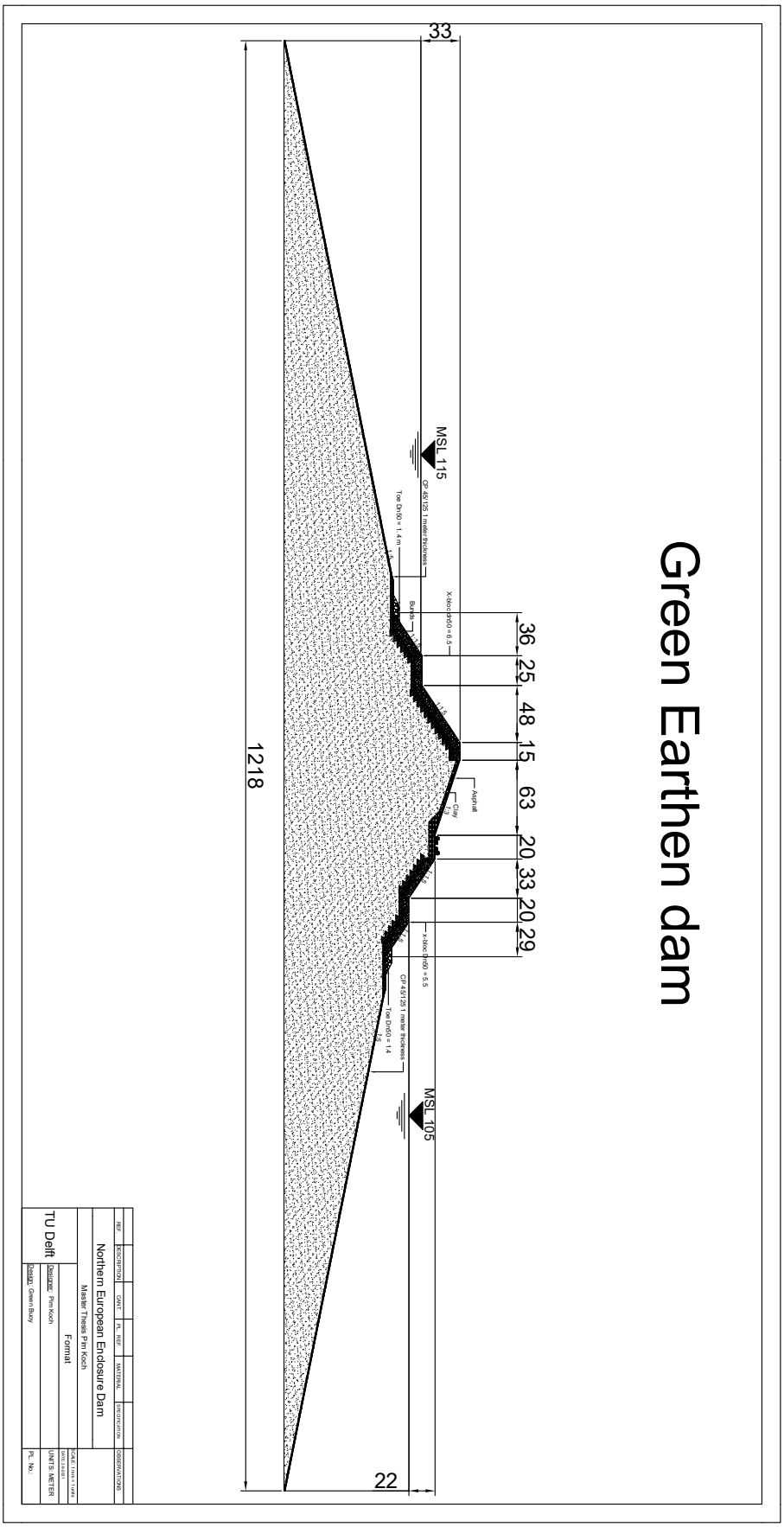

Figure I.6: Autocad drawing Earthen Caisson Dam.

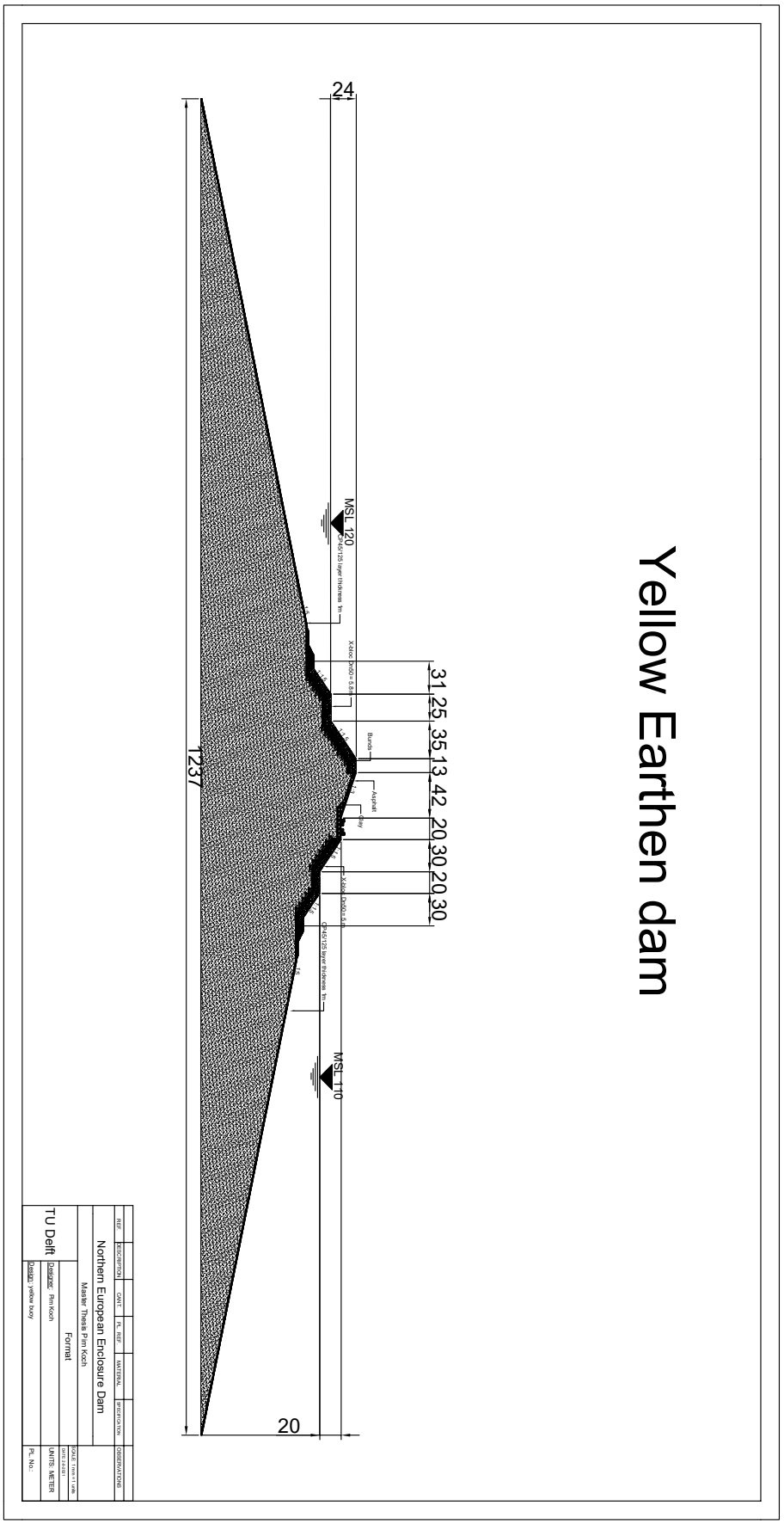

Figure I.7: Autocad Earthen Yellow Caisson Dam.

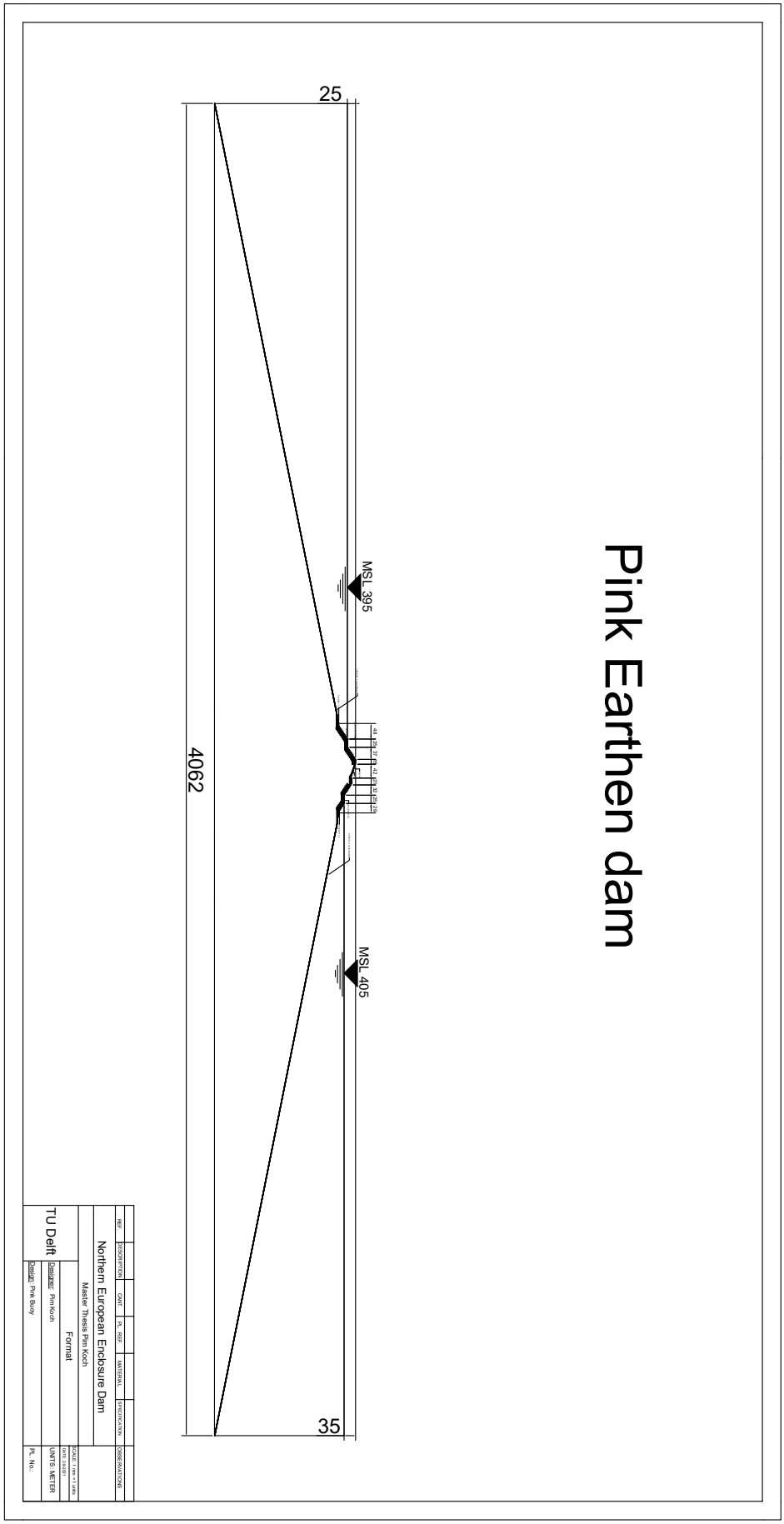

Figure I.8: Autocad drawing Pink Earthen Dam.

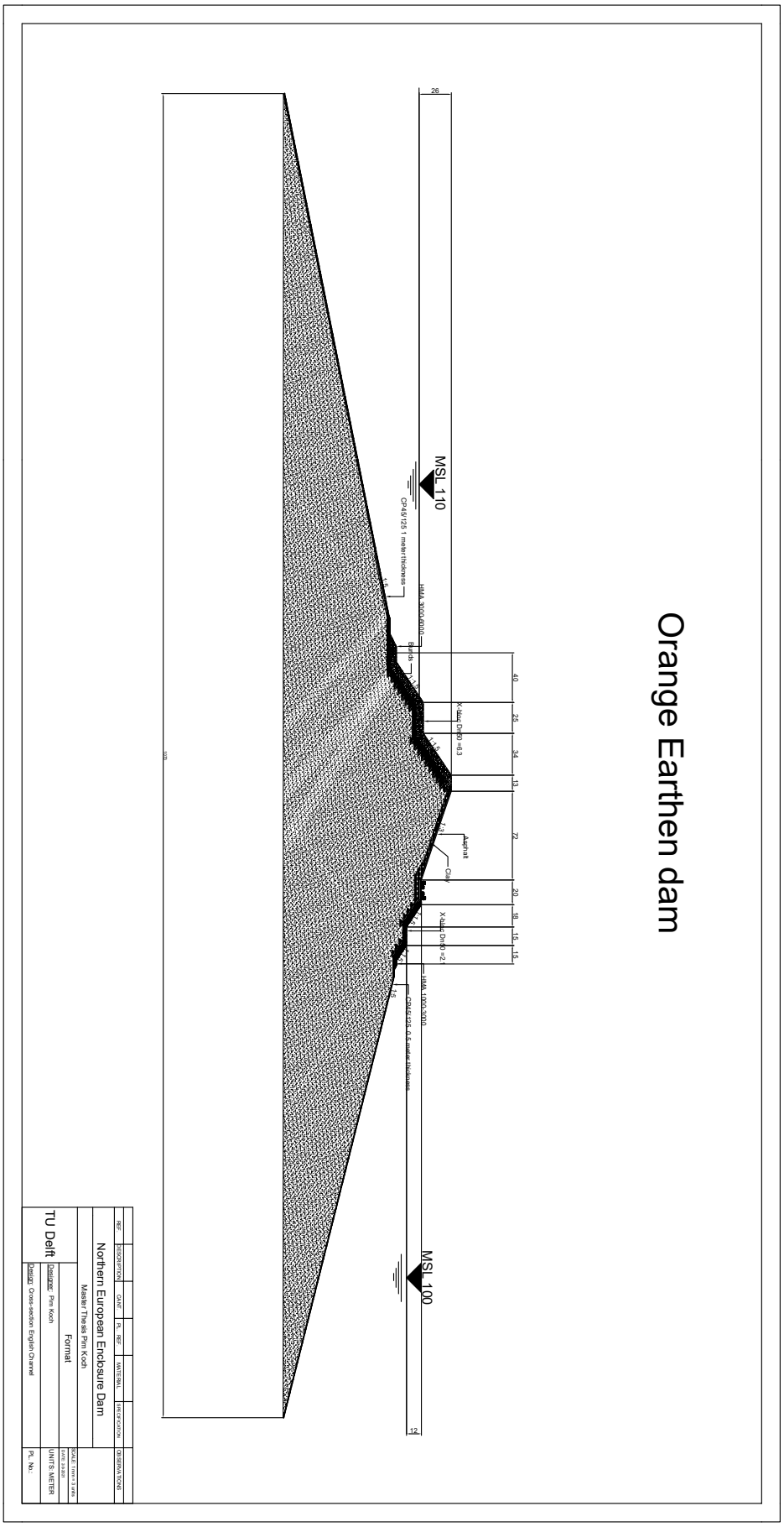

Figure I.9: Autocad drawing Orange Earthen Dam.